A NEW MULTI-FACETED FRAMEWORK FOR DECIPHERING DIPLODOCID ONTOGENY

by

David Cary Woodruff

A thesis submitted in partial fulfillment
of the requirements for the degree

of

Master of Science

in

Earth Sciences

MONTANA STATE UNIVERSITY
Bozeman, Montana

January 2015

DEDICATION

I dedicate this work to the late Mr. John Bell Hatcher. Like myself, Hatcher was raised a farm boy who headed to a distant city to pursue his dreams and a deep scientific passion. In 1884 Hatcher got the opportunity to work one-on-one with one of the most preeminent paleontologists of his day, Othneil Charles Marsh. For nearly a decade Hatcher traveled the American west collecting fossils for Marsh, and becoming a rising star in the Yale based lab. However, Hatcher wanted to be an active and contributing paleontologist, a dream severely demonized in Marsh's presence. So in 1890 Hatcher left Marsh's company and set off to blaze his own trail. Yet sadly, Hatcher's short career lacks the prestigious laurels and deserving recognition in the paleontological annals. Succumbing to Typhoid fever in 1904, Hatcher had a seemingly promising career ahead of him that was dotted with notoriety and achievements during his years at Princeton University and the Carnegie Museum of Natural History.

Today Hatcher is most credited with his work on ceratopsian dinosaurs. Hatcher famously discovered the first specimen of the cerastopsian "*Torosaurus*", and several of his scientific works revolve around these dinosaurs, most notably "The Ceratopsia". Yet I would argue that Hatcher's greatest paleontological accomplishments were in regards to his work on sauropods. Working for the Carnegie Museum of Natural History, Hatcher heavily explored and collected in the Morrison Formation of Colorado. In Colorado, Hatcher discovered and named the enigmatic sauropods *Haplocanthosaurus priscus* and *H. delfsi*. However Hatcher's *magnum opus* bar none was his description of *Diplodocus carnegii* in 1901. To this day "*Diplodocus* (Marsh): Its Osteology, Taxonomy, and Probable Habits, with a Restoration of the Skeleton" remains one of the most distinguished paleontological monographs. Not only is the monograph executed with exquisite precision and detail, but Hatcher's keen insight and understanding of sauropods is prophetic to this day.

Hatcher was one of the first to consider the significance of ontogeny and biomechanics in sauropods. In regards to ontogeny, he noted that the species "*Diplodocus lacustrius*" was only characterized by its small size and slender build. From this dubious assessment he noted that size was an unsuitable character, and that "*D. lacustrius*" merely represented an immature *Diplodocus*. In terms of biomechanic forethought, in 1901 Hatcher wrote, "The Sauropoda have been considered as the least specialized of the Dinosauria, and in many respects this is doubtless true, but in its adaptation for the application of those mechanical principles which combine maximum strength with minimum weight and increased surface for muscular attachment, the vertebral column of *Diplodocus* exhibits a remarkable degree of specialization, unsurpassed if not unequaled by other vertebrates". All sauropod biomechanic work done since, in one guise or another, directly descends from this astute observation. John Bell Hatcher's legacy lives on today as strong as ever, and I gratefully thank him for his contributions and inspiration which has had such a profound impact on my own work.

ACKNOWLEDGEMENT

“Qui si convien lasciare ogni sospetto; ogni viltà convien che qui sia morta.”
-Dante Alighieri “The Divine Comedy – Inferno” Canto III, lines 14-15
“Here one must leave behind all hesitation; here every cowardice must meet its death.”

Graduate school is no simple or trivial task. And all serious and worthwhile endeavors should present an extreme challenge. I have slipped, stumbled, fallen, limped, and crawled along the way, but I can proudly say that I did not give up. I may not have run the fastest time, but by God I completed the race. There certainly were days I wanted to throw in the towel, but I was able to preserve because of my committee. Drs. Horner, Varricchio, and Woodward all laudably guided me. As Virgil to Dante, the path was harrowing, and along the way there were times for friendly support and others for tough love, but it was critical guidance in any guise. My committee’s care for my success is directly visible from this support and guidance. I am and will always be eternally thankful and grateful for their support. I would not be standing where I am today if were not for these individuals, and I know I will progress and thrive because of them.

“Poca favilla gran fiamma seconda.”
-Dante Alighieri “The Divine Comedy – Paradiso” Canto I, line 34.
“A great flame follows a little spark.”

TABLE OF CONTENTS

TABLE OF CONTENTS - CONTINUED

LIST OF TABLES

LIST OF FIGURES

Figure Page

LIST OF FIGURES – CONTINUED

LIST OF FIGURES – CONTINUED

ABSTRACT

Since sauropod dinosaurs lack the extravagant cranial features that are important to tracking ontogenetic trajectories (changes through growth), sauropods generally garner less focus on development than those dinosaurs with expressive cranial displays. The apparent lack of features that radically change through ontogeny has even led some to speculate that sauropods exhibited isometric growth. Yet within the past decade a small number of morphologic features have been demonstrated to undergo significant morphologic change; thus maturity can be tracked in ways other than histologic analysis (bone microstructure). The recognition of features that change dramatically through ontogeny hints at significant phylogenetic and biomechanical consequences in the immature sauropod condition. However the topic of morphologic ontogenetic change in sauropods is highly debated, with some question as to the validity of these apparent patterns. The current study will attempt to recognize additional morphologic and histologic features that can be used to infer maturity in diplodocid sauropods. By examining a broad range of features that span every aspect of the skeleton, the goal of this analysis is to substantiate previous ontogenetic inferences and conclusions. The findings of this analysis indicate that contrary to previous notions, diplodocid sauropods underwent radical ontogenetic changes in several skeletal elements. This analysis also establishes a suite of morphologic and histologic attributes that in combination can be used as a guide to identify maturational status in other diplodocid specimens. In addition this study also raises question to the validity of small bodied sauropod specimens that were previously recognized as distinct species.

Manuscript Information Page

D. Cary Woodruff
Journal of Morphology
Status of Manuscript:
____ Prepared for submission to a peer-reviewed journal
____ Officially submitted to a peer-review journal
____ Accepted by a peer-reviewed journal
_X _ Published in a peer-reviewed journal

Wiley Periodicals Inc.
2014
Volume 275, Issue 9

THE ANATOMY OF THE BIFURCATED NEURAL SPINE AND ITS OCCURRENCE WITHIN TETRAPODA

Contribution of Authors and Co-Authors

Manuscript in Chapter 1

Author: D. Cary Woodruff

Contributions: Conceived and implemented the study design. Collected and analyzed data. Wrote the manuscript.

THE ANATOMY OF THE BIFURCATED NEURAL SPINE AND ITS OCCURRENCE WITHIN TETRAPODA

Woodruff, D.C. 2014. The Anatomy Of The Bifurcated Neural Spine And Its Occurrence Within Tetrapoda. Journal of Morphology. 275: 1053-1065.

ABSTRACT

Vertebral neural spine bifurcation has been historically treated as largely restrictive to sauropodomorph dinosaurs; wherein it is inferred to be an adaptation in response to the increasing weight from the horizontally extended cervical column. Because no extant terrestrial vertebrates have massive, horizontally extended necks, extant forms with large cranial masses were examined for the presence of neural spine bifurcation. Here, I report for the first time on the soft tissue surrounding neural spine bifurcation in a terrestrial quadruped through the dissection of three Ankole-Watusi cattle. With horns weighing up to a combined 90 kg, the Ankole-Watusi is unlike any other breed of cattle in terms of cranial weight and presence of neural spine bifurcation. Using the Ankole-Watusi as a model, it appears that neural spine bifurcation plays a critical role in supporting a large mobile weight adjacent to the girdles. In addition to neural spine bifurcation being recognized within nonavian dinosaurs, this vertebral feature is also documented within many members of temnospondyls, captorhinids, seymouriamorphs, diadectomorphs, Aves, marsupials, artiodactyls, perissodactyls, and Primates, amongst others. This phylogenetic distribution indicates that spine bifurcation is more common than previously thought, and that this vertebral adaptation has contributed throughout the evolutionary history of tetrapods. Neural spine bifurcation

should now be recognized as an anatomical component adapted by some vertebrates to deal with massive, horizontal, mobile weights adjacent the girdles.

INTRODUCTION

Within the paleontological literature, the bifurcated neural spine is predominantly attributed to Sauropodomorph dinosaurs and secondarily to Aves (Osborn, 1898; Hatcher, 1901; Osborn and Mook, 1921; Wedel et al., 2000; Tsuihiji, 2004; Schwarz et al., 2007; Tambussi et al., 2012; Woodruff and Fowler, 2012; Wedel and Taylor, 2013). For the purposes of this article, the term bifurcation shall strictly adhere to Janensch's (1929) definition to indicate a laterally paired neural spine apex. Unfortunately for comparative studies, there are no extant large herbivorous quadrupeds with large horizontally extended necks (i.e., proper sauropod analogs, and the numerous flaws with the many proposed extant analogs are addressed in depth by Coombs, 1975). As such, this study examined the vertebral columns of extant Cervidae and Boviadae (and other artiodactyls and perissodactyls). Characterized by large cranial ornamentation (composed of horn or antler), these features represent extreme masses positioned off of the shoulder girdles. Cervidae and Boviadae with extremely exaggerated cranial displays relative to body size were the primary study objective. The African Zebu cattle Ankole-Watusi is generally accepted as *Bos primigenius taurus* (Grubb, 2005); however, some classify it as *Bos taurus macroceros* (Dürst, 1899), *Bos Zebu africanus Sanga* (Keller, 1905), or a variation of *Bos africanus* (Grigson, 2000). Here, I will simply refer to it as the Ankole-Watusi. The Ankole-Watusi is a modestly sized bovine [cows weigh 400–540 kg, bulls weigh 450–725 kg (Desilva and Fitch, 1995)] but it is renowned because it holds the record for

the largest horns of any living animal, with a horn circumference of 95.25 cm and a span of nearly 243 cm (Folkard, 2003). These dimensions place the Ankole-Watusi amongst the largest horned animals to have ever lived (alongside other extinct bovids, such as *Syncerus antiquus*, *Bison latifrons*, and *Pelorovis oldowayensis*; Fig. 1). By dissecting the axial columns of three World Watusi Association pure Ankole-Watusi cows (four [MOR OST1613], sixteen [MOR OST1614], and nineteen years old [MOR OST1616]; Fig. 2), this study is the first to document the anatomy associated with neural spine bifurcation in an extant large terrestrial herbivorous quadruped.

MATERIALS AND METHODS

Termination of the three Ankole-Watusi cows was conducted in full accordance with guidelines and policies of the American Veterinary Medical Association, the Montana Farmers Association, the Montana Cattlemen's Association, and the Montana Beef Council, using a high impact blow to the temple that destroyed the brain. After dissection, the majority of the processed meat was donated to the Gallatin Valley Food Bank of Bozeman, Montana. A larger sample size would have been preferred for this study, however, the combination of the Ankole-Watusi being indigenous to Africa, and that the three cows were donated for this project were dominating variables that limited the study sample.

To prepare the skeletal material, the vertebral column was disarticulated into several large sections. Each section contained articulated segments then had a wire run through the neural canal. This wire ensured that during cleaning no vertebrae managed to become loose and out of sequence. Each large section was numbered and then

individually placed in a 120 quart stock pot where warm water maceration was applied to remove all of the soft tissues. Once each section was cleaned, all vertebrae were placed in numbered serial sequence and appropriately labeled including a Museum of the Rockies Osteology Collection number (MOR OST 1613, 1614, and 1616).

In addition to the macroscopic examinations, histological nondecalcified microscopic thin sections were produced from the 19-year-old cow's neural spines and a desiccated section of the intact nuchal ligament was taken from the 4-year-old cow in order to examine the microstructures of these soft tissues. The neural spine slides were prepared by Lauder Histology and the nuchal ligament slides were prepared by the Montana Veterinary Diagnostic Lab. Before thin sectioning, the nuchal ligament sample was rehydrated in a solution of alcohol, water, and carbonate of soda following the methods of Ruffer (1921). To prepare the samples for nondecalcification, the sample is first dehydrated in a series of water/formaldehyde calcium acetate mixtures and afterward transferred to a mixture of absolute ethanol/anaesthetic ether. Next the sample is transferred to a series of low-viscosity cellulose (LVN) solutions. The LVN evaporates, forming a firm gel that is then hardened by exposure to chloroform vapor. Once the section is completely hardened a section is cut. The section is then washed in a 10% solution of sodium ethylenediaminetetraacetic acid (EDTA), and dehydrated again in a graded series of water/ethanol mixtures. After the second dehydration, the sample is left in a solution of paraffin wax and chloroform. Once the wax hardens, a smaller sample is sectioned on a microtome and mounted on a plastic slide (Linder et al., 1981). A stain is then applied and the section is ground following standard histological techniques (see

Padian and Lamm, 2013).

RESULTS

Dissection

Before removal of the hide it was observed that in the hypothesized region of bifurcation, a portion of the back was rather flat compared to the sloping curvature immediately anterior and posterior to it. With the removal of the hide, it was evident that despite basic superficial similarities, Ankole-Watusi differs in several respects from typical domestic cattle. Dorsal to thoracic (T) 1–3 sits at the posterior portion of the *m. rhomboid*. In several bovid species and breeds, this is the locationof the large "shoulder hump," which is greatly expressed in the related Brahma (*Bos primigenius indicus*) breed; the Ankole-Watusi instead has a much smaller cervico-thoracic hump. Nevertheless, the posterior portion of the m. rhomboid in the Ankole-Watusi cervico-thoracic hump was quite robust and bulbous in three dimensions (Fig. 3).

Aside from the proportional discrepancy of the *m. rhomboid*, the musculature of the Ankole-Watusi was nearly identical to that of ordinary domestic cattle (collectively *Bos primigenius*). However, a dramatic difference was observed in the morphology of the primary axial ligaments (Figs. 3 and 4). The nuchal ligament (*ligamentum nuchae*) and the supraspinous ligament (*ligamentum supraspinale*) comprise the dorsally situated ligaments that attach to the apices of the spinous processes (Grey, 1858; Dimery et al., 1985; Dzemski and Christian, 2007). The nuchal ligament extends from the external occipital protuberance of the skull to cervical (C) 7, while the supraspinous ligament continues from C-7 to the sacrum (Grey, 1858; Dimery et al., 1985; Dzemski and

Christian, 2007). In typical cattle breeds, the nuchal ligament attaches posteriorly at the sacrum and anteriorly attaches to the neural spine apexes; at the cervicothoracic transition the lamellar portions branch from the main nuchal body and attach to C 2-7, and culminate in a robust attachment at the external occipital protuberance (Budras and Habel, 2003; Ashdown et al., 2010). As in domestic cattle, the nuchal ligament of the Ankole-Watusi attaches posteriorly at the sacrum and continues dorsally along the neural spines. However, at the region of thoracic bifurcation (the same "flat" area observed externally) the nuchal ligament splits into left and right halves. As opposed to splitting and then continuing anteriorly along the lateral dorsal margins of the neural spines, the Ankole-Watusi nuchal ligament splits and then extends ventrally on each lateral side. Once the nuchal ligament is ventral to the bulbous portion of the m. rhomboid, the nuchal ligament exhibits a convex curve. From this curve, the nuchal ligament bifurcates: the ventral portion terminates and attaches to the lateral spine surfaces of C 3-4, while the dorsal portion continues along the lateral surface of the cervical series before the two halves finally merge at the neural spine of C-2. The ligament finally tapers out at the external occipital protuberance. Because such a dramatic difference was observed in the ligament complex anterior and posterior to C-7, for the purpose of this article, the nuchal ligament and supraspinous ligament will collectively be referred to as the nuchal ligament, consisting of the ligament complex extending from the external occipital protuberance to the sacrum.

In addition to the unique branching and pathway of the nuchal ligament, its dorsal aspect warranted study. Along both lateral margins of the spine apices was a differing

tissue. This secondary tissue was pale yellow to white, as opposed to the nuchal ligament's golden yellow, and had a slightly pitted or textured surface, different from the fibrous nuchal. This particular tissue was extremely hard and required scissors for severing. This tissue itself did not fill the entirety of the trough of bifurcation; it appeared to be embedded within the nuchal ligament, adhering primarily to the apex of each neural spine process. Filling the remainder of the trough was a distinguishable interspinal ligament [in mammals this ligament is continuous, while in birds it is discontinuous and referred to as the *ligamentum elasticum interlaminare* (Tsuihiji, 2004)]. The interspinal ligament was not restricted to the bifurcation trough; it extended from the trough to the immediately anterior and posterior neural spines. During hot water maceration of the 4-year-old thoracic section, the nuchal ligament and surrounding features were shed together (Fig. 5). This approximately 18.5 cm long section was desiccated for study. Examination of the underside of this complex in situ, suggested that this hard tissue was interpreted to be cartilage (a sample of which was documented histologically). These cartilaginous caps are "heart"- shaped, and the widest portion is anteriorly situated. Each cartilaginous cap attaches to a neural spine apex and is embedded within the nuchal ligament [similarly observed in crocodilians as the *lamina processus spinosi* (Frey, 1988)]. From there, each interspinal ligament is attached to the ventral side of each cartilaginous cap and to the nuchal ligament.

A great deal of morphologic change was observed in the morphology of bifurcated spines between the 4- and 16-year-old Ankole-Watusi cows (Figs. 6 and 7, Table 1). Bifurcation occurs in the neural spines of T 6-10 in the 4-year-old cow. The

neural spines are inclined on average approximately 40° to the centrum. In the thoracic series, bifurcation begins and ends rather suddenly: T-5 is not bifurcated, but T-6 is fully bifurcated; full bifurcation is present in T-10, but only scalloping of the anterior and posterior portions is present in the neural spines in T-11 and 12. In the bifurcated thoracic vertebrae, the neural spine apices are enlarged and inclined approximately 10° to the neural spines. The neural spine apex of T-6 is widened and the bifurcation trough is a narrow "U"-shape 1.6 cm in depth. From T 7-9, the neural spine apices widen to form a very pronounced and steep "V"-shaped trough. This is most defined in T-8 where the trough is 3 cm deep. At T-10 the neural spines have nearly rejoined, leaving a barely open "keyhole." The anterior face of each bifurcated apex is broad and slightly rounded. However, the posterior faces have a prominent keel and are steeply inclined into the bifurcation trough. From T-11 posteriorly, the neural spines are not bifurcated and exhibit the typical bovine morphology. From neural canal to spine apex, the neural spine is fairly uniform in thickness. The anterior face forms a prominent keel along the midline, whereas the posterior face is distally very broad, progressively tapering toward the apex. Small degrees of bifurcation were also observed in a few cervical vertebrae. C-3 has a short and stocky neural spine, but the apex is weakly bifurcated with a wide "U"-shaped trough. C-5 is the second cervical with apparent bifurcation. The neural spine is long and anteriorly inclined with a bulbous apex. The bifurcation of C-5 is nowhere near as dramatic as the others, and C-5 should be described as slightly or incipiently bifurcated. C-4 is missing the unfused portion of the neural spine apex; however, considering that C-3 and 5 are bifurcated, it would be logical to reconstruct the same condition in C-4.

In the 16-year-old cow, neural spine bifurcation occurs in C 3-5, T 6-13, and in lumbar (L) 1. In gross morphology, these neural spines are very similar to those from the 4-year-old cow. In which, the onset and offset of bifurcation is rather sudden. In T-6, the neural spine apex is very bulbous and bifurcation is only incipient. In T-7 and 8, the spine apices have widening troughs with bony margins surrounding them. In T-6 through 8, a horizontal projection runs from the posterior portion of the spine apex. T-9 exhibits bifurcation in the more classic sense. The bifurcation trough is a wide "U"-shape 0.5 cm deep. T-10 and 11 exhibit asymmetric bifurcation. From T-11 through 13 and L-1, the neural spine apexes exhibit very dramatic pronounced and rugose protuberances. From T-12 to L-1, the bifurcation troughs decrease in height significantly. The apices change from bulbous in the preceding neural spines to laterally expanded. From T-12 through the remaining presacral vertebrae, the pre and postzygapophyses become more elongated and interlocked. Posteriorly, the intervertebral mobility becomes more restricted. L-3 and 4 are interlocked in such a way that the two cannot be separated. Also as in the 16-year-old, there is bifurcation in the cervical column. C-3 through 5 exhibit bifurcation reminiscent of the 4-year-old cow. The bifurcation is strongest (and asymmetric) in C-3, reducing to incipient bifurcation in C-5.

In addition to the variation in bifurcation, other neural spine features also show distinct differences (Fig. 8). As in the 4-year-old cow, the neural spines of the 16-year-old cow have a prominent keel along the anterior midline; the posterior face is distally very broad and progressively tapers toward the apex. However, in T-6 through 8 the anterior facing keel is greatly enlarged. Situated at the proximal end of the neural spine,

the keel is approximately half the length of the neural spine and protrudes roughly 1 cm from the neural spine.

Unlike the 4-year-old cow, in the 16-year-old cow, the posterior side of the neural spine has numerous tubercles. These tubercles are roughly paired and situated on either side of the posterior midline. Another interesting and possibly ontogenetic feature is the morphology of foramina along the posterior side of the neural spine. In the 4-year-old cow, small foramina were irregularly and infrequently distributed on some neural spines. In the 16-year-old cow, these foramina are much larger and are on nearly all posterior sides of the neural spines. These foramina, like those in the 4-year-old, are distal to the neural spine. However, unique to the 16-year-old cow is the presence and degree of these features on the posterior side of the neural spines. Some of these circular, irregularly dispersed canals are foramina, but several are much larger (on the order of centimeters) and irregularly shaped. The fossa-like features are roughly ovoid and extend deep into the neural spine. Only in T-8 and 9, do these fossae appear to have roughly symmetric counterparts. These fossae are present in T-6 through 11.

Slide Descriptions

The nondecalcified neural spine sections (MOR OST1616 1-6) from the 19-year-old cow represent spines apices that were once strongly bifurcated, and through ontogeny were highly remodeled resulting in a nonbifurcated spine (as observed in the 16-year-old cow and the world record holding Ankole-Watusi steer “Lurch,” Fig. 9). Under magnification, the border of the neural spine apex is highly irregular, which denotes enthesis. Commonly studied under injuries such as “tennis elbow,” “jumper’s knee”

(Benjamin et al., 2002), and Achilles tendinosis (Cormick, 2010), enthesis is defined as the insertion point of a ligament or tendon into bone via Sharpey's Fibers. At this junction, the collagen fibers of the connective tissue are mineralized through metaplasia (Benjamin et al., 2002). Enthesis can be fibrous or fibrocartilaginous. The enthesis within the Ankole-Watusi neural spines is fibrocartilaginous. In fibrocartilaginous enthesis, there are four transitionary zones, and in the Ankole-Watusi thin section between the bone and soft tissue is a region of calcified cartilage known as the "tidemark" or "blue line" indicative of the third transitionary zone (Mescher, 2010). Enthesis has also been previously reported from the vertebrae of the macronarian sauropod *Camarasaurus* (Ikejiri et al., 2005; Organ and Adams, 2005).

In addition to the neural spines slides from the 19-year-old cow, nondecalcified sections were prepared from the suspected cartilage from the preserved nuchal ligament belonging to the 4-year-old cow (MOR OST1613 1-8). In thin section, this tissue has abundant cartilaginous matrix that produced chondrocytes dispersed throughout a fibrous matrix, indicative of fibrocartilage (Hall, 2005; Fig. 10). Because these tissues are nodules of cartilage located near bone and are formed within a ligament, they should be identified as sesamoids (Currey, 1984; Hall, 2005; Vickaryous and Olson, 2007). The function of a sesamoid is to protect the connective tissue (in this case the nuchal ligament) and to increase the ligament's mechanical effect (Currey, 1984; Vickaryous and Olson, 2007). Fibrocartilage has been documented to undergo endochondral ossification (Vickaryous and Olson, 2007), so potentially the "pathological" appearance and spinous projections observed in the more mature Ankole-Watusi [and the crocodilian

lamina processus spinosi (Frey, 1988)] are indicative of this ossification. The identification of fibrocartilage within the nuchal ligament also supports fibrocartilaginous enthesis in the neural spine.

DISCUSSION

In the Ankole-Watusi, I would theorize that the modified vertebral morphology (i.e., spine bifurcation and associated nuchal morphology) is due to the large weight of the horns. Although the horn cores themselves are very spongy and cavernous, the weight alone is still significant. In the case of the Ankole-Watusi cows used in this study, the weight of the skull detached from C-1 and defleshed for the 4-year-old was 28.58 kg and 51.26 kg for the 16-year-old cow. When the World Record holding Ankole-Watusi steer "Lurch" (MOR OST1615) died at the age of 14, it was calculated that his horns weighed over 45 kg each. As in the 16-year-old cow, "Lurch's" neural spines and vertebrae exhibit numerous growths, protuberances, and fusion. While these osteological oddities could initially appear to be pathologies, considering the immense weight of the skull, they most parsimoniously represent the vertebral column's attempt tocope with the increasing stresses. If the development of spine bifurcation is attributed to the cranially situated weight, I theorize that the nuchal ligament is likewise modified in a similar response. In addition, among several extant artiodactyls (including members of Bovidae, Cervidae, Camelidae, and Giraffidae), perissodactyl (Equidae), and even Carnivora (including members of Felidae, Canidae, and Ursidae), none exhibited a nuchal ligament reminiscent of the Ankole-Watusi (Fig. 11). Therefore, it should be regarded that the

highly modified soft and mineralized tissues observed in the Ankole-Watusi as directly attributable to the massive cranially situated weight.

Phylogenetic Distribution of Neural Spine Bifurcation

From this new work, it has been demonstrated that bifurcation of the neural spines is a significant biomechanical adaptation for vertebrates that evolved this feature. Conditionally being treated as restricted to amniotes, this assumption could indicate that neural spine bifurcation was one vertebral feature associated with amniote axial evolution [another being the pleurocentrum becoming the primary vertebral element (Romer, 1956)]. However, neural spine bifurcation is documented to be found outside of Amniota within reptilomorphs, and even anamniotes (Fig. 12). Within the numerous captorhinids [*Labidosaurus hamatus* (Cope, 1895)], seymouriamorphs (Seymouria), and diadectomorphs [*Tseajaia campi* (Vaughn, 1964)] that exhibit spine bifurcation, the bifurcation is restricted to the dorsal series (Sumida, 1990); while in the temnospondyl *Eryops*, the spine bifurcation is restricted to the anterior caudal vertebrae. Sumida (1990) strongly suggests that the vertebral morphologies seen in these basal tetrapods are adaptations associated with locomotion, and this analysis would strongly agree. Besides the aforementioned basal tetrapods, bovids, and well documented sauropods and ratites, this analysis has also observed neural spine bifurcation in the Stegosauridae dinosaurs *Stegosaurus* and *Miragaia longicollum* (Mateus et al., 2009), the Carnotaurinae dinosaur *Carnotaurus sastrei* (Bonaparte, 1985), the Megalosauroidea *Condorraptor currumili* (Rauhut, 2005), the Dromaeosauridae *Austroraptor cabazai* (Novas et al., 2009), within Afrotheria including *Arsinoitherium zitteli* (Beadnell, 1902), and members of

Elephantidae, artiodacyls such as *Capreolus* and *Stockoceros conklingi* (Stock, 1930), cetaceans such as *Delphinapterus leucas* (Cope, 1890), perissodactyls such as *Chalicothere*, marsupials such as *Diprotodon optatum* (Owen, 1838), in the felid *Smilodon populator* (Lund, 1842), in flightless birds such as *Raphus cucullatus* (Newton and Newton, 1869), members of Gastornithidae, Dinornithidae, Aepyornithidae, Dromornithidae, and in Primates (von Eggeling, 1922) to name a few (Fig. 13).

This widespread distribution suggests that neural spine bifurcation represents a significant vertebral adaptation throughout tetrapod evolution. However, the question remains as to why these organisms with drastically differing body forms and life habits develop spine bifurcation in the first place?

In 1922, the German anatomist H. von Eggeling concluded that within Primates the bifid spinous process was a mechanism contributing to increased bipedal equilibrioception (von Eggeling, 1922). To maintain bipedal equilibrioception, our cranium is continuously making unnoticeable microadjustments to maintain proper fluid balance in the semicircular canals. von Eggeling (1922) proposed that as humans evolved larger brains and a morebipedal stance, the cervical column needed a way to support the neck while maintaining heightened mobility. von Eggeling's (1922) major line of evidence was that from prosimians to lesser apes to humans, the degree of bifurcation increases.

von Eggeling's (1922) connection between mobility and spine bifurcation would appear to provide the answer. Be it a heavy neck, heavy brain, heavy tail, or heavy horns, regardless of the specifics, all of these represent some form of a proportionally large,

mobile weight adjacent to the shoulder or pelvic girdles. The anterior caudal bifurcation observed within diplodocids, *Stegosaurus*, and *Eryops*, would seem supportive of a laterally mobile tail, the posterior cervical bifurcation of the Aves and diplodocids appears to provide greater cervicothoracic mobility, and the dorsal bifurcation of captorhinids, seymouriamorphs, and diadectomorphs pertinent to the highly mobile vertebral column during locomotion (*sensu* Sumida, 1990). While the connection between mobility and spine bifurcation is supported and enforced within these examined tetrapods, it must be stated that at this time it is not fully understood as to why neural spine bifurcation appears restricted to particular vertebral segments and as to why bifurcation morphology varies. It may be that the location and degree of bifurcation within each of these tetrapods is dependent on several variables such as cranial and body mass, stance, and distance the weight is offset, amongst other considerations. Biomechanical testing is imperative to begin to answer these questions, but the one certainty is that neural spine bifurcation appears to be far more complex than previously suggested.

CONCLUSIONS

Bifurcation of the neural spines is theorized as one possible biomechanical adaptation within tetrapods for sustaining a large, mobile weight adjacent to the girdles. Coinciding in tandem with the spine bifurcation is an enlarged and highly specialized nuchal ligament. Modified for its elastic efficiency, the nuchal ligament is the most modified soft tissue structure associated with vertebral spine bifurcation. While vertebral bifurcation was largely treated as if present primarily in sauropod dinosaurs and ratites,

new recognition and documentation of this feature indicates that it is far more diverse and in fact present in basal tetrapods. This phylogenetic distribution indicates that while being one form of weight sustainment, neural spine bifurcation has had a much longer and complex evolutionary history than previously recognized.

ACKNOWLEDGEMENTS

The author thanks J. Carroll and D. Gilbert for donating the Ankole-Watusi cows used for this study. J. Wolf donated the vertebral column from the late "Lurch." V. Base and the World Watusi Association provided useful information, support, and assistance. T. and S. Swart and the entire crew at Budget Game Processing allowed the use of their facilities to perform the dissections. J. Horner provided financial support throughout this project. Extreme thanks and gratitude to J. Ohrstrom for continuing support to the Museum of the Rockies paleontology graduate student fund. R. Crum of Rocky Mountain Beetle Works provided the preparation of the three cow skulls. D. Lauder of Lauder Histology Inc. made the Ankole-Watusi neural spine slides, and T. Goins of the Montana Veterinary Diagnostic Lab created the Ankole-Watusi nuchal ligament slides. A. Costopoulos and McGill University's Anthropology Department shared pictures and information of the Ankole-Watusi skeletons that they are currently excavating and preparing. Countless thanks and gratitude to the dissection team: K. Wescamp, B. Baziak, J. Heuck, D. Fowler, E. Fowler, J. Scannella, H. Woodward, M. Knell, A. Poust, and Z. Cooper. Thanks to S. Gibson for deciphering the Ankole-Watusi thin sections. Thanks to the Museum of the Rockies, Montana State University, and to J. Horner and D. Varricchio for assistance in acquiring and housing the Ankole-Watusi cows for this

study. D. Anduza provided the drawings of the Ankole-Watusi nuchal ligament. J. Horner, K. Padian, M. Starck, J. Scannella, E. Fowler, K. Nordén, L. Cerretti, and two anonymous reviewers generously revised earlier drafts of this manuscript.

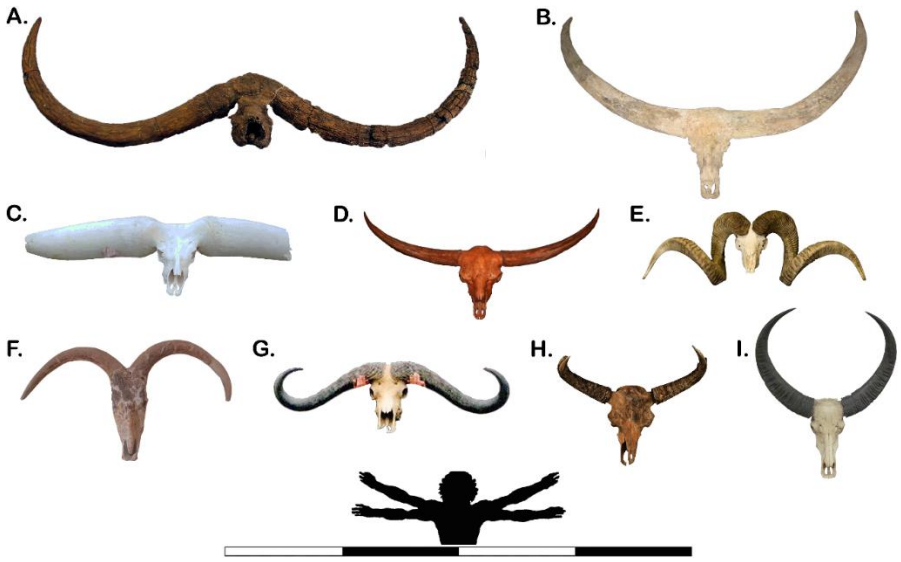

Figure 1. Cranial comparison of large extinct and extant bovids with breadth of horns. A. *Syncerus antiquus*, 3.6 m, image by K. Garrett. B. *Bubalus paleokerabau*, 2.43 m, image by T. Lindgren. C. Ankole-Watusi "Lurch," 2.43 m, image by T. Dobbs. D. *Bison latifrons*, 2 m. E. *Ovis ammon polii*, 1.9m. F. *Pelorovis oldowayensis*, 1.83 m. G. World record *Syncerus caffer*, 1.6 m. H. *Bison priscus*, 1 m, from Zazula et al. (2009). I. *Bubalus bubalis*, 1 m. All skulls to scale. Scale bar = 4 m; Leonardo da Vinci's "*Vitruvian Man*" illustrates size comparison to a 1.83 m tall human.

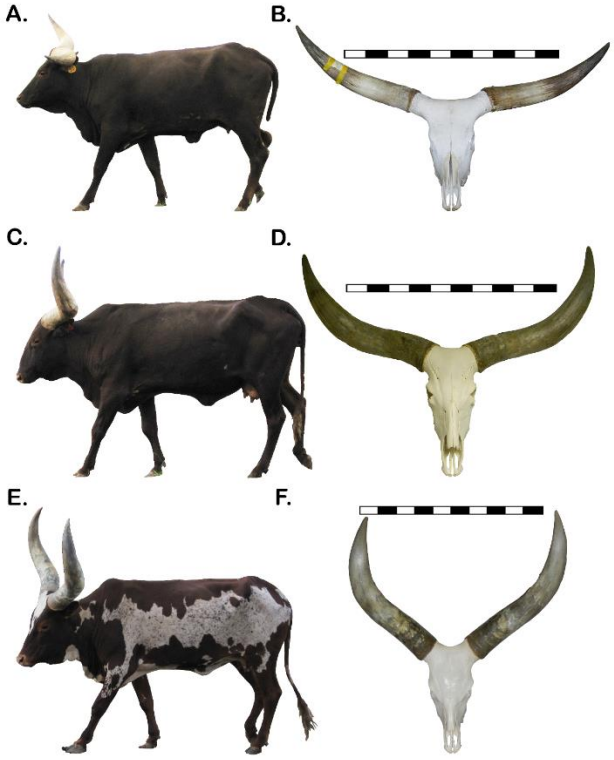

Figure 2. Ankole-Watusi cows used for this study. A. Four-year-old (MOR OST 1613). C. Sixteen-year-old (MOR OST 1614). E. Nineteen-year-old (MOR OST 1616). B. Four-year-old skull. D. Sixteen-year-old skull. F. Nineteen-year-old skull. Not to scale. Scale bar for B, D, and F = 1 m.

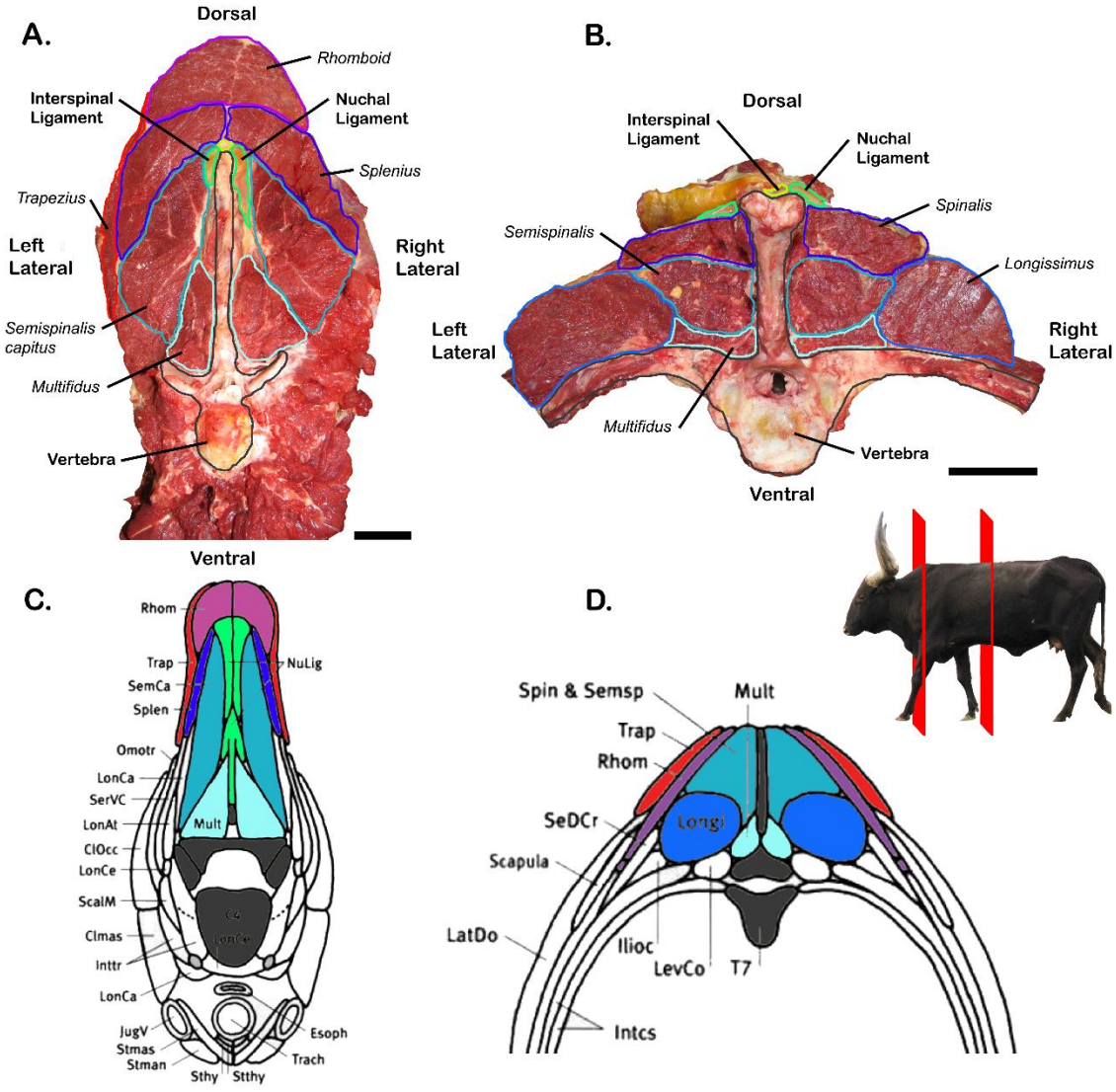

Fig. 3. Musculature comparison of Ankole-Watusi cow versus typical domesticated cattle. Anterior view of cervico-thoracic "hump" of Ankole-Watusi (A) and domestic cattle (C). Posterior view of mid-thoracic vertebra of Ankole-Watusi cow (B) and domestic cattle (D). C and D modified from Goldfinger (1981). Red planes on the sixteen-year-old Ankole-Watusi cow indicates approximate location of transverse sections. Images not to scale. Scale bar for A and B = 5 cm.

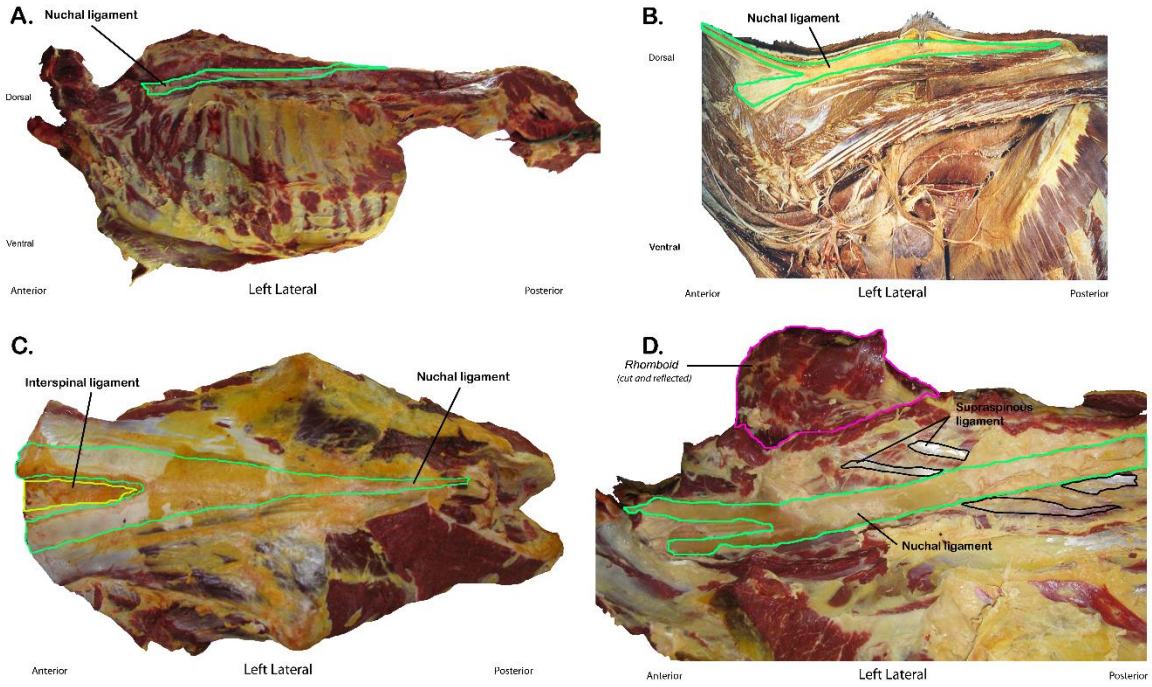

Figure 4. Musculature of the four-year-old Ankole-Watusi cow. A. Torso with skull, limbs, and tail removed in left lateral view, nuchal ligament in corresponding green. B. Nuchal ligament of a typical domestic cow in the same orientation to illustrate the different nuchal paths (modified from Ashdown et al., 2010). C. Dorsal view of the pelvic region of A illustrating the bifurcation of the nuchal ligament. D. anterior portion of A in closer view. In A, the *m. rhomboid* has been entirely removed along with the anteriorly bifurcating portion of the nuchal ligament, and a majority of the surficial musculature. Not to scale.

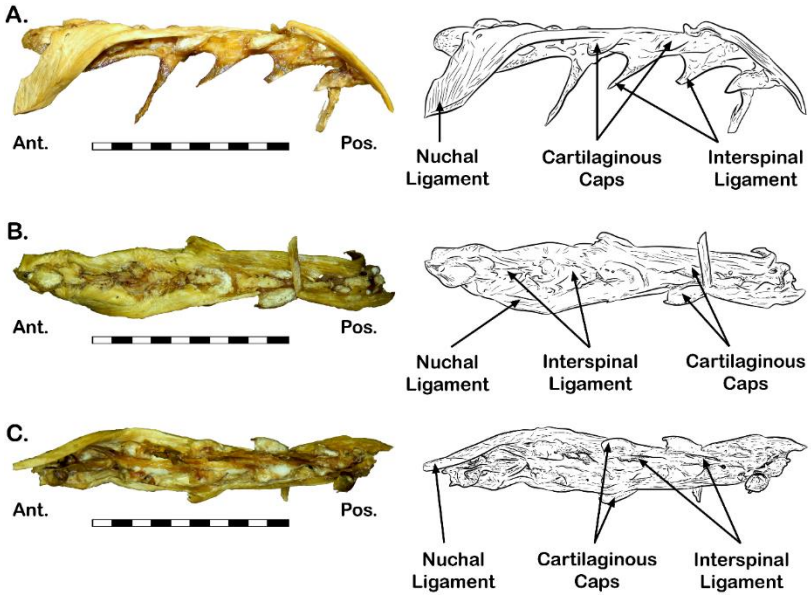

Figure 5. Preserved portion of nuchal ligament from the four-year-old Ankole-Watusi cow (MOR OST1613). A. Nuchal ligament in left lateral view, drawing to highlight the nuchal ligament, fibrocartilage sesamoids, and interspinal ligament. B. Nuchal ligament in dorsal view. C. Nuchal ligament in ventral view. Ant. (anterior); Pos. (posterior). Drawings by D. Anduza. All images to scale. Scale bar = 10 cm.

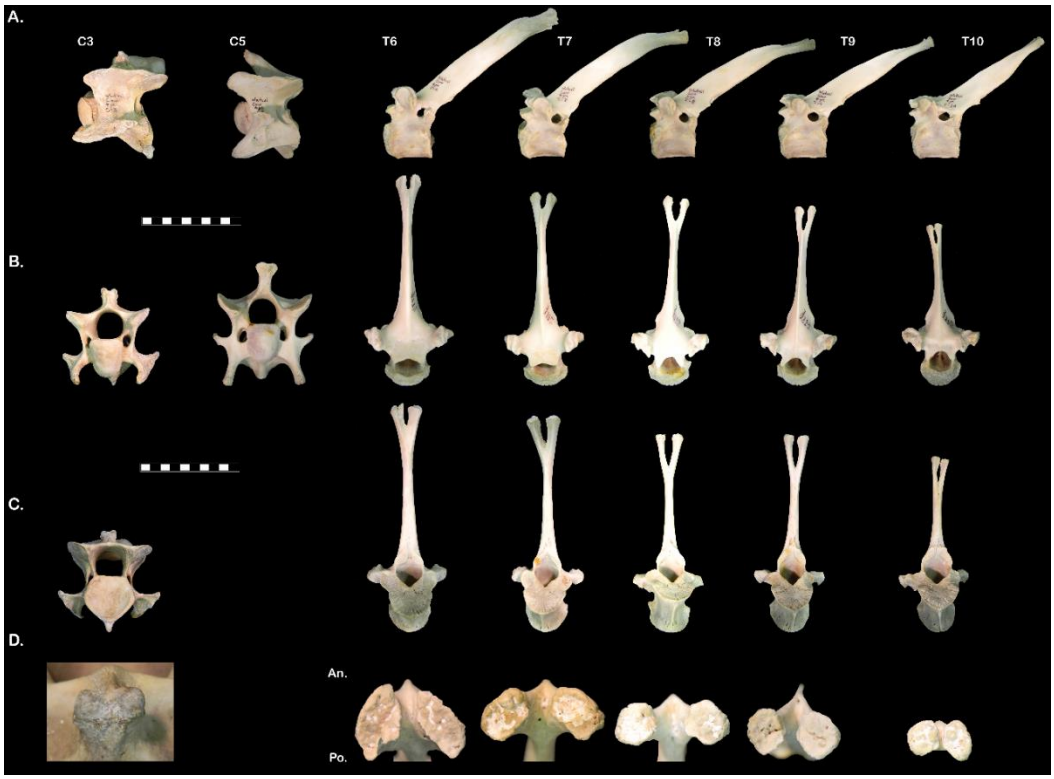

Figure 6. Vertebrae exhibiting neural spine bifurcation within the four-year-old Ankole Watusi cow (MOR OST1613). A contains C-3 and 5, and T-6 through 10, in left lateral view. B. Vertebrae in anterior view. C. Vertebrae in posterior view. D. Dorsal viewof neural spines; all in same orientation, Anterior (An.) and Posterior (Po.) marked on T-6 in row D. Rows A-C all to scale, scale bar = 10 cm, Row D not to scale.

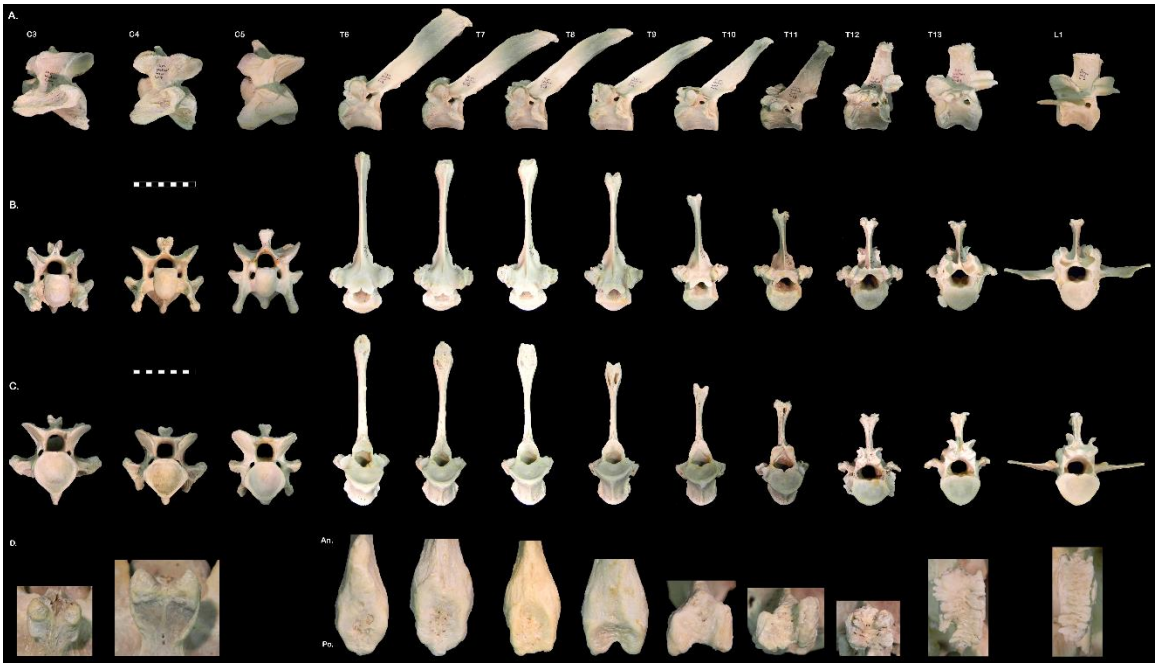

Figure 7. Vertebrae exhibiting neural spine bifurcation within the sixteen-year-old Ankole-Watusi cow (MOR OST1614). A contains C-3 through 5, T-6 through 13, and L-1 in left lateral view. B. Vertebrae in anterior view. C. Vertebrae in posterior view. D. Dorsal view of neural spines; all in same orientation, Anterior (An.) and Posterior (Po.) marked on T-6 in row D. Rows A–C all to scale, scale bar = 10 cm, Row D not to scale.

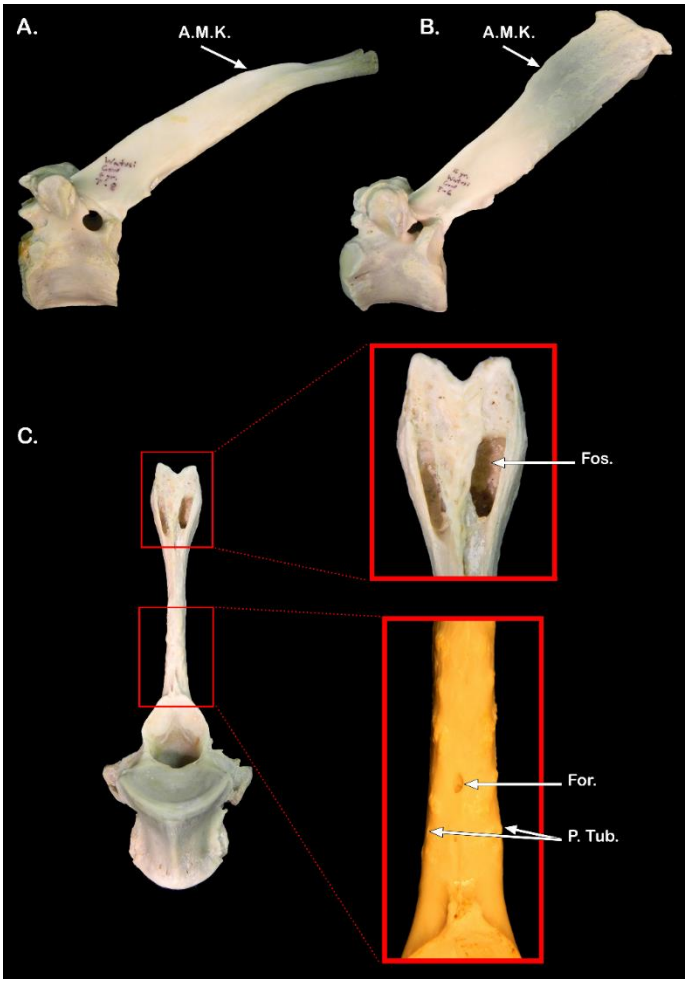

Figure 8. Vertebral features within the Ankole-Watusi. A. T-8 from the four-year-old cow (MOR OST1613), left lateral view. B. T-6 from the 16-year-old cow (MOR OST1614), left lateral view; A.M.K. indicates the anterior midline keel. C. T-6 from the 16-year-old cow (MOR OST1614), posterior view. Red inset boxes highlight neural spine apex and distal portion of neural spine; Fos. = fossae, For. = foramina, and P. Tub. = paired tubercles. All features indicated with a white arrow. Not to scale.

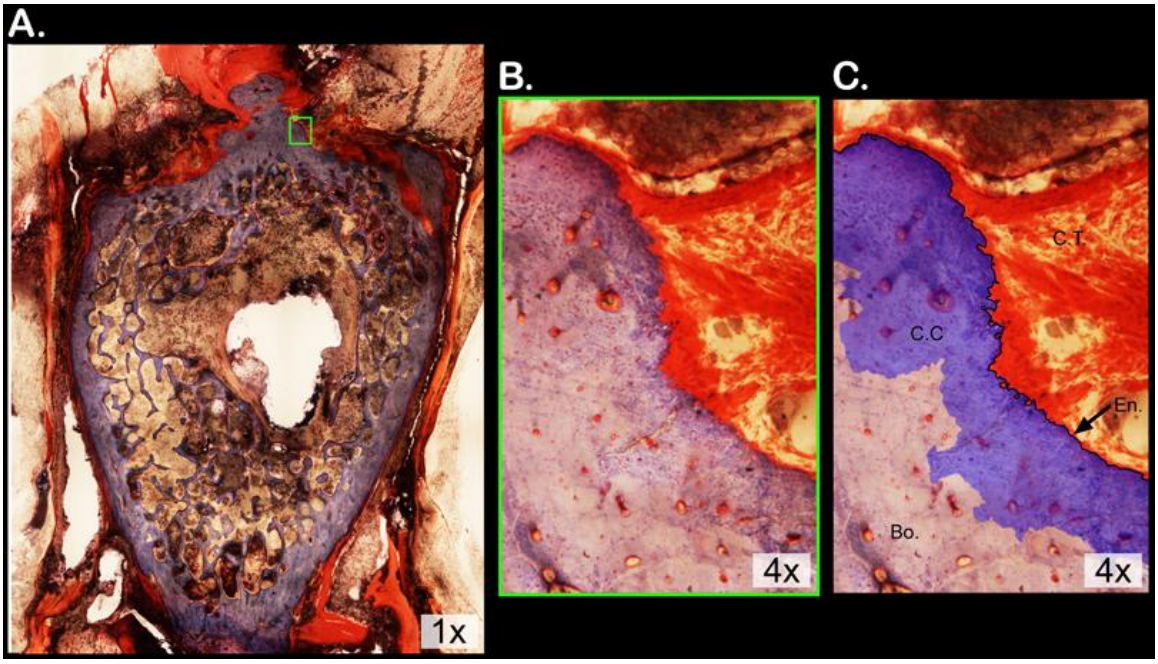

Figure 9. A. Histological thin section of nineteen-year-old Ankole-Watusi (MOR OST1616) neural spine apex in anterior view; scale bar = 1 cm. B. 4X magnification of selected area in green box from A displaying the zone of enthesis. C. Same image as B, but with key. The zone of calcified cartilage (C.C.) highlighted in darker blue, bone (Bo.), connective tissue (C.T.), and point of enthesis (En.) highlighted with a black line. Stain is Aniline Blue.

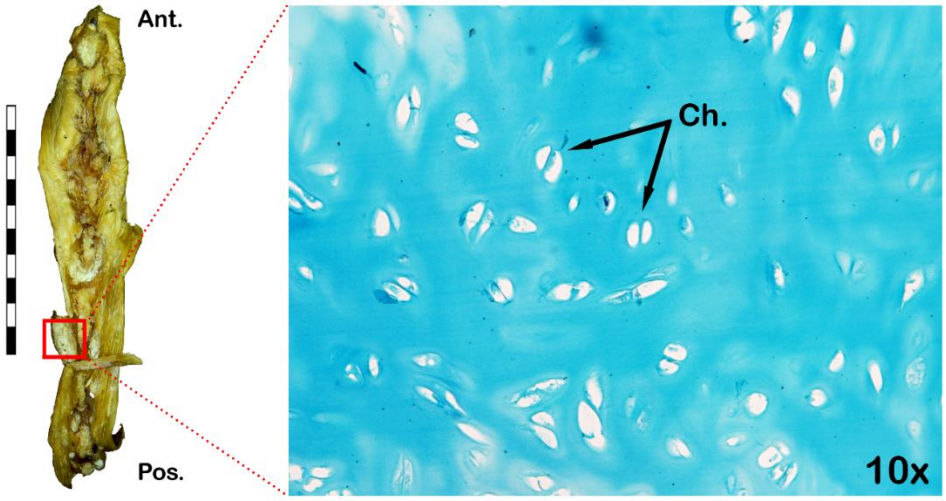

Figure 10. Histological thin section of the desiccated nuchal ligament from the four-year-old Ankole-Watusi cow (MOR OST1613). Arrows point to the abundant chondrocytes (Ch.) dispersed throughout the fibrocartilage matrix. Stain is Alcian Blue.

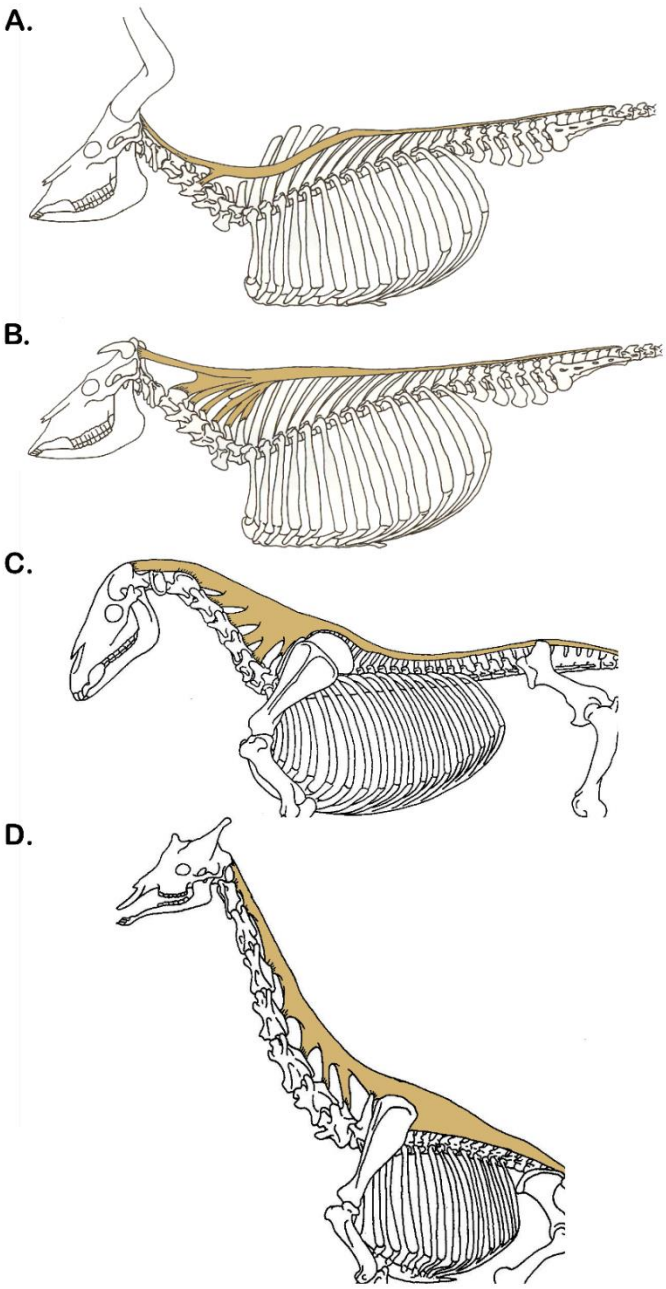

Figure 11. Lateral comparison of the nuchal ligament (in yellow) in an Ankole-Watusi (A), typical domesticated cow (B), domesticated horse (C), and giraffe (D). Not to scale. Drawings by DCW.

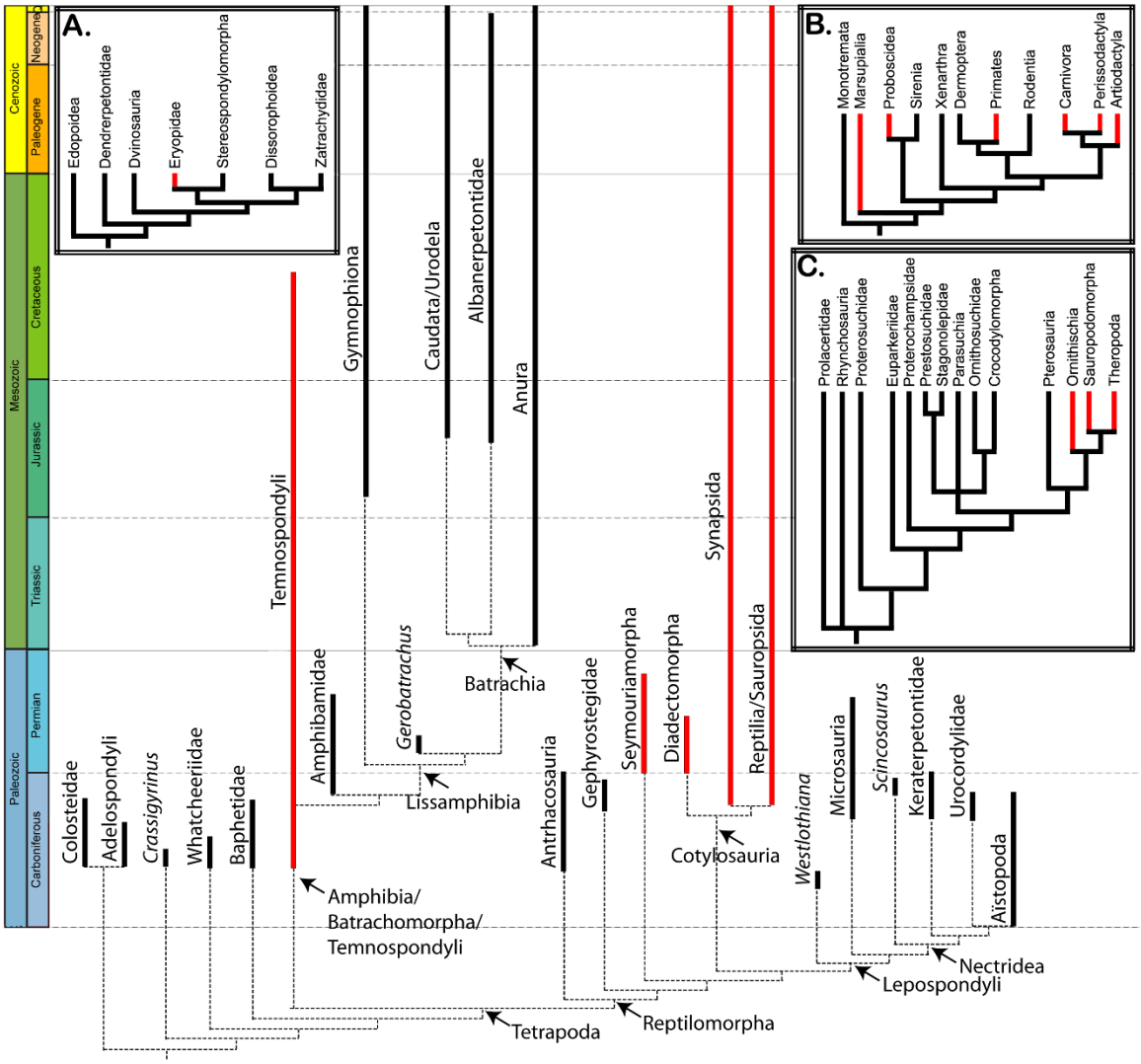

Figure 12. Time calibrated phylogenetic distribution of neural spine bifurcation within Tetrapoda. Lineages possessing spine bifurcation highlighted in red. A. Temnospondyli phylogeny with families exhibiting spine bifurcation in red. B. Mammalia phylogeny with orders exhibiting spine bifurcation in red. C. Sauropsida phylogeny with orders exhibiting spine bifurcation in red. A, B, and C not time calibrated. Courtesy of T. Holtz and modified from http://www.geol.umd.edu/~tholtz/G331/lectures/331vertsII.html.

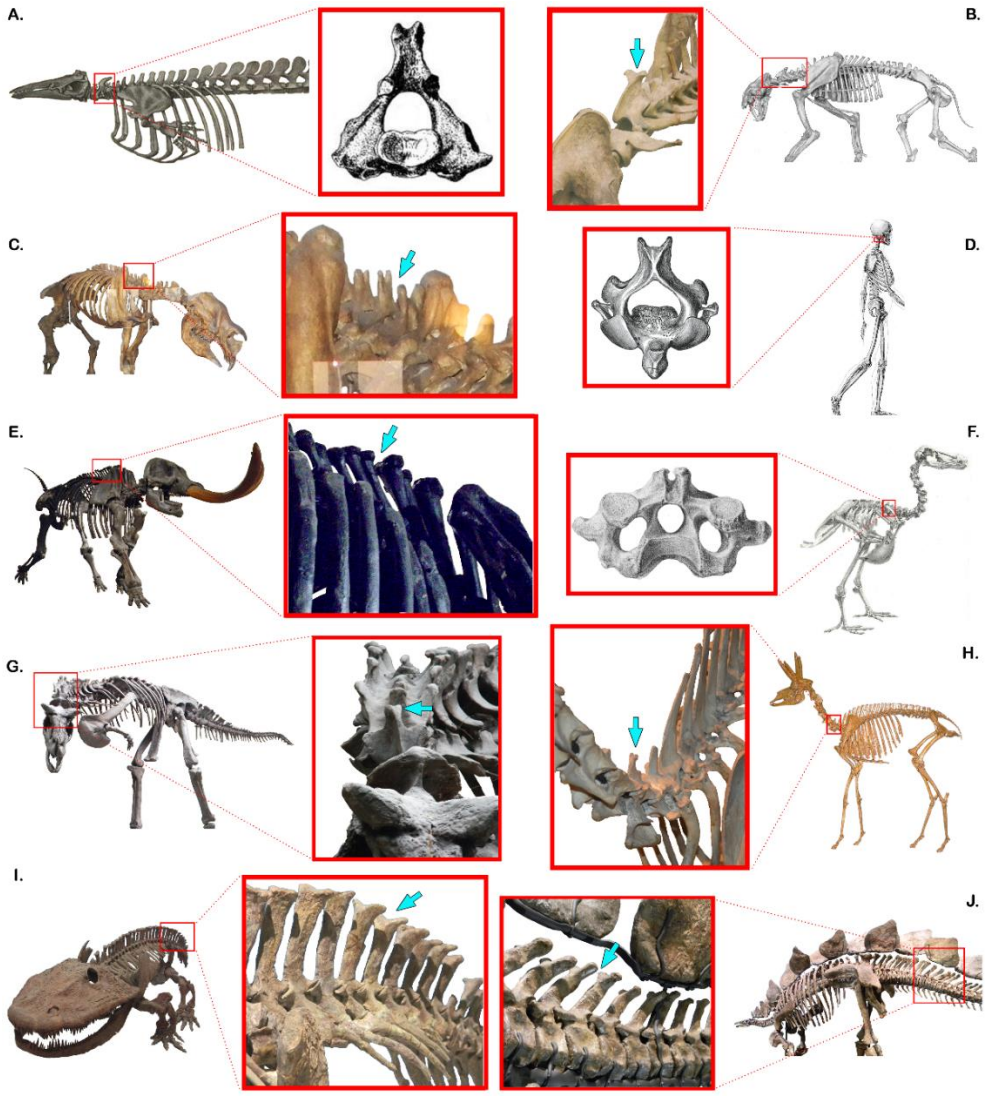

Figure 13. Neural spine bifurcation in extinct and extant tetrapods. A. *Delphinapterus leucas*, red inset box highlighting cervical bifurcation in second cervical vertebra (Cope, 1890; Post, 2012). B. *Smilodon populator*, red inset box highlighting cervical bifurcation in oblique anterior view. C. *Diprotodon optatum*, red inset box highlighting posterior cervical and anterior thoracic bifurcation in anterior oblique view. D. *Homo sapien*, red inset box highlighting cervical bifurcation in the second cervical vertebra (from Grey, 1858) in anterior view. E. *Mammut americanum*, red inset box highlighting anterior thoracic bifurcation in oblique posterior ventral view. F. *Raphus cucullatus*, red inset box highlighting 13th cervical vertebra (from Newton and Newton, 1869). G. *Carnotaurus sastrei*, red inset box highlighting cervical bifurcation in anterior view. H. *Stockoceros conklingi*, red inset box highlighting cervical bifurcation in anterior oblique view. I. *Eryops*, red inset box highlighting caudal bifurcation in anterior oblique view. J. *Stegosaurus ungulatus* (CM 11341), red inset box highlighting caudal bifurcation in oblique anterior view. Blue arrows mark bifurcation. Not to scale.

Table 1. Depth and width of Ankole-Watusi neural spine bifurcation. Units in cm.

	Depth (of bifurcation)	Width (of apex)
4-yr. old		
C3	0.3	1.2
T6	1.6	2.4
T7	2.8	2.6
T8	3	2.5
T9	2.5	1.9
T10	1.9	1.4
16-yr. old		
C3	0.4	1.9
C4	0.2	2.1
T7	0.2	2.1
T8	0.4	2.1
T9	0.5	2
T10	0.4	2.2
T11	0.5	2.6
T12	0.3	2.4
T13	0.3	2.2
L1	0.2	1.7

REFERENCES CITED

Ashdown RR, Done SH, Barnett SW. 2010. Color Atlas of Veterinary Anatomy, Vol. 1, Amsterdam: The Ruminants (Mosby). pp 272.

Beadnell HJL. 1902. A Preliminary Note on *Arsinoitherium zitteli*, Beadn., from the Upper Eocene Strata of Egypt. National Printing Department.

Benjamin M, Kumai T, Milz S, Boszczyk BM, Boszczyk AA, Ralphs JR. 2002. The skeletal attachment of tendons—Tendon 'entheses.' Comp Biochem Physiol A Mol Integr Physiol 133: 931-945.

Bonaparte JF. 1985. A horned Cretaceous carnosaur from Patagonia. Natl Geogr Res 1: 149-151.

Budras K-D, Habel RE. 2003. Bovine Anatomy: An Illustrated Text. Hanover, Germany: Schlütersche. pp 138.

Coombs WPJ. 1975. Sauropod habits and habitats. Palaeogeogr Palaeoclimatol Palaeoecol 17:1-33.

Cope ED. 1890. The cetacea. Am Nat 24: 599-616.

Cormick W. 2010. Enthesopathy—a personal perspective on its manifestations, implications and treatment. Aust J Ultrasound Med 13: 19–23.

Currey JD. 1984. The Mechanical Adaptations of Bones. Princeton University Press. Princeton: New Jersey. pp 294.

Desilva U, Fitch J. 1995. Ankole-Watusi. From Breeds of Livestock Project, Oklahoma State University Department of Animals Sciences. Available at: http://www.ansi.okstate.edu/breeds/cattle/. Last accessed on 2013.

Dimery NJ, Alexander RM, Deyst KA. 1985. Mechanics of the ligamentum nuchae of some artiodactyls. J Zool 206: 341-351.

Dürst JU. 1899. Die Rinder Von Babylonien, Assyrien Undü Agypten Und Ihr Zusammanhang Mit Den Rindern Der Alten Welt; Georg Reimer: Berlin, Germany.

Dzemski G, Christian A. 2007. Flexibility along the neck of the ostrich (Struthio camelus) and consequences for the reconstruction of dinosaurs with extreme neck length. J Morphol 268:701-714.

Folkard C. 2003. Guinness Book of World Records. New York: Guinness World Records Ltd. pp 288.

Frey E. 1988. Anatomie des Küorperstammes von *Alligator mississippiensis* Daudin. Stuttgarter Beitrüage zur Naturkunde 24: 1-106.

Goldfinger E. 1981. Animal Anatomy for Artists. Oxford University Press, Oxford: United Kingdom. pp 256.

Grey H. 1858. Anatomy: Descriptive and Surgical. London: Parker & Son. pp 983.

Grigson C. 2000. *Bos africanus* (Brehm)? Notes on the archaeozoology of the native cattle of Africa. In: Blench RM, MacDonald KC, editors. The origins and development of African livestock. pp 38-60.

Grubb P. 2005. "*Bos taurus primigenius*". In: Wilson DE, Reeder DM, editors. Mammal Species of the World, 3rd ed. Johns Hopkins University Press. Baltimore: Maryland. pp 637-722.

Hall BK. 2005. Bones and Cartilage: Developmental and Evolutionary Skeletal Biology. Academic Press. San Diego: California. pp 792.

Hatcher JB. 1901. *Diplodocus* (Marsh): Its osteology,taxonomy, and probable habits, with a restoration of the skeleton. Mem Carnegie Mus 1: 1-63.

Ikejiri T, Tidwell V, Trexler DL. 2005. New adult specimens of *Camarasaurus lentus* highlight ontogenetic variation within the species. Thunder-Lizards: The Sauropodomorph Dinosaurs. In: Tidwell V, Carpenter K, editors. Bloomington, IN: Indiana University Press. Pp. 154-179.

Janensch W. 1929. Die Wirbelsaule der gattung *Dicraeosaurus* Palaeontographica (Supplement 7) 3: 39-133.

Keller C. 1905. Naturgeschichte Der Haustiere. Berlin, Germany: Paul Parey.

Linder JF, Longhurst P, Johnson NW. 1981. A paraffin-celloidin embedding method for studying soft-hard tissue interfaces. Arch Oral Biol 26: 753-755.

Mateus O, Maidment SC, Christiansen NA. 2009. A new longnecked ‘sauropod-mimic’ stegosaur and the evolution of the plated dinosaurs. Proc Royal Soc B Biol Sci 276: 1815-1821.

Mescher AL. 2010. Junqueira’s Basic Histology: Text & Atlas. Mcgraw-hill medical, New York: New York. pp. 480.

Novas FE, Pol D, Canale JI, Porfiri JD, Calvo JO. 2009. A bizarre Cretaceous theropod dinosaur from Patagonia and the evolution of Gondwanan dromaeosaurids. Proc Royal Soc London B Biol Sci 276: 1101-1007.

Organ CL, Adams J. 2005. The histology of ossified tendon in dinosaurs. J Vertebrate Paleontol 25: 602-613.

Osborn HF. 1898. Additional characters of the great herbivorous dinosaur *Camarasaurus*. Bull Am Mus Nat Hist 10: 219-233.

Osborn HF, Mook CC. 1921. *Camarasaurus*, *Amphicoelias*, and other sauropods of Cope. Mem Am Mus Nat Hist 3: 247-387.

Padian K, Lamm ET. 2013. Bone Histology of Fossil Tetrapods: Advancing Methods, Analysis, and Interpretation. University of California Press, Oakland: California.

Post L. 2012. The Whale Building Book: A Step-By-Step Guide To Preparing And Assembling Medium Sized Whale Skeletons. print on demand. pp. 1-69.

Rauhut O. 2005. Osteology and relationships of a new theropod dinosaur from the Middle Jurassic of Patagonia. Paleontology 48: 87-110.

Romer AS. 1956. Osteology of the Reptiles. University of Chicago Press, Chicago: Illinois. pp. 1-772.

Ruffer MA. 1921. Studies in the Palaeopathology of Egypt. Chicago, IL: University of Illinois Press. Pp. 1-372.

Schwarz D, Frey E, Meyer CA. 2007. Pneumaticity and soft tissue reconstructions in the neck of diplodocid and dicraeosaurid sauropods. Acta Palaeontol Pol 52: 167-188.

Stock C. 1930. Quarternary antelope remains from a second cave deposit in the Organ Mountains, New Mexico. Los Angel Mus Sci Ser Paleontol 2: 1-18.

Sumida SS. 1990. Vertebral morphology, alternation of neural spine height, and structure in Permo-Carboniferous tetrapods, and a reappraisal of primitive modes of terrestrial locomotion. University of California Press, Oakland: California.

Tambussi CP, de Mendoza R, Degrange FJ, Picasso MB. 2012. Flexibility along the neck of the Neogene terror bird *Andalgalornis steulleti* (Aves Phorusrhacidae). PLoS One 7(5): e37701.

Tsuihiji T. 2004. The ligament system in the neck of *Rhea americana* and its implication for the bifurcated neural spines of sauropod dinosaurs. J Vertebrate Paleontol 24: 165-172.

Vaughn PP. 1964. Vertebrates from the Organ Rock shale of the Cutler Group, Permian of Monument Valley and vicinity, Utah and Arizona. J. Paleont 38: 567-583.

Vickaryous MK, Olson WM. 2007. Sesamoids and ossicles in the appendicular skeleton. Fins and Limbs: Evolution, Development and Transformation. In: Hall BK, editor. Chicago, IL: University of Chicago Press. pp 323-341.

von Eggeling H. 1922. Die Gabelung der Halswirbeldornen undihre Ursache. Anat Anz 55: 33-94.

Wedel MJ, Taylor MP. 2013. Neural spine bifurcation in sauropod dinosaurs of the Morrison Formation: Ontogenetic and phylogenetic implications. Palarch's J Vertebrate Palaeontol 10: 1-34.

Wedel MJ, Cifelli RL, Sanders RK. 2000. Osteology, paleobiology, and relationships of the sauropod dinosaur *Sauroposeidon*. Acta Palaeontol Pol 45: 343-388.

Woodruff DC, Fowler DW. 2012. Ontogenetic influence on neural spine bifurcation in Diplodocoidea (Dinosauria: Sauropoda): A critical phylogenetic character. J Morphol 273: 754-764.

Zazula GD, MacKay G, Andrews TD, Shapiro B, Letts B, Brock F. 2009. A late Pleistocene steppe bison (*Bison priscus*) partial carcass from Tsiigehtchic, Northwest Territories, Canada. Quat Sci Rev 28: 2734-2742.

Manuscript Information Page

D. Cary Woodruff, Denver W. Fowler, John R. Horner
Status of Manuscript:
_ X_ Prepared for submission to a peer-reviewed journal
____ Officially submitted to a peer-review journal
____ Accepted by a peer-reviewed journal
_ __ _ Published in a peer-reviewed journal

A NEW MULTI-FACETED FRAMEWORK FOR DECIPHERING DIPLODOCID ONTOGENY

Contribution of Authors and Co-Authors

Manuscript in Chapter 2

Author: D. Cary Woodruff

Contributions: Conceived and implemented the study design. Collected and analyzed data. Prepared histological slides. Wrote the manuscript.

Co-Author: Denver W. Fowler

Contributions: Helped conceive aspects of the study design. Provided feedback on drafts of the manuscript.

Co-Author: Dr. John R. Horner

Contributions: Helped conceive the study design. Provided histological and ontogenetic expertise and funding. Provided feedback on drafts of the manuscript.

A NEW MULTI-FACETED FRAMEWORK FOR DECIPHERING DIPLODOCID ONTOGENY

D. Cary Woodruff[1,2]*, Denver W. Fowler[1,2], John R. Horner[1,2]

[1,2] *Museum of the Rockies, Department of Earth Sciences, Montana State University, Bozeman, MT, USA,*

**sauropod4@gmail.com*

ABSTRACT

Determining maturity in sauropod dinosaurs is difficult due to the fact that Lines of Arrested Growth (LAGs) are destroyed or obscured due to rapid secondary remodeling. Although a complimentary system has been devised utilizing relative amounts of remodeling (Histologic Ontogenetic Stage [HOS]; youngest HOS = 1, oldest =13) most assessments of sauropod maturity are based on osteological features such as neurocentral fusion. To better assess indications of maturational status, and to test recent assertions about ontogenetic change of gross skeletal features, we examined cranial and postcranial material from over twenty non-adult sized diplodocid individuals (up to two-thirds the body length of *Diplodocus carnegii* [Carnegie Museum specimen CM 84] and *Apatosaurus louisae* [CM 3018]) from the late Jurassic Morrison Formation (latest Oxfordian – earliest Tithonian). Along with macroscopic examination of cranial, vertebral, and limb elements, in select specimens we also examined pneumatic structures via computed axial tomography and histology of thoracic ribs, neural spines, and limb bones. We found consistent combinations of morphologic features which, combined with histology, can be used to ascertain maturity. The fifteen small diplodocids (approximately

one-third body length; maximum femur length 120 cm) from the Mother's Day Quarry (MDQ) display non- to weakly bifurcated cervical and dorsal neural spines, acamerate to camerate centra, and two to six preserved LAGs in thoracic ribs. Individuals larger than the MDQ specimens (approximately two-thirds body length; femur length ~125 cm) have more developed internal pneumatic structures, greater neural spine bifurcation, preserve up to eight LAGs, and are HOS 9. This contrasts with the larger and presumably skeletally mature sauropods (CM 84 and CM 3018) that have complex pneumatic structures such as pervasive camerae in the centrum and neural arch, exaggerated neural spine bifurcation that now includes the anterior caudals, and have reached HOS 12 or 13. Further, all of the small skulls examined (Academy of Natural Sciences [ANS] 21122, Sauriermuseum Aathal [SMA] 0004, SMA 0011, and Museum of the Rockies [MOR] 700, 592, 7029) possess a postparietal foramen, which has been suggested to be an apomorphy of Dicraeosauridae, but which is absent in large skulls (such as CM 84) suggesting that it may be an ontogenetic character seen only in young individuals. These findings suggest that significant morphological change occurred during the ontogeny of diplodocid sauropods, and that erecting new taxa on the basis of small-bodied holotypes should be approached with caution.

INTRODUCTION

Ontogenetic studies in dinosaurs largely rely on morphologic comparisons of cranial features (i.e. horns, frills, and crests; Dodson, 1975; Hopson, 1975; Sampson et al., 1997; Carr, 1999; Evans et al., 2005; Horner and Goodwin, 2006; 2009; Scannella and Horner, 2010; Campione and Evans, 2011). As sauropods do not possess extravagant

cranial displays (that are so beneficial in recognizing ontogenetic trajectories), the quantity of ontogeny based works on Sauropoda is spare compared to other dinosaurian orders. Since sauropods lack the apparent basic necessity for ontogenetic studies, the work done on them has to depend largely on histology. These histologic studies examine the microstructural morphology of the bone and the degrees of bone remodeling to determine relative maturity of a range of individuals (such as the Age Class assignments of Curry [1999] and the Histologic Ontogenetic Stage [HOS] of Klein and Sander [2008]).

Recently several sauropod studies have reported morphologic attributes that can be used to denote maturity. Whitlock et al. (2009) documented the cranial changes between immature and mature specimens of *Diplodocus*, which include: proportionally larger orbits, rounded and narrower pre-maxilla, and a more posteriorly situated tooth row. Wedel (2003; 2005; 2009) has demonstrated that the complexity of pneumatic architecture has not only increased through sauropodomorph phylogeny, but appears to likewise increase through ontogeny. While Woodruff and Fowler (2012) showed that in small – presumably immature - diplodocids, vertebral neural spines were rounded to weakly bifurcated, while in large – presumably adult- diplodocids, the neural spines were fully bifurcated. Thus Woodruff and Fowler (2012) suggested that neural spines bifurcated through ontogeny, and that the degree of bifurcation could be used to infer maturity.

While some of these morphologic features have been incorporated into our understanding of sauropod ontogeny, the findings of Woodruff and Fowler (2012) have

not been universally accepted. In regards to Woodruff and Fowler (2012) there are two contention points: 1) the unknown precise serial placement for isolated vertebrae, and 2) the proper identification of maturational states to corroborate said morphological interpretations (Hedrick et al., 2012; Wedel and Taylor, 2013). As Woodruff and Fowler (2012) was a preliminary report, the maturational status of specimens were assessed solely on morphology (similar to the Morphologic Ontogenetic Stage [MOS] of Carballido and Sander [2013]). While many of the opposing issues are legitimate points, it has been suggested that histologic analysis may not be necessary due to specific features attributable to maturity (such as vertebral arch fusion; Wedel and Taylor, 2013). We would challenge this statement and instead argue that histologic analysis is the only repeatedly proven methodology to determine a specimen's maturational state. This current analysis set out to determine if the inferred maturational statuses of Woodruff and Fowler (2012) could be substantiated via a histologic examination. In addition we also want to see if there are any other morphologic or histologic features that could likewise be used to demonstrate maturity. In order to execute these questions, a large scale analysis was conducted on the diplodocids *Apatosaurus* and *Diplodocus* (Table 1), which included overall vertebral morphology (cervical, dorsal, and anterior caudal vertebrae), vertebral pneumatic morphology, histologic ontogenetic stage (HOS; Klein and Sander, 2008) assessment of femora, age determinate histology of thoracic ribs, and neural spine histology (of cervical and dorsal vertebrae).

Our findings indicate that diplodocids underwent radical ontogenetic trajectories comparable to other dinosaur groups. In addition to validating the proposed maturity

inferences of Woodruff and Fowler (2012), this analysis also establishes other suites of characters that in combination can be used as a guide to identify maturational states of other diplodocid specimens. Furthermore, the findings of this study raise questions to the validity of several small bodied Diplodocoidea holotypes that display a combination of small stature in tandem with basal and derived characters.

INSTITUTIONAL ABBREVIATIONS

Academy of Natural Sciences, ANS; American Museum of Natural History, AMNH; Carnegie Museum of Natural History, CM; Brigham Young University, BYU; Cincinnati Museum Center, CMC; Dinosaur National Monument, DNM; Houston Museum of Natural Science, HMNS; Judith River Foundation, JFR; Museum of the Rockies, MOR; Museum of Western Colorado, MWC; National Science Museum, Tokyo, NSMT; Sam Nobel Oklahoma Museum of Natural History, OMNH; Sauriermuseum Aathal, SMA; Science Museum of Minnesota, SMM; Texas Memorial Museum, TMM; University of Kansas Natural History Museum, KUVP; Yale Peabody Museum, YPM.

METHODS AND MATERIALS

This analysis uses Size (S) 1, S2, S3, and S4 to refer only to the body lengths of the specimens examined. S1 denotes individuals ≤ 2 meters (m) in body length, S2 2 - 10 m, S3 10 - 20 m, and > 20 m S4. This categorization does not account for life history events (such as sexual maturity, percentage of body size, or histologic morphology), and only designates relative sizes.

Specimens examined macroscopically were photographed from multiple angles (if possible) and all measurements were taken with digital calipers, cloth, or retracting

measuring tapes. For histological sampling, sites were chosen as follows (Figure 1): in regards to thoracic ribs, sections were removed just distal to the capitulum and tuberculum (following the methods of Waskow and Sander, 2014). From S2 specimens entire transverse sections of the thoracic ribs were taken, while in S3 and S4, a medial section was removed distal to the capitulum and tuberculum. Finally for limb elements (femora), core sections were removed from the anterior face of the middle of the diaphysis. A longitudinal orientation line was drawn on the periosteal surface, and thin sections were taken perpendicular to this line (Stein and Sander, 2009). If a core broke while boring, the fragments were pieced back together as best as possible. No bone was cut in its entirety to remove sample material. The bone that is lost due to the cutting blade (called kerf loss) results in adjoining flush edges. During restoration work, these flush edges can result in the element having a different measurement (usually shorter). For samples in this analysis, previously occurring cracks and fractures were exploited if possible. A section of bone containing the desired sample location that had been glued together could be removed (with applied heat or a dissolvent), from which the section could be molded and casted. From here the casted piece could be reinserted, and the element fully restored.

The coring bits pioneered by Stein and Sander (2009) allow for a cylindrical sample of bone to be removed, and this can be performed in a variety of locations (such as a collection room, a lab, and even on a mounted specimen). These bits are cylindrical tools consisting of a flat end with sintered or galvanized diamond grit. We personally found that these flat end bits created a significant degree of friction and often caused

flaking or chipping of the periosteal surface. Instead we had greater success with a serrated core bit. In like manner when sawing across wood grain, sheet woods, or delicate materials such as plexiglass, the presence of smaller and finer blade teeth in tandem produce a smoother cut. In addition to the serrated tip, we found a bit that separated into two sections (known as a two-part bit) to be invaluable. With a traditional bit, the core can become lodged and extremely difficult to remove, and attempted removal can damage or destroy the bone core. However, using a 35 mm two-part bit (Bosch™) allows for a coin (under 35 mm in circumference) to be placed on the bone surface without interfering with the cutting surface. If the core becomes lodged in the bit, the bit can simply be separated and a larger diameter bolt (such as a carriage bolt) can be inserted into the distal half and used to indirectly push on the bone core via the coin (opposed to direct pressure on the bone surface which could cause damage; Figure 2).

In addition to the information pertaining to the core bit itself, we found other useful techniques to aid in the coring process. In the case of a delicate periosteal surface, a thick layer of fossil preservative (such as Vinac) can be applied to the selected surface. Once dry, a layer of five minute epoxy can be placed on top of the thick preservative layer, which prevents external flaking, and subsequently cored through. Afterwards acetone can be used to clean the area surrounding the bore hole, and the surface of the core if desired. In regards to lubricant, Stein and Sander (2009) suggest making a clay reservoir around the core to contain the lubricant (in most cases water). This works and keeps the mess to a minimum, but using a squirt bottle to apply a soap and water solution to the bit provides the same effect and does not over saturate the bone. The water cools

the bit, while the soap provides extra lubrication. Remember to apply frequent lubrication, and always avoid dry bone dust or overheating of the bit (which will turn the metal red to orange).

In the case of a delicate cortex, a stepwise progression is best. In this case it is best to core a short distance into the bone (a few mm), extract the bit, and inject some form of penetrating glue into the scored area. Heating the bone with a blow dryer (we suggest a commercial hair dryer) prior to the introduction of glue will aid the bone in absorbing the glue. Allowing for ample drying time (several hours) is imperative, otherwise the bit can become gummed up and will be more susceptible to catching. If the bit and core do become gummed up or glued together, soaking the bit in a cup filled with an adhesive remover (such as *CYANO*-OFF!™) overnight will dissolve the glue and resolve all issues. Doing this stepwise progression will stabilize both the core and surrounding area.

All samples used for histological analysis were prepared following the methods and techniques demonstrated in Padian and Lamm (2013). Samples were first embedded in a Silmar two-part epoxy resin (SIL95BA-41), and once cured, two transverse slices (~2-4 mm thick) were cut from the embedded block using a Felker 41-AR tile saw. Slices were then pre-mount ground on the surface to be glued to the glass slide using 320 grit and then 600 grit silicon carbide paper. After this initial grinding, the sample is mounted to frosted glass slides using a Devcon two-part epoxy glue. Then using a Buehler Ecomet 4 Variable Speed Grinder-Polisher, the thin sections were polished using Buehler silicon carbide paper sequentially from a 60 grit to an 800 grit finish (60 grit initially to get 1

mm above the thickness of the glass slide, 120 grit to 750 μm thick, 180 grit to 500 μm thick, 320 grit to 300 μm thick – or when a color change occurs in the bone, 600 grit to ~150 μm thick – or when light easily passes through the bone, 800 grit to buff out remaining scratches). However final slide thickness varied, and depended entirely on desired optical clarity. Finished slides were photographed using a Nikon Optiphot-Pol polarizing microscope equipped with a Nikon DS-Fi1 digital camera, and compiled with NIS-Elements BR 3.0 software. Histological descriptions follow those established by Francillon-Vieillot et al. (1990), De Ricqles et al. (1991), Castanet et al. (1992), and Huttenlocker et al. (2013), while long bone descriptions follow the HOS of Klein and Sander (2008). (Histological terminology can be found in Table 2).

Skeletal Features

CAT scans of pneumatic architecture

The question of ontogenetic development of vertebral pneumatic architecture is strongly inferred (Wedel, 2003), but has yet been tested or fully documented. In this analysis we examined the overall morphology of the cervical and dorsal centra pneumatic structures for our ontogenetic series (Figure 5), and we examined the internal pneumatic structures of nine cervical and dorsal vertebrae using Computer Axial Tomography (CAT scan). In agreement with importance of serial position, only cervical and dorsal vertebrae from known or strongly approximated position were scanned. The scanned elements consist of two late anterior to early middle cervical vertebrae from two individuals (MOR 714 and MOR 790), two anterior dorsal vertebrae from two individuals (MOR 790 and MOR 592), and three posterior dorsal vertebrae from three individuals (MOR 790, MOR

592, and MOR 957). Each specimen was examined via frontal and transverse sections. Definitions and usage of pneumatic architecture follows those established by Wedel et al. (2000; Table 2).

Computer Axial Tomography scans (CAT scan) of cervical and dorsal vertebrae were performed by Advanced Medical Imaging at Bozeman Deaconess Hospital in Bozeman, MT, USA. The scan resolution varied based on the dimensions of the vertebra and ranged from every 2 mm up to 5 mm. Scan data were uploaded into the DICOM Viewer OsiriX for multi-plane study, with individual planes being analyzed using the image processing program ImageJ (Abramoff et al., 2004).

Vertebral Neural Spines

Other than the debated morphologic changes (Woodruff and Fowler, 2012), diplodocid neural spines have not been examined histologically in regards to ontogeny. To determine if neural spine microstructure changes, four neural spine apices (two posterior cervical vertebrae [MOR-790 un-numbered and MOR 592 8-24-90-91] and two anterior dorsal vertebrae [MOR 790 8-21-95-238 and MOR 592 8-22-90-15) were coronally sampled to demonstrate relative structural change (if any) between varying body sizes.

Thoracic Ribs

In lieu of the aforementioned difficulties involved with sauropod limb histology, Waskow and Sander (2014) recently demonstrated that thoracic ribs record cyclical growth marks. The identification and recognition of recordable growth histories in sauropods is paramount and finally allows for histological age determination (opposed to

maturational inference [HOS] and tabulated longevity calculations). In their thorough analysis throughout the entirety of a *Camarasaurus* thoracic rib cage, Waskow and Sander (2014) showed that sampling within the proximal third, but distal to the capitulum and tuberculum, of thoracic ribs one through three recorded the most intact and complete history of growth marks (LAGs).

In this analysis we sampled the thoracic ribs of four diplodocids from the data set (MOR 790 7-24-96-95, MOR 790 7-27-8-96, MOR 592, CM 94). The specimens were selected by maturity (smaller - presumably less mature, larger - presumably more mature) with known or associated limb elements. Waskow and Sander (2014) state that corresponding limbs (femora) are important in calculating the animal's mass, and that such age determining analyses require both elements for complete and comparative results. For isolated thoracic ribs, comparisons to well documented rib series were used to approximate serial position (*Camarasaurus* - Osborn and Mook, 1921; *Dicraeosaurus* – Janensch, 1929; *Apatosaurus* – Gilmore, 1936).

In terms of the age assessment of the diplodocids in this dataset, for the time being, we prefer to estimate individual age based on preserved LAG counts. From the preserved LAG record, both Griebeler et al. (2013) and Waskow and Sander (2014) use a retro-calculation method to formulate age estimates. For the retro-calculation, the minimum and maximum distance between LAGs must be measured. Lines are then drawn along the short and long axis, with the origin representing the hypothetical original center of the rib. From there the previously measured distances are marked until reaching the origin and thus attaining a hypothetical maximum age value. While this methodology

is convenient, straightforward, and simplistic, this retro-calculation method implies uniform growth. Many studies have shown that immature dinosaurs had much faster growth rates (Curry, 1999; Horner et al., 2000; Padian et al., 2001; Horner and Padian, 2004; Erickson et al. 2001; Erickson, 2005; Lee and Werning, 2008; Woodward and Lehman, 2009; Horner et al., 2010), so the distances between LAGs should be greater during early development. Thus we believe that the retro-calculation methods should represent maximum age estimates. However this retro-calculation method will be beneficial in the analysis of specimens with significantly more remodeling in which LAG counts are obscured, and thus maximum age estimations can be proposed.

Femora

In regards to long bone (particularity femora) histology, this analysis relied heavily on the highly informative sample set of Klein and Sander (2008). Consisting of eighty-five femoral sections (out of one hundred and eighty-five total), the Klein and Sander (2008) database was used as the primary piece of evidence for long bone histologic ontogenetic change (see Figure 3 of Klein and Sander, 2008). Two individuals from this study's dataset were sectioned and compared to the Klein and Sander (2008) samples to support previously inferred and hypothesized maturational states. Histological designations for femora in this analysis follow the numerical and alphabetical designations of Klein and Sander (2008). The histological ontogenetic stage (HOS) of Klein and Sander (2008) follows a 13 part maturational system – HOS 1 being the youngest animal, HOS 13 the oldest – which consists of a 7 part alphabetical hierarchy

denoting bone microstructure – bone Type A having no primary osteons, bone Type G being completely secondarily remodeled (Klein and Sander, 2008; Table 2).

Body mass estimations were calculated for fifty-four diplodocid femora (Table 3) following the allometry based body mass formula of Mazzetta et al. (2004). Additional mass estimation methods that incorporate multiple elements (such as humeral and femoral circumference; i.e. Campione and Evans, 2012) and histologic data (Sander and Tuckmantel, 2003; Lehman and Woodward, 2008; Griebeler et al., 2013) should produce more accurate estimates because these methods incorporate more variables regarding the individual life histories. The diplodocid dataset in this analysis lacks the required inclusive life history variables (i.e. corresponding femur and humerus [Campione and Evans, 2012], or histologic markers - LAGs or polish lines [Sander and Tuckmantel, 2003; Griebeler et al., 2013]). As such the most agreeable method that can be incorporated with this dataset is that of Mazzetta et al. (2004). Once mass values were calculated, 10% was deducted to account for pneumaticity (*sensu* Wedel, 2003). Yet it must be noted that since the degree of pneumatization at different body sizes is not known, we decided to treat each body length and body mass equally, and deduct a standard value of pneumatization.

RESULTS

Morphologic Data

Neural Spine Bifurcation

As stated previously, one of the two contention points to the Woodruff and Fowler (2012) findings is that within diplodocids, neural spine bifurcation does not

follow an ontogenetic trajectory (Wedel and Taylor, 2013). A significant portion of this opposing viewpoint rests in isolated elements where precise serial placement is at best an approximation (such as the collective material from the Mother's Day Quarry); and we completely agree and uphold that serial position is extremely important in regards to spine bifurcation.

Since Woodruff and Fowler's (2012) initial report, subsequent inquiry by this analysis has examined material representing a significant portion of known Morrison diplodocids collected to date (and this analysis is ongoing by DCW). As spine bifurcation is a more muted point to this paper, we shall restrict the majority of spine bifurcation discussion to the Supplementary Information. In addition to the numerous isolated elements, enough associated, formerly articulated, and articulated specimens irrevocably demonstrate and uphold the inescapable conclusion that neural spine bifurcation does indeed develop ontogenetically.

Postparietal Foramen

The cranial foramen known as the postparietal foramen, has been inferred as a synapomorphy of Dicraeosauridae (Salgado and Bonaparte, 1991; Harris, 2006a; Remes, 2009; Whitlock, 2011), a local autapomorphy for the Plateosauria *Massopondylus* and *Plateosaurus* (Knoll et al 2012), the basal Sauropoda *Spinophorosaurus* (Knoll et al., 2012), and the diplodocids *Tornieria* (Upchurch et al., 2004; Remes, 2009) and *Kaatedocus* (Tschopp and Mateus, 2012). Yet outside of *Kaatedocus*, *Tornieria*, and the taxonomically debated *Suuwassea* (Lovelace et al., 2007; Whitlock and Harris, 2010), no members of Diplodocidae or Morrison Formation equivalent sauropods are supposed to

possess this cranial feature (Harris, 2006a; Whitlock and Harris, 2010; Hedrick et al., 2012).

In 2010, Balanoff et al. reported an *Apatosaurus* sp. braincase (BYU 17096) with a postparietal foramen, making it the first definitive Apatosaurinae to possess this feature. Subsequent examinations of the *Apatosaurus* (SMA 0011 and MOR 700) and *Diplodocus* (MOR 592 and MOR 7029) reveal that all of these specimens possess a postparietal foramen (Figure 3). The exact morphology of the foramen can be difficult to discern due to damaged margins, but in general it is ovoid in shape. In some specimens the foramen's greatest axis is transverse to the long axis of the skull (MOR 700), while in others it is parallel to the long axis of the skull (SMA 0011).

Macroscopic Examination Of Pneumatic Structures

The smallest diplodocid of the dataset (SMA 0009; S1), represents an animal with an approximately 50 cm long cervical series. Macroscopically the cervical vertebrae appear acamerate (fossae do not invade centrum). The pneumatic fossae (not leading to internal chambers) of the cervical series are structurally simple, consisting of a shallow oval that runs the major length of each centrum. In the mid cervical vertebrae the pneumatic fossae have an average depth of 4 mm, while in the posterior cervical the depth increases up to 8 mm. In the anterior most and posterior cervical vertebrae, an accessory lamina can be observed dividing the pneumatic fossae. In the anterior-most cervical vertebrae, this accessory lamina is well developed thus creating an anterior and posterior fossa; while in the posterior most cervical vertebrae these laminae are weakly expressed (Figure 4).

The next size range consists of individuals with cervical series up to approximately 3 m in length (S2). Individuals representing this size range, such as SMA 0004, the *Apatosaurus* CM 3390, and the *Barosaurus lentus* specimens AMNH 7530 and AMNH 7535, all exhibit procamerate to camerate (degrees of pervading complexity into the centrum) cervical vertebrae. In this size class all of the pneumatic fossae are deepened and well defined. Distributed throughout the mid and posterior cervicals from SMA 0004, AMNH 7530, and AMNH 7535 are smaller foramina (on the order of a few cm in greatest breadth, and leading to internal chambers), many of which are bounded by new accessory laminae. As in the previous size range, the fossae and foramina of the anterior cervicals are shallower than those in the posterior cervical vertebrae. The anterior fossae/foramina range from a depth of 7 mm to the low teens, while those posteriorly range in the high teens to as deep as 24 mm in SMA 0004. Additionally, the primary accessory laminae along with both the posterior centroparapophyseal and the postzygodiapophyseal laminae are more developed and pronounced (Figure 3).

The next size range collectively represents S3 and S4 specimens. However, within this collected range there are two discernible groups. The first group represents specimens with cervical series lengths 4-6 m in length (S3), such as the *Apatosaurus excelsus* CM 555, and the *Diplodocus* specimens SMA 0003 and MOR 592. As in the S2s, the fossae and foramina continue to increase in size and depth. Likewise, all of the associated laminae continue development, expansion, and proliferation. The final size range denotes the S4 condition. The primary difference observed between the S3s and S4s is the degree and abundance of fossae and foramina. In examining the *Diplodocus*

carnegii CM 84, the degree and occurrence of foramina and laminae is dramatically increased (Figure 3). The greatest concentration of these laminae are still in the mid and posterior cervical, but in the S4 condition these features even proceed into the anterior portion of the cervical series. In some of these foramina-prolific centra, such as C-11 of CM 84, the degree of laminae gives the appearance of a network of honeycomb.

Computed Axial Tomography

In the smallest late anterior to early middle cervical vertebra (MOR 714 7-22-3-53), the centrum is acamerate and appears to lack any secondary pneumatic structures. In both frontal and transverse views, the portion of the median septa bounded by the fossae has a fairly uniform thickness. Also in frontal view the lateral margins of the condyle are rather bulbous at their extremities. In the S2 late anterior to early middle cervical vertebra of MOR 790 8-10-96-204, we see in comparison to MOR 714 7-22-3-53 that the median septa has continued thinning. The most dramatic change is the pneumatic structures of the condyle; in frontal view the condyle has deep excavations, as in MOR 714 7-22-3-53, but in MOR 790 8-10-96-204 the lateral margins of the condyle have continued to thin and taper. The bulk of the condyle is composed of large camerae (larger rounded cavities with a regular pattern) as observed in other sauropod condyles (Wedel, 2003; Schwarz and Fritsch, 2006; Schwarz et al., 2007). The posterior portion of the cotyle also seems to possess camerae. Unfortunately no larger specimens could be ascertained for this study, so we can only speculate on further ontogenetic development (Figure 5).

Collectively, the dorsal vertebrae represent a more complete trajectory (in total consisting of five scanned vertebrae). In the S2 anterior dorsal, MOR 790 8-21-95-238,

the median septa is uniformly thin and in frontal view the pneumatic fossae pervade deeply into the condyle. Both the condyle and cotyle of MOR 790 8-21-95-238 are deeply penetrated by pneumatic fossae. It would also appear that internal pneumatic structures are nearly non-existent. In frontal view only one possible small camera is observed in the condyle. In the S3 specimen, MOR 592 8-22-90-75, there is continuing invasion of the pneumatic fossae into the condyle. Due to lateral shearing, the median septa is highly fragmented. In frontal view it would appear that MOR 592 8-22-90-75 lacks any internal pneumatic structures. However in transverse view there are several camerae and camellae (smaller angular cavities with an irregular pattern) primarily along the peripheral margins of the centrum. MOR 592 8-22-90-75 also marks the first appearance of pneumatic structures within the neural arch. Those in the arch would likewise appear to consist of camerae and camellae (Figure 6).

The posterior dorsal series exhibits perhaps the best ontogenetic development of the pneumatic structures. The S2 specimen, MOR 790 7-8-95-17, is structurally simple. The centrum is acamerate and lacks any sort of internal pneumatic structures (as hypothesized by Wedel, 2003). In addition the medially shallow lateral fossae produce a very thick median septa. In the S3 specimen, MOR 592 8-22-90-77, the lateral pneumatic fossae extend medially into the centrum producing an overall thinner median septa. In addition to the thinning of the median septa, numerous internal pneumatic structures are also present. The cotyle would appear to consist of a complex of fairly interconnected camerae with some less numerous camellae; while the condyle would appear to contain primarily interspersed camellae. There also appears to be some fine camerae and

camallae in the neural arch as well. The S4 posterior dorsal vertebra (MOR 957 6-29-92 29#1) is significantly larger than MOR 592 8-22-90-77; unfortunately a suitable intermediate specimen was not available for study. The most notable feature of MOR 957 6-29-92 29#1 is the elaborate and extensive pneumatization. The lateral pneumatic fossae have extended deep into the centrum to produce a median septa that in certain locations is under 2 cm in thickness. In frontal view both the condyle and cotyle are completely composed of large (several cm in greatest length) extensive camerae. In transverse view there is even more apparent pneumatization. The thin median septa and large camerae of the centrum are still evident, and the neural arch hosts a series of elongate camerae. These neural arch camerae gently arc medially towards the neural canal, and their overall size decreases dorsally while the dividing septa increase in thickness dorsally (Figure 7).

Ontogenetic Data

As histology is the only conclusive way to determine skeletonchronology, the majority of the ontogenetic data used in this analysis relies on enhanced sampling of multiple skeletal elements.

Neural Spine Histology

In the S2 posterior cervical (MOR-790 un-numbered) and anterior dorsal (MOR 790 8-21-95-238) the inter-trabecular spaces are fine and generally divided into two size ranges: those well under 1 mm and those equal to or larger than 1 mm (however in MOR-790 [un-numbered] a few of the inter-trabecular spaces are up to 3.5 mm in greatest length; Figure 8). In the un-bifurcated MOR-790 [un-numbered], the apex of the neural

spine is more compact with the bulk of the more cancellous bone loosely oriented in a convex arc across the width of the neural spine.

In the bifurcated MOR 790 8-21-95-238, the lateral margin is primarily compact with the more cancellous bone restricted to the medial margin of the split spine. This feature is likewise observed in the S3 posterior cervical (MOR 592 8-24-90-91) and anterior dorsal (MOR 592 8-22-90-15). In the bifurcated MOR 592 8-24-90-91 there are two ranges of inter-trabecular sizes (far more of the larger spaces), and the spaces are distributed throughout the spine apex (Figure 8). In addition, the lateral margin of MOR 592 8-24-90-91 is more compact with the largest inter-trabecular spaces being restricted along the medial border. In MOR 592 8-22-90-15 the inter-trabecluar spaces are elongate and generally much larger than those from previous specimens (approximately 3 mm or larger). The lateral margin of the spine apex is primarily compact with a more cancellous medial periphery. A proper ontogenetic series is needed to verify if these results are legitimate, but potentially these specimens indicate that throughout ontogeny, inter-trabecular spaces increase in size and orientation, and as bifurcation of the spine develops, differing bone morphologies occupy different proportions of the spine apex.

Thoracic Rib Histology

The smallest specimens sampled represent the hypothetical extremes recorded from the Mother's Day Quarry. As previously addressed, the Mother's Day Quarry represents a bone bed of at least fifteen immature diplodocids with femora lengths between 102 and 120 cm (both S2). Unfortunately, the Quarry material is largely disarticulated and disassociated, so serial position or association is an approximation at

best. If the femora extremes represent the minimum and maximum size range, we likewise concluded that the smallest and largest anterior most thoracic ribs do as well.

Within the smallest Mother's Day thoracic rib (MOR 790 7-24-96-95; Figure 9), the bone microstructure is predominantly woven (highly disorganized; i.e. fast growth). The bone is highly vascularized, and throughout there are numerous resorption cavities (~1 mm in greatest diameter). The vascular canal orientation throughout is principally longitudinal and reticular. In the vicinity of the cranial intercostal ridge, the periosteal cortex vascular canal orientation is uniformly longitudinal, while the medial most portion transitions from longitudinal to reticular. Secondary osteons are principally located adjacent to the deep cortex trabecular bone and within the cranial intercostal ridge. This varying microstructural anatomy within a single section is why Waskow and Sander (2014) emphasize that thoracic ribs should not be cored; sampling in three different locations could yield three entirely different life history interpretations. While there are no continuous LAGs or indications of growth cessation, there are numerous smaller, semi- opaque, and non-continuous line segments. These segments are primarily concentrated into two distinct regions, and these regions collectively are much thicker than a LAG. In-between these segments are smaller zones of slower, but continuous growth. As such we identify these regions as annuli (Francillon-Vieillot et al., 1990). Annuli represent a slowing of osteogenesis, not an annual cessation (as in the case of LAGs; Castanet et al., 1992). Therefore we theorize that this individual records a minimum of two annual growth markers.

The presumed largest represented thoracic rib from the Mother's Day Quarry is MOR 790 7-27-8-96 (Figure 9). Like the smallest Mother's Day specimen, MOR 790 7-27-8-96 is highly vascularized with numerous resorption cavities (up to ~2 mm in greatest diameter). Adjacent to the deep cortex trabecular bone is a relatively large (up to several mm in thickness) zone of secondary remodeling. Within this remodeled zone up to two generations of secondary osteons are observed. The remainder of the medial cortex is comprised of woven bone with a few secondary osteons infrequently dispersed. Endosteally the vascular canal orientation exhibits longitudinal and laminar zones, while the outer most cortex transitions from laminar to longitudinal canals. And like the smaller MDQ thoracic rib, the cranial intercostal ridge is highly remodeled and consists of Haversian bone comprising up to four generations of secondary osteons. MOR 790 7-27-8-96 does preserve distinct and discernable LAGs. These preserved LAGs are largely restricted to the outer portion of the cortex, and there are a recorded minimum of six preserved LAGs.

The S3 size range is represented by the *Diplodocus* MOR 592 (Figure 10). As in the S2 thoracic ribs, MOR 592 is highly vascularized with numerous resportion cavities. The cranial intercostal ridge is composed entirely of dense Haversian bone, however the medial portion of the rib records pertinent life history information. Adjacent to the deep cortex trabecular bone, there is a large (approximately 2 cm) zone of highly vascular, longitudinal, woven bone. While this zone is composed of longitudinal vascular canals, these canals are arraigned in radial rows (Francillon-Vieillot et al., 1990). Immediately adjacent to this highly vascularized longitudinal zone for the remainder of the cortex is a

zone of less vascularized primary bone. In this outer-most zone the vascular canal orientation transitions from longitudinal to reticular. MOR 592 records a minimum of eight LAGS; however no LAGs are visible within or prior to the highly vascularized longitudinal zone.

The S4 specimen is represented by the paratype of *Diplodocus carnegii* (CM 94; Figure 11). As in all of the aforementioned thoracic ribs, that of CM 94 is highly vascularized and possesses a dense network of deep cortex trabecular bone. However unlike the previous thoracic ribs, that of CM 94 has proportionally a much larger and more extensive zone of secondary remodeling (up to three generations of secondary osteons) adjacent to the deep cortex trabecular bone. The periosteal portion of the cortex is comprised of fibrolamellar bone. The vascular canal orientation of the entire section is longitudinal. No radial zones as in MOR 592 are observed in CM 94. Zones of longitudinal vascular canals are bracketed by LAGs; these canals are found in episodic groupings of either predominantly larger or smaller canal diameters. Perhaps these bands are representative of episodic growth. Within the outermost four to five mm of the cortex there is a decrease in vascularity, which is represented by both occurrence and size of vascular canals. The thoracic rib of CM 94 records a minimum of twenty-four LAGs. In addition to the high LAG count, the outermost portion of the cortex records three to four closely spaced LAGs LAGs in low vascularized tissue. We believe that this zone is an external fundamental system (EFS; the histologic indicator of growth cessation). The presence of an EFS indicates that CM 94 was skeletally mature (and potentially the same may hold true for the slightly larger holotype CM 84), and therefore these size ranges do

indeed represent the previously assumed skeletally mature sizes of *D. carnegii*.

Femoral Histology

Mother's Day Quarry Femora

The work of Klein and Sander (2008) strongly suggests a linear relationship between femoral length and HOS in sauropods; thus this trend suggests that the largest Mother's Day Quarry femur (MOR 790 7-23-95-122, 120 cm long; S2; Figure 12) should theoretically represent the oldest animal from the quarry. With a cortex 11.29 mm thick, endosteally there is a large region of Haversian bone, periosteally grading into a scattered region of secondary remodeling. Further periosteally, the remainder of the cortex comprises a very thin unit of Types D and E bone. Klein and Sander (2008) report that growths marks may appear in Type E bone (although extremely rare); however no growth marks are visible in MOR 790 7-23-95-122. The bone morphology indicates MOR 790 7-23-95-122 - presumably the most skeletally mature individual - represents HOS 7 out of 13.

MOR 592 Femur

The medullary cavity of the S3 *Diplodocus* MOR 592 is large with a cortex 29.51 mm thick (Figure 13). From the medullary cavity there is a large zone of Haversian bone, while periosteally secondary osteons become less frequent within the primary tissue. Type E bone predominates for the remainder of the cortex. In the case of the MOR 592 femur, at least one LAG is present along the periosteal margin. MOR 592 representing HOS 9 out of 13 is consistent with femoral length versus HOS found by Klein and Sander (2008). The lack of a cortex consisting entirely of Haversian bone and the lack of an EFS

indicates that skeletochronologically, MOR 592 is immature. Histological and morphologic examinations both verify and substantiate the conclusions of Woodruff and Fowler (2012) that MOR 592 is indeed an immature *Diplodocus*.

DISCUSSION

Morphologic Evidence

Pneumatic Architecture, Cranial Foramen, and Femoral Proportions

Wedel (2005) demonstrated the importance and implications of pneumaticity within sauropod vertebrae (particularly in regards to mass estimations). In regards to quantifying the pneumatic potential, Wedel (2005) proposed the calculation of the air space proportion (ASP) - which is the volume of air versus the volume of bone. The ASP methodology is simplistic, and relies on a two color image. One color delineates the volume of the bone in cross section, and the other color represents the area filled by pneumatic structures (see Wedel [2005] for the full methodology). A simple calculation comparing the pixel count of bone to air will result in an ASP value. Out of the spectrum of sauropods examined, Wedel (2005) had a degree of variability, but noted that most sauropod vertebrae contained approximately 50% air by volume, comparable to avian ASP values. Additionally Wedel (2005) noted that the execution of ASP was still in its infancy; the location of the section in a given vertebra and the serial position could greatly affect the calculated ASP. However, Wedel (2003; 2005; 2009) demonstrated that vertebral pneumatic complexity has increased through sauropodomorph phylogeny. Thus ASP increases in tandem with pneumatic complexity.

ASP should be considered an important character, however in this analysis we felt cautious in the quantification of ASP. For the CAT scanned vertebrae, we attempted to view transverse slices near the mid-point of the pneumatic foramen and transversely through the length of the centrum. In viewing the cervical vertebrae scan data, the anterior and posterior pneumatic foramen slices vary, so in calculating ASP, perhaps an average from multiple fixed locations would give an overall vertebral ASP. Regardless of the quantified ASP, in examining the scan data, one can clearly see (particularly within the dorsal vertebrae) that the pneumatic architecture increases in complexity throughout ontogeny (as demonstrated by Wedel, 2003). Quantifying the ASP will be important in regards to comparing taxa and calculating evolutionary trends; but initially we see that the complexity follows a developmental trajectory, and it is another example of derived juveniles exhibiting basal adult morphologies.

Interestingly, while the scans reveal general pneumatic architecture, we would stress they are not a true 1:1 reflection of the actual pneumatic morphology. When the S3 MOR 592 8-22-90-75 was scanned, the results showed that the neural spine had a dense outer cortex with a less dense interior. Within the neural spine there were only a few laterally restricted, small inter-trabecular spaces. Yet thin sectioning revealed a completely different outcome. The dense periosteal most margin was verified, but the entirety of the internal aspect was instead occupied by cancellous bone with large inter-trabecular spaces. This discrepancy could be explained as an issue with scan resolution-whereas finer structures could become less distinguishable with lower resolution. Perhaps rescanning with both finer resolution and intensified contrast could clarify some of these

issues. In addition to these possible adjustments, a comparative study examining the results between scan images and complete enhanced sections of each vertebra would be worthwhile.

In regards to the postparietal foramen, the recognition of this cranial feature in several Morrison diplodocid specimens indicates that it is not a synapomorphic or autapomorphic trait restricted solely to Dicraeosauridae and isolated Sauropoda genera. Harris (2006a) has suggested that this foramen was used for photoreception (i.e. a pineal eye). Within the diplodocids that possess a postparietal foramen, it is present only in skulls under ~40 cm in length. The larger and presumably more mature diplodocid skulls (CM 11161, USNM 2672, USNM 2673, and CM 11162) all lack this foramen. The presence/absence of this foramen between less and more mature individuals would suggest that within Diplodocidae, the postparietal foramen is an ontogenetic cranial feature (further support that both *Suuwassea emilieae* and *Kaatedocus siberi* are in fact immature animals; Woodruff and Fowler, 2012; Woodruff et al., 2013; Woodruff and Fowler, 2014; Figure 3).

A histologic examination of the postparietal foramen has yet to be conducted, but it raises the question as to the proper terminology to be used in addressing this feature. Amongst the immature diplodocid skulls with this feature, it would appear that it initially represents a posterior opening between the sutural margins of the parietals (~1cm), and that through ontogeny this gap is reduced by the fusing parietals. By definition a foramen is a static opening (Grey, 1858), so in regards to the diplodocid condition, foramen is not an appropriate term. In 1979 J. A. Hopson concluded that these cranial “foramen” were in

actuality fontanelles. A fontanelle is defined as the temporary membranous gap between developing cranial bones (Grey, 1858). So if this feature is indeed ontogenetic within diplodocids, then fontanelle would be the more appropriate term. However it must be stated that currently the cranial ontogeny of dicraeosaurids is unknown. Potentially dicraeosaurids could retain this cranial opening throughout ontogeny – thus foramen, while in diplodocids this trajectory could be peramorphic, therefore neither term is suitable. In lieu of a histological examination which could possible elucidate the proper term, we suggest for the time being using Balanoff et al.'s (2010) more neutral phrasing of "postparietal aperture".

The large femora dataset acquired for diplodocid body mass estimations has likewise allowed for the examination of femoral ontogeny (Figure 14). Some studies suggest that few limb changes – if any - are apparent between maturational states (Wilhite and Curtice, 1998; Wilhite, 1999; Wilhite, 2003; Bonnan, 2004); thus at least sauropod limbs may have developed in a more isometric manner. Yet in examination of the dataset, subtle ontogenetic femoral trends are observed. These general trends appear to apply to both *Diplodocus* and *Apatosaurus*. In many of the immature individuals the femoral head appears inclined at a greater angle to the long axis of the diaphysis (more pronounced in *Diplodocus*), and in the larger and more mature forms the femoral head angle becomes more perpendicularly oriented. Likewise the medial condyle becomes much more pronounced (especially in *Apatosaurus*) in the larger and more mature individuals. Finally, in regards to femoral proportions, in the immature diplodocids, the fourth trochanter is situated proportionally more proximally, while in more mature

individuals this trochanter is generally situated at approximately the mid-point of the diaphysis (Figure 4). A proper thin-plate spline analysis (such as those used in Wilhite and Curtice, 1998; Wilhite, 1999; Wilhite, 2003; Bonnan, 2004) is required to accurately quantify these changes and to possibly detect other proportional changes. This superficial examination would suggest that while minor, these femoral changes indicate allometric development.

Ontogenetic Compilation

In exceptional ontogenetic studies, entire growth trajectories are represented which allow for accurate histologic and morphological comparisons (such as the 50 *Maiasaura peeblesorum* of Woodward et al., in review; to the 56 *Psittacosaurus* of Zorigt in prep; and the 100+ *Triceratops* of Scannella and Fowler, 2014). While Morrison diplodocids are by far one of the most common and best represented of all North American dinosaurs, taphonomic biases, stratigraphic resolution, and taxonomic uncertainties generally result in largely piecemeal specimens. While some basic ontogenetic information is hypothesized (such as HOS, and cranial, pneumatic, and neural spine development), there is in large part frustratingly sparse ontogenetic information. Compared to the previously mentioned exceptional series, individually some of the features examined in this analysis weakly support an ontogenetic trend, or the particular dataset is statistically too small to make accurate inferences (such as neural spine histology and CAT scans of pneumatic structures). In lieu of such a diplodocid series, an encompassing set of histologic and morphologic features together create a

system of supportive characters, and collectively we call this system the Sauropod Ontogeny Scale (SOS; Table 4).

In like manner to the Nash Equilibrium Theory (Nash, 1950), the individual characters of SOS may seem insignificant or minor; however by not forcefully competing (i.e. histologic characters trump morphological characters, or vice versa), each is individually significant while simultaneously supportive of the others and the end result is a more parsimonious and larger scale outcome. And that outcome is a methodology that can be used to more accurately predict and infer diplodocid maturational statuses and conditions.

As an example, let us examine the S3 *Diplodocus* MOR 592. A histologic section of the 124.5 cm long femur designates it as HOS 9. Morphologic examination shows that the posterior cervical vertebrae are in the initial stages of spine bifurcation, while the dorsal vertebrae exhibit spine bifurcation that is more reminiscent on the adult morphology. CAT scans of the vertebrae illustrate a thinning of the median septa and interspersed camellae and camerae within the condyle and cotlye. The calculated body mass is 3,205 kg. Histology of the thoracic ribs record a minimum of eight preserved LAGs. All of these characters in combination define the SOS Stage 3 condition. Opposed to solely using HOS or degree of spine bifurcation to determine a relative maturational state, or thoracic rib data to determine a minimum age, the SOS method creates a larger depiction of the histological and morphological attributes of each size range, thereby creating a better representation of the animal as a whole.

Potentially the SOS method even has the capabilities to be applied towards fragmentary and isolated diplodocid elements. While the predictive capabilities based on a single element are less absolute than multi element analysis, it none the less reinforces that every piece of data is significant. Another agreeable factor to the SOS method is that every specimen in every institution collectively creates a more accurate index. A seemingly relatively insignificant isolated femur that can be sampled will reveal HOS. HOS coupled with femur dimensions could contribute to the range (such as HOS range and calculated body mass) of the particular growth stage. Likewise from an isolated cervical vertebra, the degree of spine bifurcation and pneumaticity could be noted, and the neural spine could be sampled, while the entire vertebra could be CAT scanned. So much data is potentially harvestable from a presumed "useless bone". As presented, the SOS method is preliminary and in its infancy, and undoubtedly more specimens and characters will and should be added to increase its accuracy in predictive capabilities. And likewise the SOS method as presented applies thus far uniformly to Diplodocidae. However with further analysis it may be warranted or necessary to have family and/or genera specific SOS tables.

CONCLUSION

Every individual skeletal feature examined in this study demonstrates that each quantifiably changes through ontogeny. More importantly than the recognition of a single feature’s ontogenetic trajectory is that all of the features we examined substantiate one another in terms of inferred maturational states. The inclusion of multiple elements, and both histologic and morphologic analyses, uniformly supports and upholds one another.

More important than the outcome of a single perspective is the recognition of a suite of defining histologic and morphologic characters for each maturational range. Here defined as the Sauropod Ontogeny Scale, this comparative scale allows for far more ontogenetic inferences to be made towards applied specimens, and importantly it allows for a much more complete and accurate picture of the animal as a whole to be constructed (Figure 15).

ACKNOWLEDGEMENTS

We would like to thank G. Ohrstrom and E. and J. Sands for their gracious and continuing support to the MOR Paleontology Department. Without the time and consideration of all the museum staff and collection managers, none of this work would have been possible. We humbly thank K. Siber and the entire staff and family of the Sauriermuseum Aathal; O. Wings and H. Mallison at the Museum für Naturkunde – Leibniz Research Institute for Evolution and Biodiversity; C. Mehling and M. Norell at the American Museum of Natural History; A. Henrici, M. Lamanna, C. Beard, D. Berman, and D. Pickering of the Carnegie Museum of Natural History; T. Daeschler and the Academy of Natural Sciences; S. Lucas and the New Mexico Museum of Natural History; and M. Sander, K. Waskow, N. Klein, and DFG Research Unit 533 from the Steinmann Institute for Geology, Mineralogy, and Paleontology. K. Ugrin and the staff of Advanced Medical Imaging at Bozeman Deaconess Hospital generously donated their time and use of their CAT scanner. H. Woodward and D. Varricchio provided invaluable insight and assistance through manuscript revision and preparation. Further we would like to thank R. Wilhite, J. Foster, M. Wedel, M. Taylor, B. Hedrick, J. Harris, E.

Prondvai, K. Stein, K. Stevens, J. McIntosh, G. Storrs, L. Freedman-Fowler, J. Scannella, K. Nordén, and B. Baziak for expert advice and assistance, review, and continuing support throughout this project. And finally thanks to S. Hartman for allowing us the use of his sauropod reconstructions. This manuscript represents contribution number three to The Morrison Formation Dating Project.

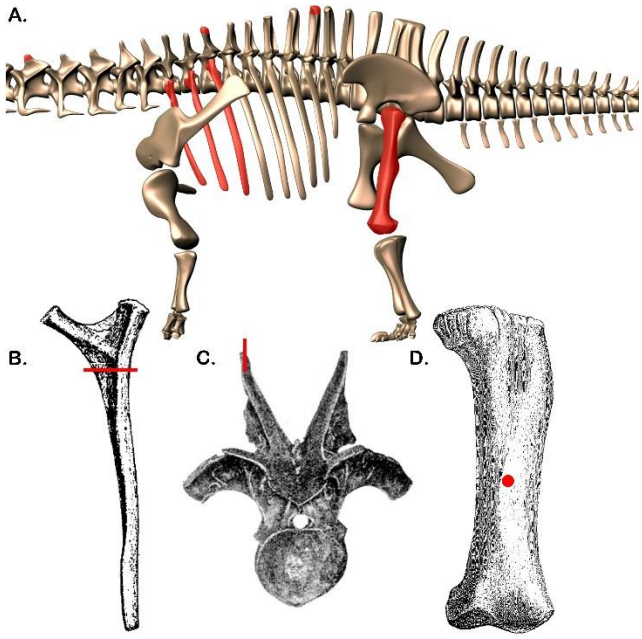

Figure 1: Elements histologically sampled for this analysis. A. Digital reconstruction of *Apatosaurus* (by K. Stevens) with sampled elements highlighted in red. Approximate location of sampling in thoracic ribs (B; from Gilmore, 1936), neural spines (C; from Hatcher, 1901), and femora (D; from Gilmore, 1936).

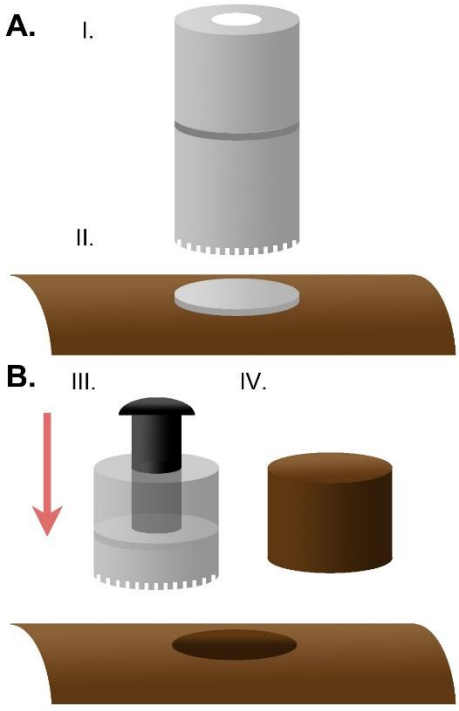

Figure 2: Schematic of coring bit method used in this analysis. A. A two part core bit (I) with a coin placed on the bone surface (II). B. The core bit separated with a bolt inserted to push on the coin (III) to extract the bone core (IV).

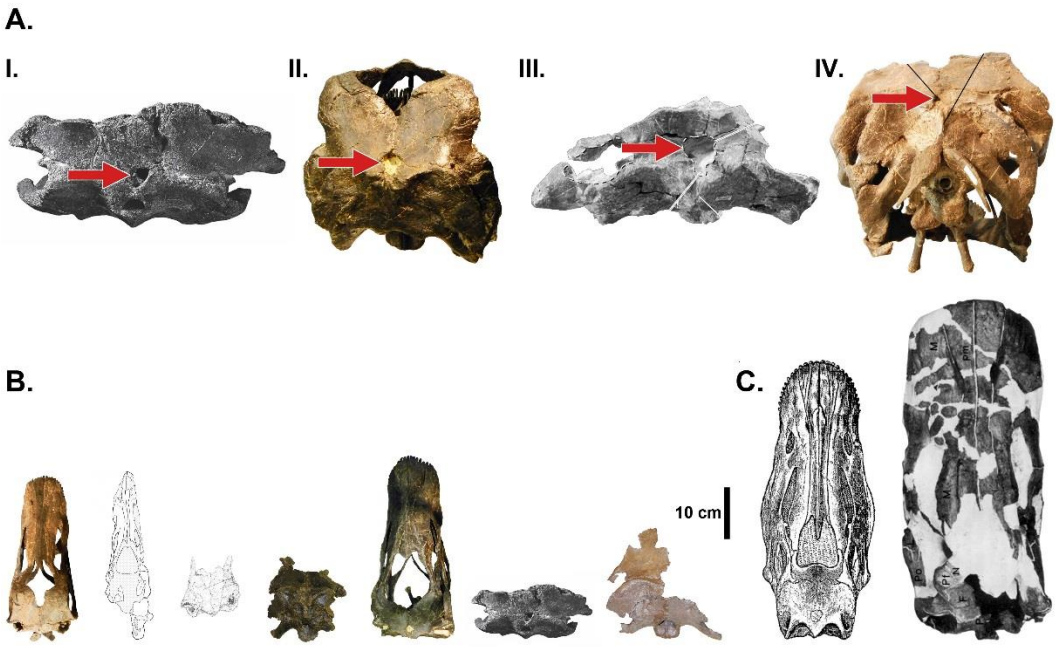

Figure 3: Presence of the Post Parietal Foramen within Diplodocidea. A. Diplodocid specimens with the Post Parietal Foramen – I. ANS 21122, II. SMA 0011, III. BYU 17096, IV. SMA 0004. B. and C. Diplodocid skulls illustrating the presence of the Post Parietal Foramen in immature animals (B.), and its absence in mature animals (C.) – from left to right: SMA 0004, CM 11255, SMM P. 84.15.3, MOR 700, BYU 17096, SMA 0011, ANS 21122, MOR 592, USNM 2672, and CM 11162. Skulls in B. and C. to scale.

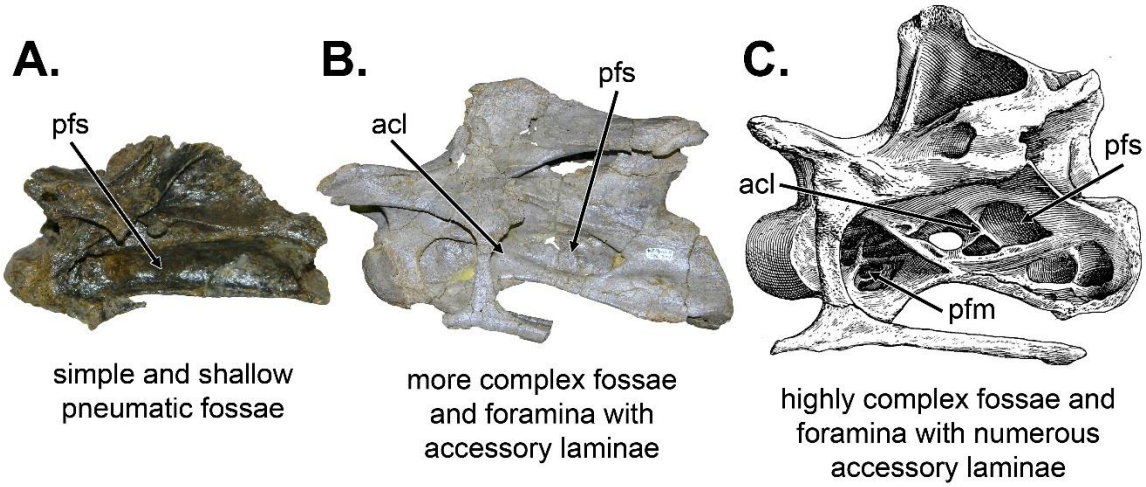

Figure 4: Macroscopic pneumatic architecture in diplodocid cervical vertebrae. A. MOR 714 7-22-3-53, B. MOR 790 8-10-96-204, C. CM 84 (from Hatcher, 1091). Increasing pneumatic complexity and maturity from A to C.

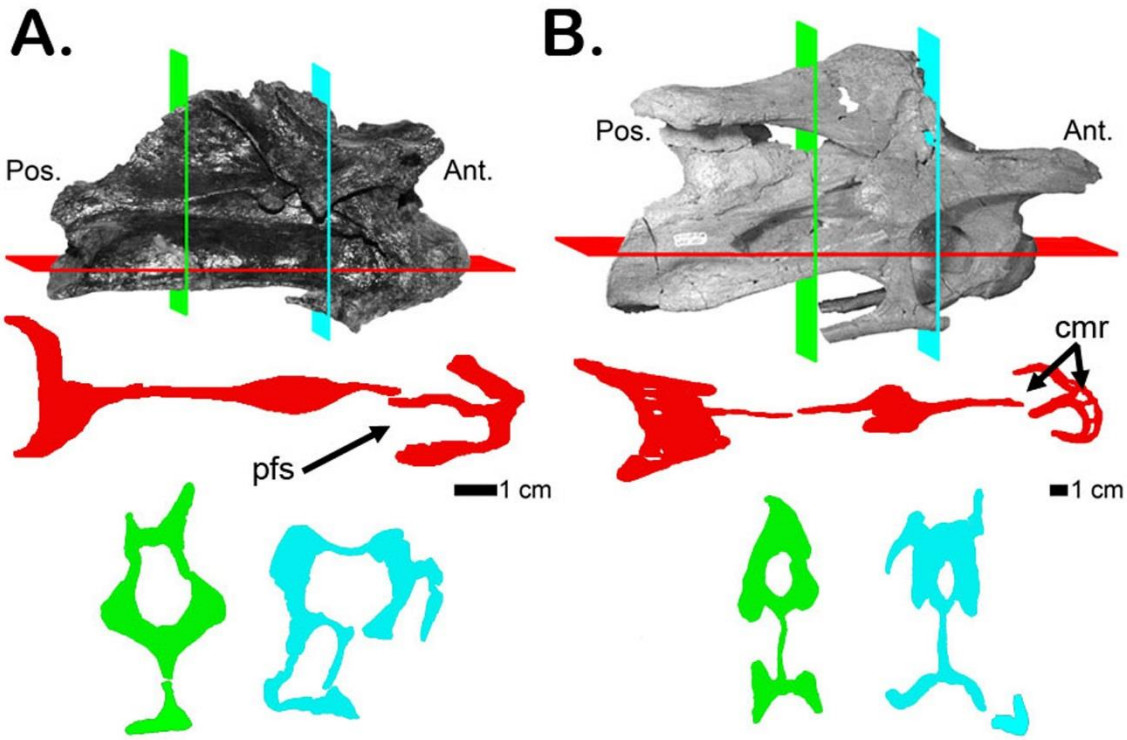

Figure 5: CAT scans of diplodocid anterior cervical vertebrae. A. MOR 714 7-22-3-53, B. MOR 790 8-10-96-204. Colored planes in A. and B. correspond to CAT scan sections for each respective vertebrae. pfs = Pneumatic Fossa, cmr = Camera (Wedel, 2003).

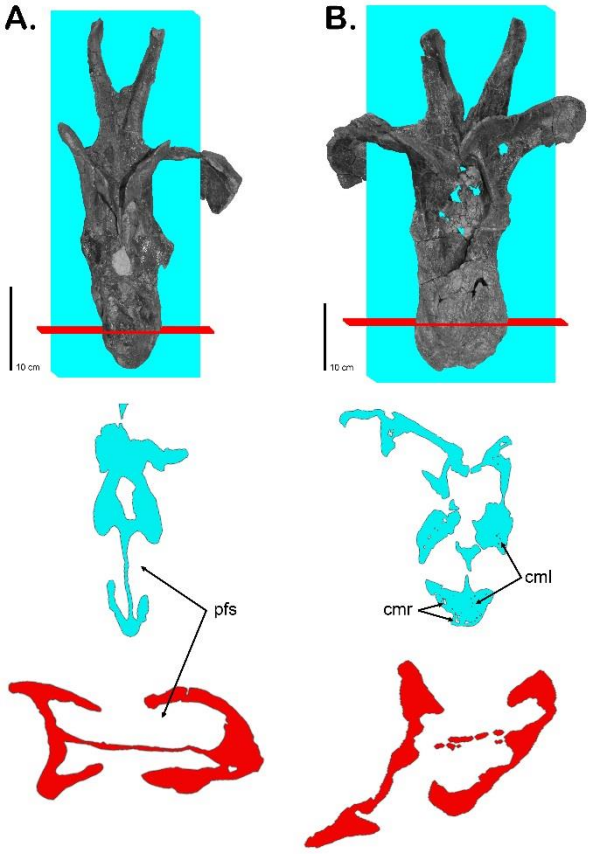

Figure 6: CAT scans of diplodocid anterior dorsal vertebrae. A. MOR 790 8-21-95-238, B. MOR 592 8-22-90-15. Colored planes in A. and B. correspond to CAT scan sections for each respective vertebrae. pfs = Pneumatic Fossa, cmr = Camera, cml = Camella (Wedel, 2003).

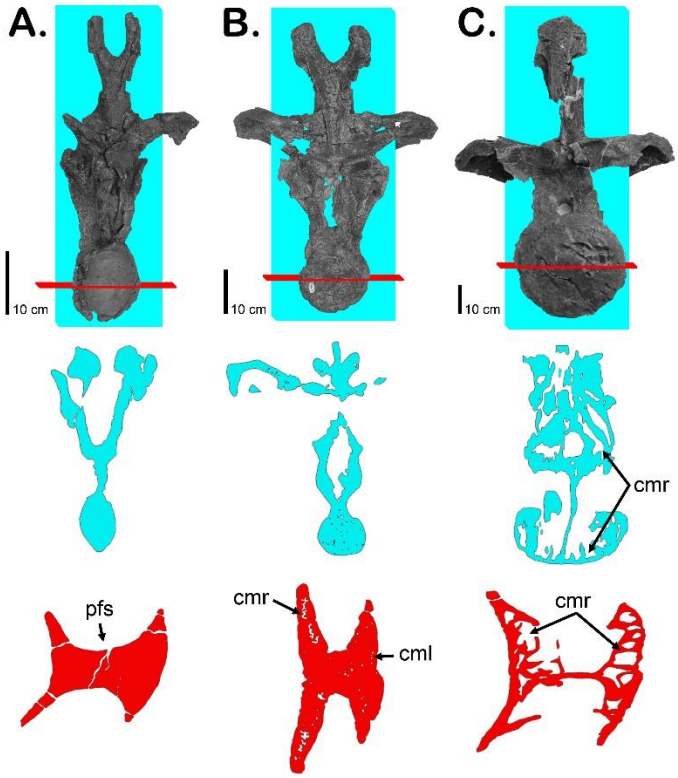

Figure 7: CAT scans of diplodocid posterior dorsal vertebrae. A. MOR 790 7-8-95-17, B. MOR 592 8-22-90-77, C. MOR 957 6-29-92#1. Colored planes in A. and B. correspond to CAT scan sections for each respective vertebrae. pfs = Pneumatic Fossa, cmr = Camera, cml = Camella (Wedel, 2003).

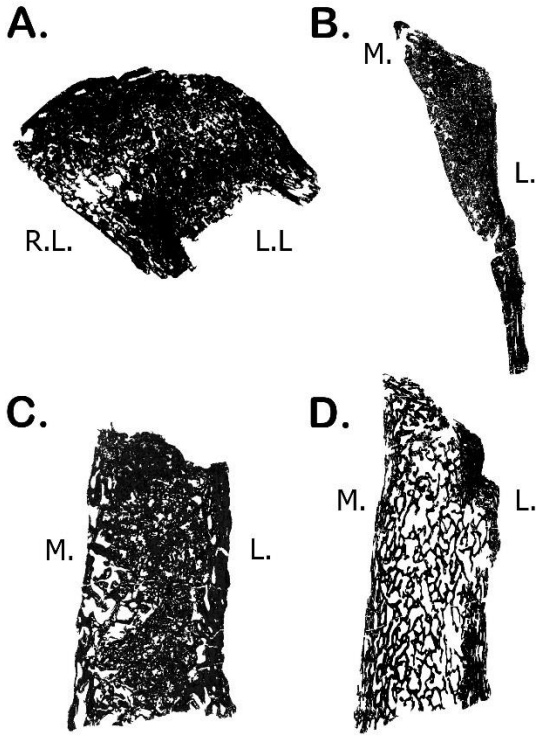

Figure 8: Posterior cervical and anterior dorsal vertebrae neural spine histology. A. Posterior cervical MOR 790 (*un-numbered*), B. Anterior dorsal 790 8-21-95-238, C. Posterior cervical MOR 592 8-24-90-91, D. Anterior dorsal MOR 592 8-22-90-15. R.L. (right lateral), L.L (left lateral), M. (medial), L (lateral). Not to scale.

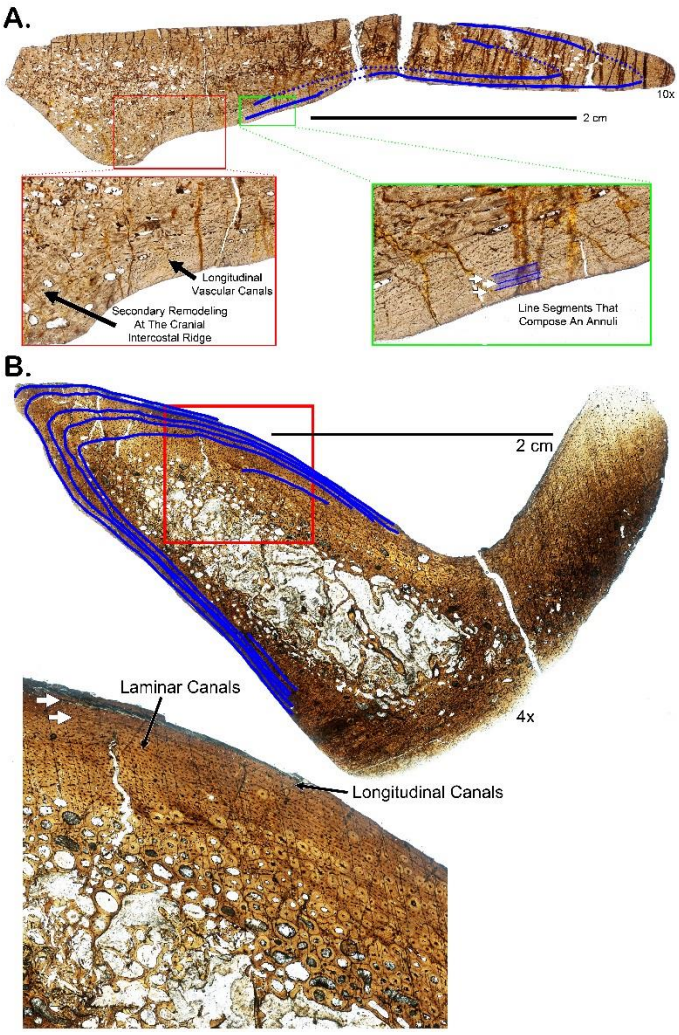

Figure 9: A. Histologic sections of the SOS Stage 2 *Diplodocus* MOR 790 7-24-96-95 (10x) and B. MOR 790 7-27-8-96 (4x) thoracic ribs. A. MOR 790 7-24-96-95 records a minimum of two annuli (blue lines). Red insert box highlights bone microstructure differences between the cranial intercostal ridge and lateral margins with longitudinal vascular canals. Green insert box highlights a sample of the segments that comprise one of the growth markers (an annuli, highlighted in blue). B. MOR 790 7-27-8-96 records a minimum of six LAGs (blue lines). Red insert box highlights the microstructure and shows the vascularity patterns while the white arrows denote two of the LAGs present.

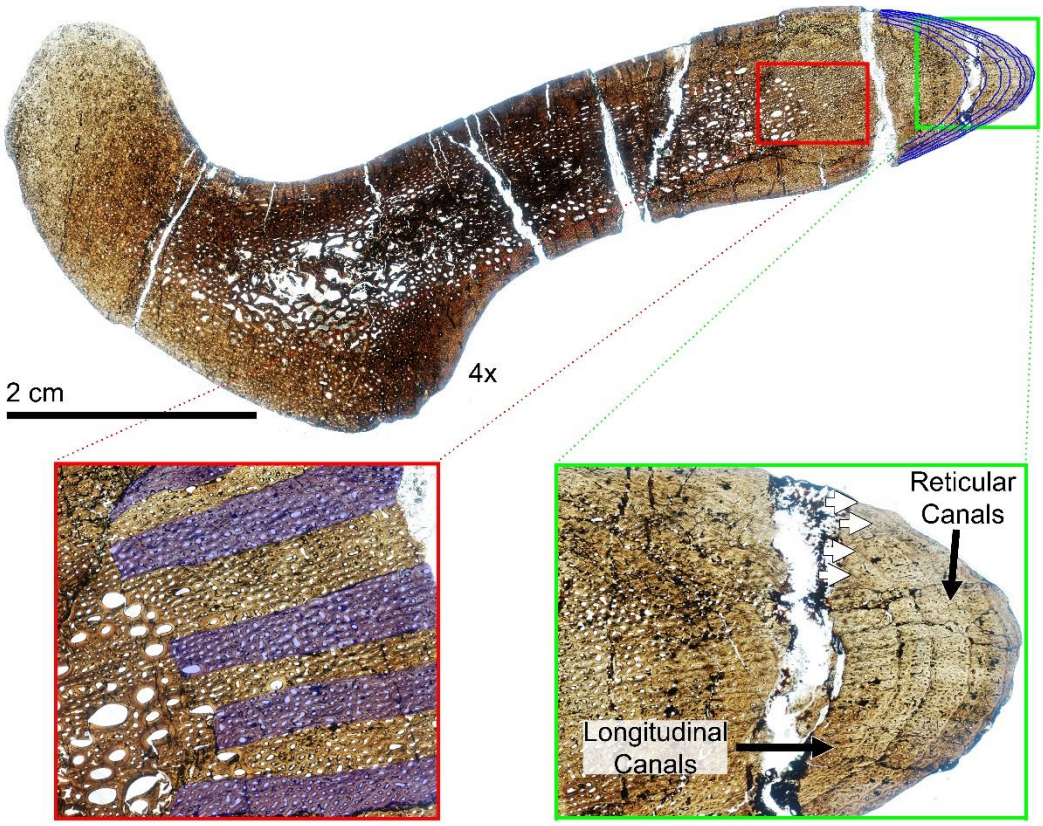

Figure 10: Histologic section of the SOS Stage 3 *Diplodocus* MOR 592 thoracic rib at 4x. MOR 592 records a minimum of eight LAGs (blue lines). Red insert box highlights the organization of longitudinal vascular canals in radial rows (alternating rows highlighted in blue). Green insert box highlights the vascularity patterns with white arrows denoting four of the LAGs present.

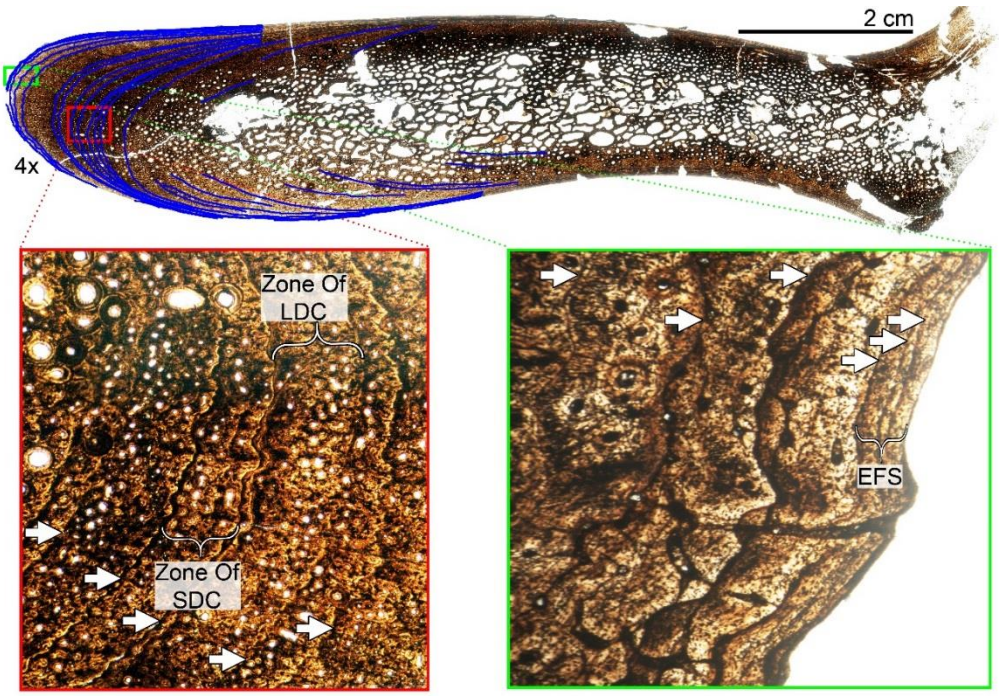

Figure 11: Histologic section of the SOS Stage 4 *Diplodocus* CM 94 (*Diplodocus carnegii* paratype) thoracic rib at 4x. CM 94 records a minimum of twenty-four LAGs (blue lines). Red insert box highlights the episodic zones of large (LDC) and small (SDC) diameter longitudinal vascular canals with white arrows denoting some of the LAGs present. Green insert box highlights the outermost cortex which records the presence of an EFS. White arrows denote LAGS present, with the EFS bracketed.

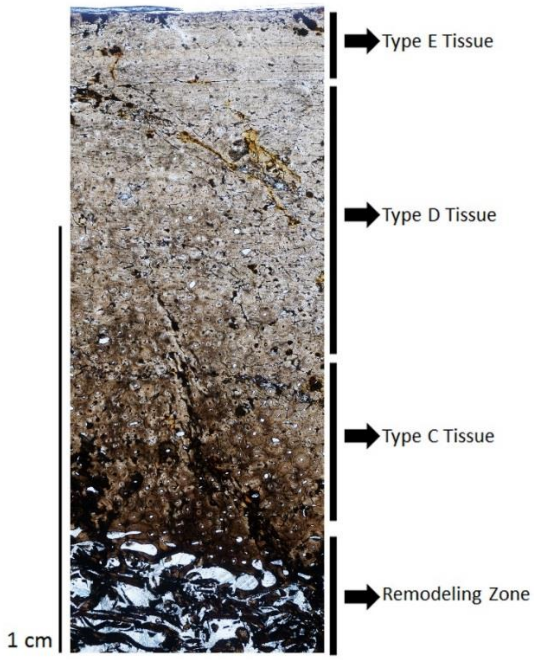

Figure 12: Histologic section of the SOS Stage 2 *Diplodocus* MOR 790 7-23-95-122 femur at 4x. MOR 790 7-23-95-122 is HOS 7 out of 13.

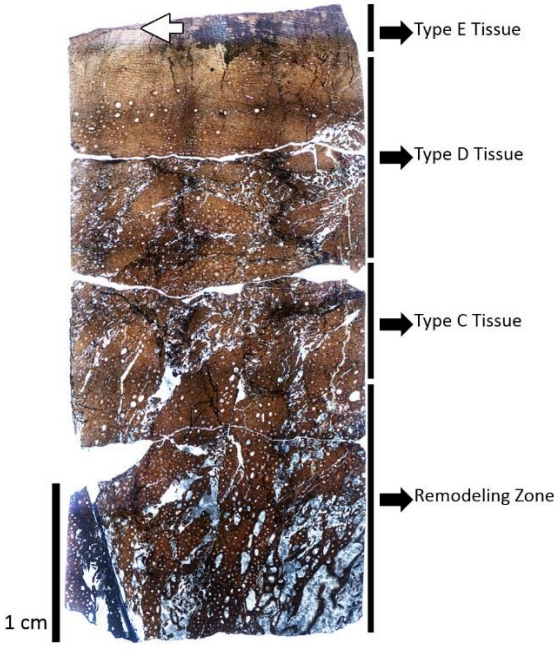

Figure 13: Histologic section of the SOS Stage 3 *Diplodocus* MOR 592-35 femur at 4x. White arrow marks one observable LAG. MOR 592 is HOS 9 out of 13.

Figure 14: Selection of the diplodocid femoral dataset used throughout this analysis which illustrates ontogenetic shifts. Top row *Diplodocus* sp., from left to right: CM 33976, CM 33991, CM 21788, CM 30762, MOR 790 7-5-97-7, AMNH 5855, MOR 700 7-27-91-40, MOR 790 7-23-95-122, MOR 592-35, CM 21752, SMA 0008, SMA "Brosemli", CM 21745, CM 84; Bottom row *Apatosaurus* sp., from left to right: AMNH 613, OMNH 1279, AMNH 606, MWC 5439, CM 21784, CM 33997, CM 30766, MOR 700 7-24-91-31, NSMT-PV-20375 (from Upchurch et al., 2004), AMNH 353, CM 87, SMA 0014, CM 85, MOR 857 7-16-92-30, MWC "Moffit Co. Apato.". Scale bar = 10 cm. Overlapping colored lines illustrate femoral changes through ontogeny – for *Diplodocus* sp. MOR 790 7-5-97-7, MOR 790 7-23-95-122, and CM 84, and *Apatosaurus* sp., CM 33997, MOR 700 7-24-91-31, and MWC "Moffit Co. Apato.".

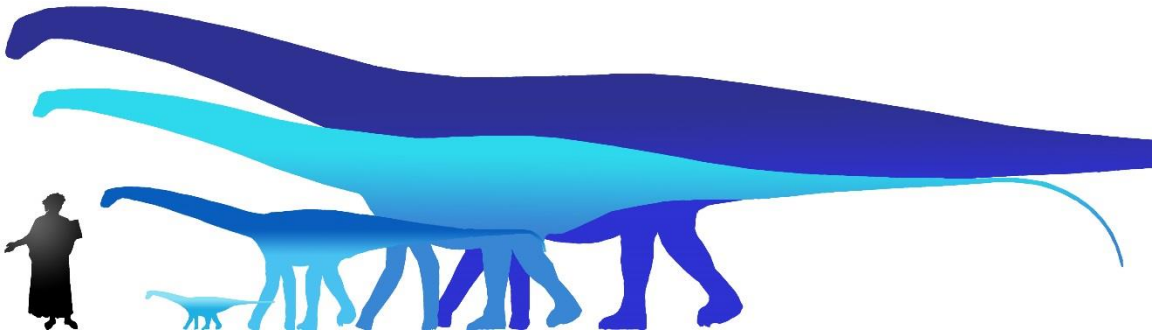

Figure 15: An ontogenetic trajectory in consideration of morphologic attributes for the Morrison diplodocid *Diplodocus*. Note diplodocids, and certainly all other sauropods, did not skeletally develop along an isometric trajectory. Human scale bar is Dante Alighieri from Domenico di Michelino's "*La commedia illumina Firenze*", depicting Dante as 1.63 m tall. Modified silhouette of *Diplodcus carnegii* CM 84 by S. Hartman and available via PhyloPic under the Creative Commons Attribution-ShareAlike 3.0 Unported License.

Table 1: Sauropod specimens examined in this analysis.

Specimen Number	Material Examined	Taxonomy
AMNH 353	Femur	*Apatosaurus* (McIntosh, 1990)
AMNH 435	Femur	*Apatosaurus* (*this analysis*)
AMNH 606	Femur	*Apatosaurus* (*this analysis*)
AMNH 613	Femur	Diplodocidae (*this analysis*)
AMNH 5855	Femur	*Diplodocus*, *Barosaurus* (Mook, 1917; McIntosh, 2005)
AMNH 6341	Vertebrae	*Barosaurus* (Lull, 1919)
AMNH 7530	Vertebrae	*Barosaurus* (Michelis, 2004)
AMNH 7535	Vertebrae	*Barosaurus* (Michelis, 2004)
AMNH 7539	Femur	*Diplodocus* (*this analysis*)
ANS 21122	Vertebrae, Femur, Skull, Thoracic Ribs	*Suuwassea*, Apatosaurinae (Harris, 2006a,b; Woodruff and Fowler, 2012)
BYU 601-17103	Femur	*Apatosaurus* (Wilhite, 2003)
BYU 725-4889	Femur	*Diplodocus* (Wilhite, 2003)
BYU 725-9026	Femur	*Diplodocus* (Wilhite, 2003)
BYU 725-11421	Femur	*Diplodocus* (Wilhite, 2003)
BYU 725-12155	Femur	*Diplodocus* (Wilhite, 2003)
BYU 725-13369	Femur	*Diplodocus* (Wilhite, 2003)
BYU 725-13643	Femur	*Diplodocus* (Wilhite, 2003)
BYU 725-13670	Femur	*Diplodocus* (Wilhite, 2003)
BYU 725-16569	Femur	*Diplodocus* (Wilhite, 2003)
BYU 725-16610	Femur	*Diplodocus* (Wilhite, 2003)
BYU 17096	Skull	*Apatosaurus* (Balanoff et al., 2010)
BYU Fe-4-DM197	Femur	*Diplodocus* (Wilhite, 2003)

BYU Fe-5-DM172	Femur	*Diplodocus* (Wilhite, 2003)
CM 84	Vertebrae, Femur	*Diplodocus* (Hatcher, 1901)
CM 85	Femur	*Apatosaurus* (McIntosh, 1981)
CM 87	Femur	*Apatosaurus* (McIntosh, 1981)
CM 94	Vertebrae, Femur, Thoracic Ribs	*Diplodocus* (Hatcher, 1901)
CM 555	Vertebrae	*Apatosaurus* (McIntosh, 1981)
CM 563	Vertebrae	*Apatosaurus* (Gilmore, 1936)
CM 566	Femur	*Apatosaurus* (McIntosh, 1981)
CM 572	Vertebrae	*Haplocanthosaurus* (Hatcher, 1903)
CM 879	Vertebrae	*Haplocanthosaurus* (Hatcher, 1903)
CM 3018	Vertebrae, Femur, Skull	*Apatosaurus* (Gilmore, 1936)
CM 3390	Vertebrae	*Apatosaurus* (McIntosh, 1981)
CM 11161	Skull	*Diplodocus* (Berman and McIntosh, 1978)
CM 11162	Skull	*Apatosaurus* (Berman and McIntosh, 1978)
CM 11338	Vertebrae	*Camarasaurus* (Gilmore, 1925)
CM 21785	Femur	*Apatosaurus* (McIntosh, 1981)
CM 21788	Femur	*Diplodocus* (Wilhite, 2003)
CM 30762	Femur	*Diplodocus* (Wilhite, 2003)
CM 30766	Femur	*Apatosaurus* (Wilhite, 2003)
CM 33976	Femur	*Apatosaurus*, *Diplodocus* (Wilhite, 2003, *this analysis*)
CM 33991	Femur	*Diplodocus* (McIntosh, 1981)
CMC VP 7747	Femur	Diplodocidae, *Diplodocus* (Meyers, 2004; Woodruff and Fowler, 2004)
CMNH 10039	Femur	*Apatosaurus* (Wilhite, 2003)

CMNH 10380	Vertebrae	*Haplocanthosaurus* (Wilhite, 2003)
DNM 3781	Femur	*Diplodocus* (Wilhite, 2003)
HMNS 175	Limb	*Diplodocus* (Holland, 1924)
JRF 220	Vertebrae	*Camarasaurus* (*this analysis*)
KUVP 1351	Femur	*Apatosaurus* (Wilhite, 2003)
MOR 592	Vertebrae, Femur, Skull, Thoracic Ribs, Cervical Ribs	*Amphicoelias*, Dicraeosauridae, *Diplodocus* (Wilson and Smith, 1996; Whitlock and Harris, 2010; Woodruff and Fowler, 2012)
MOR 700	Skull, Cervical Ribs	*Apatosaurus* (Woodruff and Fowler, 2014)
MOR 714	Vertebrae	Diplodocidae (*this analysis*)
MOR 790	Vertebrae, Femur, Thoracic Ribs, Cervical Ribs	Diplodocinae; *Diplodocus* (Meyers, 2004; Woodruff and Fowler, 2012)
MOR 957	Vertebrae, Femur	*Apatosaurus* (*this analysis*)
MOR 7029	Vertebrae, Skull	*Diplodocus* (Woodruff and Fowler, 2014)
MWC 5439	Femur	*Apatosaurus* (*this analysis*)
MWC "Moffit Co. Apato."	Femur	*Apatosaurus* (*this analysis*)
NSMT-PV 20375	Vertebrae, Femur	*Apatosaurus* (Upchurch et al., 2004)
OMNH 1793	Femur	*Diplodocus* (Wilhite, 2003)
OMNH 01667	Femur	*Apatosaurus* (Wilhite, 2003)
SMA 0003	Vertebrae	Diplodocidae, *Diplodocus* (Schwarz et al., 2007; *this analysis*)
SMA 0004	Vertebrae, Skull	*Kaatedocus*, Diplodocidae (Tschopp and Mateus, 2012; *this analysis*)
SMA 0009	Vertebrae, Femur, Cervical Ribs	Diplodocidae; *Barosaurus*, *Brachiosaurus* (Schwarz et al., 2007; Woodruff and Fowler, 2012; Carballido et al., 2012)
SMA 0011	Vertebrae	Diplodocidae (Klein and Sander, 2008)

SMA "Jacq"	Femur	Diplodocidae (this analysis)
SMM P84.15.2	Femur	*Apatosaurus* (*this analysis*)
TMM 993-1	Femur	*Diplodocus* (Wilhite, 2003)
USNM 2672	Skull	*Diplodocus* (Berman and McIntosh, 1978)
USNM 2673	Skull	*Diplodocus* (Berman and McIntosh, 1978)
USNM 4797	Femur	*Apatosaurus* (Wilhite, 2003)
USNM 10865	Femur	*Diplodocus* (Wilhite, 2003)
USNM 11162	Skull	*Apatosaurus* (Berman and McIntosh, 1978)
USNM 337871	Femur	*Diplodocus* (Wilhite, 2003)
WDC BS-157	Femur	*Apatosaurus* (Wilhite, 2003)
YPM 429	Vertebrae	*Barosaurus* (McIntosh, 2005)
YPM 1980	Vertebrae	*Apatosaurus* (Ostrom and McIntosh, 1966)
YPM 5862	Femur	*Apatosaurus* (Wilhite, 2003)

Table 2: Terms, definition, and usage of pneutmatic morphology and histology used in this analysis.

Pneumatic Architecture (*Wedel et al., 2000*) –

Acamerate - Pneumatic structures limited to fossae. Fossae do not significantly invade the centrum.

Procamerate - Deep fossae penetrate to median septum, but are not enclosed by ostial margins.

Camerate - Large, enclosed camerae with regular branching pattern; cameral generations usually limited to 3.

Camera – Round cavity, 5-150 mm in size, septal thickness of 2-10 mm, and a regular branching pattern.

Camella – Angular cavity, 2-20 mm in size, septal thickness of 1-3 mm, and an irregular branching pattern.

Histologic Terms (*Francillon-Vieillot et al., 1990; De Ricqles et al., 1991; Castanet et al., 1992; Huttenlocker et al., 2013*) –

Line Of Arrested Growth (LAG) – Thin bands that represent temporary arrest of osteogenesis, and are considered osteological response to predictable environmental cues.

Annuli – Translucent to opaque bands, thicker than LAGs, represent a slowing (but not a cessation) of osteogenesis.

Woven Bone – Highly disorganized arrangement of collagen fibers, which reflects a high rate of osteogenesis.

Fibrolamellar Bone – Woven bone with intervening and randomly oriented primary osteons.

External Fundamental System (EFS) – Slowly deposited parallel-fibered or lamellar tissue along the outermost cortex (closely spaced outermost series of LAGs).

Haversian Bone – Bone that is completely remodeled by secondary osteons.

Primary Osteon – Central blood vessel and surrounding concentric bone tissue.

Secondary Osteon – Osteon formed by replacement of existing bone, surrounded by an outer cement sheath.

Cancellous Bone – Highly vascular bone that contains a higher surface area to mass ratio.

Trabeculae – Rod-shaped bone tissue in cancellous bone. Provides lightweight internal support.

Longitudinal Vascular Canal – Canals oriented parallel to the long axis on the bone.

Reticular Vascular Canal – Obliquely oriented vascular canals.

Long Bone Histology – Histologic Ontogenetic Stage (HOS; *Klein and Sander, 2008*) –

HOS 1 - Cortex consists of Type A bone.

-Type A: Non-laminar organization.

HOS 2 - Cortex consists of Type A bone with Type B bone laid down in the outer cortex.

-Type B: Vascularization is mainly longitudinal, and density of vascular canals is very high. The vascular canals are large and essentially circular in cross-section, but with an irregular margin, similar to small erosion cavities of the remodeling zone. However, the small erosion cavities are easily distinguished from primary vascular canals of Type B bone by their resorption margins. Type B bone normally has no true primary osteons developed, and only a thin sheath of lamellar bone lines the vascular canals, indicating that primary osteon formation has started. No secondary osteons or growth marks.

HOS 3 - Cortex consists of Type B bone while in the inner cortex remains of Type A bone can be preserved.

HOS 4 - Cortex consists primarily of Type B bone with Type C bone laid down in the outer cortex.

-Type C: Longitudinal vascular canals in Type C bone are easy to distinguish from those in Type B by a more regularly round margin compared to the irregular longitudinal vascular canals. No secondary osteons or growth marks.

HOS 5 - Cortex consists primarily of Type C bone while in the inner cortex remains of Type B bone can be preserved.

HOS 6 - Cortex consists primarily of Type C bone with Type D bone laid down in the outer cortex.

-Type D: Vascular canals are large, but smaller than in Type C bone tissue. Vascularization is primarily laminar, but a few areas have vermiform or more

reticular organization. In Type D bone tissue, the formation of secondary osteons starts. Growth marks rare.

HOS 7 - Cortex consists primarily of Type D bone while in the inner cortex remains of Type C bone can be preserved.

HOS 8 - Cortex consists primarily of Type D bone with Type E bone laid down in the outer cortex.

-Type E: Very distinctive primary osteons. The secondary osteons between the erosion cavities in the inner cortex are more densely spaced in type E. Spread of secondary osteons into the primary cortex has started by now, resulting in scattered secondary osteons that may extend in some specimens up to the middle of the primary cortex. Growth marks may occur.

HOS 9 - Cortex consists primarily of Type E bone while in the inner cortex remains of Type D bone can be preserved.

HOS 10 - Cortex consists primarily of Type E bone with Type F bone laid down in the outer cortex.

-Type F: Remodeling by secondary osteons has increased significantly, and dense secondary osteons are deposited at least up to the middle to inner two-thirds of the primary cortex. In Type F, growth marks are usually apparent. In some specimens a change from fibrolamellar to lamellar-zonal bone and the deposition of an EFS are initiated.

HOS 11 - Cortex consists primarily of Type F bone while in the inner cortex remains of Type E bone can be preserved.

HOS 12 - Cortex consists primarily of type F bone tissue while in the outer cortex an EFS is deposited.

HOS 13 - Cortex consists of type G bone tissue which means it is nearly completely remodeled by secondary osteons.

-Type G: Almost complete remodeling of the primary cortex by secondary osteons.

Table 3: Diplodocidae Mass Table (log Body Mass = 2.955 • log Femur Circumference − 4.166; Mazzetta et al. [2004]).

Genus	Specimen Number	Femur Circumference (mm)	Body Mass (kg)	Mass - Pneumaticity (kg)
Apatosaurus	MWC "Moffat Co. Apato."	908.05	49378.59631	44440.73667
Apatosaurus	SMA "Jacq"	810	26827.06928	24144.36235
Apatosaurus	AMNH 613	805	26340.67055	23706.60349
Apatosaurus	AMNH 606	795	25385.44993	22846.90494
Apatosaurus	AMNH 7539	766	22745.52756	20470.9748
Apatosaurus	AMNH 353	725	19332.98035	17399.68231
A. louisae	CM 30766	701	17502.36514	15752.12863
A. excelsus	CM 21785	690	16703.17623	15032.8586
Apatosaurus	CM 85	678	15859.29017	14273.36116
A. excelsus	CM 87	650	14000.9972	12600.89748
Apatosaurus	CM 566	626	12527.86759	11275.08083
Apatosaurus	CM 33976	600	11051.89995	9946.709959
Apatosaurus	P25112	555	8777.801694	7900.021524
Apatosaurus	OMNH 01667	513	6956.5965	6260.93685
Apatosaurus	KUVP 1351	453	4816.928356	4335.235521
Apatosaurus	BS 157	349	2228.687292	2005.818563
Apatosaurus	CMNH 10039	310	1570.26809	1413.241281
Apatosaurus	USNM 4797	288	1263.29507	1136.965563
Apatosaurus	BYU 601-17103	216	539.896901	485.9072109
Apatosaurus	YPM 5862	184.15	336.963175	303.2668575
Apatosaurus	MWC 5439	148	176.6539566	158.9885609
Apatosaurus	MOR 957 7-16-92-30	125	107.2430331	96.5187298
diplodocid inteterminate	SMM P84.15.2	120	95.05622917	85.55060625
D. "hayi"	HMNS 175	590	10516.4145	9464.77305
Diplodocus	USMN 10865	564	9205.126313	8284.613681
Diplodocus	TMM 993-1	551	8592.172245	7732.95502
D. carnegii	CM 94	540	8095.12502	7285.612518
Diplodocus	BYU 725-13643	536	7919.211712	7127.290541
Diplodocus	BYU 725-13369	513	6956.5965	6260.93685

D. carnegii	CM 84	510	6837.067544	6153.36079
Diplodocus	BYU Fe-4-DM197	490	6074.764083	5467.287674
Diplodocus	AMNH 435	458	4975.737808	4478.164027
Diplodocus	BYU 725-11421	456	4911.804923	4420.624431
Diplodocus	AMNH 7539	455	4880.043319	4392.038987
Diplodocus	BYU 725-12155	455	4880.043319	4392.038987
Diplodocus	BB 761	451	4754.355816	4278.920235
Diplodocus	BYU Fe-5-DM172	435	4273.028154	3845.725339
Diplodocus	AMNH 5855	410	3587.37103	3228.633927
Diplodocus	MOR 592-35	409	3561.577304	3205.419574
D. longus	CM 30762	387	3024.72504	2722.252536
Diplodocus	BYU 725-16569	385	2978.766464	2680.889817
Diplodocus	MOR 790 7-23-95-122	371.5	2680.577713	2412.519942
Diplodocus	BYU 725-16610	365	2544.341575	2289.907418
Diplodocus	MOR 790 7-5-95-7	362	2483.04063	2234.736567
Diplodocus	BB 463	361	2462.826294	2216.543665
Diplodocus	BYU 725-4889	354	2324.36667	2091.930003
Diplodocus	BYU 725-9026	350	2247.610597	2022.849537
Diplodocus	USMN 337871	325	1805.574164	1625.016747
D. longus	CM 21788	317	1677.374822	1509.63734
D. longus	CM 33991	315	1646.295103	1481.665593
Diplodocus	OMNH 1793	254	871.5325918	784.3793326
Diplodocus	DNM 3781	243	764.6567709	688.1910938
Diplodocus	BYU 725-13670	162	230.7368014	207.6631213
diplodocid inteterminate	P.84.15.2	120	95.05622917	85.55060625

Table 4: The Sauropod Ontogeny Scale (SOS).

	Stage 1	Stage 2	Stage 3	Stage 4
HOS	>4	7	8	12+
Postparietal Aperture	?	Present	Present	Absent
LAGs	?	2-6	8	24+
Cervical Pneumatic Architecture	Acamerate With Shallow Fossae (4-8 mm)	Procamerate to Camerate With Deepening Fossae (7-24 mm)	Camerate With Increasing Depth & Abundance Of Fossae & Foramina	Camerate With Extensive & Numerous Fossae & Foramina
Cervical Pneumaticity (CAT Scan)	No Internal Structures	Camerae & Camellae	Thinning Median Septa With Camerae And Camellae	?
Dorsal Pneumaticity (CAT Scan)	?	Thinning Median Septa With Camerae	Thinning Median Septa With Camerae And Camellae	Extensive Camerae In Centrum & Arch
Ant. Cervical Bifurcation	No Bifurcation	No Bifurcation	Notched to Weakly Bifurcated	Fully Bifurcated
Post. Cervical Bifurcation	No Bifurcation	Weakly Bifurcated	Narrow Bifurcation	Fully Bifurcated
Ant. Dorsal Bifurcation	No Bifurcation	Narrow Bifurcation	Narrow Bifurcation	Fully Bifurcated
Post. Dorsal Bifurcation	No Bifurcation	Narrow Bifurcation	Bifurcated	Fully Bifurcated
Ant. Caudal Bifurcation	No Bifurcation	No Bifurcation	No Bifurcation	Fully Bifurcated
Neural Spine Trabeculae	?	≤ 1	≥ 3	?

(mm)

Femoral Head Orientation	?	18° - 12°	8° - 6°	0°
4th Trochanter Position	Proximal	Proximal	Proximal To Mid-Diaphysis	Mid-Diaphysis
Medial Condyle	Not Pronounced	Ventrally Expanding	Laterally Expanding	Greatly Pronounced
Femur Length (mm)	200	1,000 – 1,200	1,250	1,450+
Body Mass (kg)	>100	2,200 – 2,250	3,200	7,200+

REFERENCES CITED

Abramoff MD., Magalhaes P.J., Ram S.J. 2004. Image Processing with ImageJ. Biophotonics International, volume 11, issue 7, pp. 36-42.

Balanoff A.M., Bever G.S., Ikejiri T. 2010. The braincase of *Apatosaurus* (Dinosauria: Sauropoda) based on computed tomography of a new specimen with comments on variation and evolution in sauropod neuroanatomy. American Museum Novitates, 1-32.

Berman D.S., McIntosh J.S. 1978. Skull and relationships of the Upper Jurassic sauropod *Apatosaurus* (Reptilia, Saurischia).

Bonnan M.F. 2004. Morphometric analysis of humerus and femur shape in Morrison sauropods: implications for functional morphology and paleobiology. Paleobiology, 30: 444-470.

Campione N.E., Evans D.C. 2011. Cranial growth and variation in edmontosaurs (Dinosauria: Hadrosauridae): implications for latest Cretaceous megaherbivore diversity in North America. PLoS One, 6(9), e25186.

Campione N.E., Evans D.C. 2012. A universal scaling relationship between body mass and proximal limb bone dimensions in quadrupedal terrestrial tetrapods. Bmc Biology, 10: 60.

Carr T.D. 1999. Craniofacial ontogeny in tyrannosauridae (Dinosauria, Coelurosauria). Journal of Vertebrate Paleontology, 19: 497-520.

Carballido J.L., Sander P.M. 2013. Postcranial axial skeleton of *Europasaurus holgeri* (Dinosauria, Sauropoda) from the Upper Jurassic of Germany: implications for sauropod ontogeny and phylogenetic relationships of basal Macronaria. Journal of Systematic Palaeontology, (ahead-of-print), 1-53.

Carballido J.L., Marpmann J.S., Schwarz-Wings D., Pabst B. 2012. New information on a juvenile sauropod specimen from the Morrison Formation and the reassessment of its systematic position. Palaeontology, 55: 567-582.

Castanet J., Francillon-Vieillot H., Meunier F.J., De Ricqles A. 1992. Bone and lndividual Aging. Bone: A Treatise Volume 7: 245.

Cope E.D. 1877. On a gigantic saurian from the Dakota Epoch of Colorado. Palaeontological Bulletin 25:5-10.

Curry K.A. 1999. Ontogenetic histology of *Apatosaurus* (Dinosauria: Sauropoda): new insights on growth rates and longevity. Journal of Vertebrate Paleontology, 19: 654-665.

De Ricqlès A., Meunier F.J., Castanet J., Francillon-Vieillot H. 1991. Comparative microstructure of bone. Bone, 3: 1-78.

D'Emic M.D., Foreman B.Z. 2012. The beginning of the sauropod dinosaur hiatus in North America: insights from the Lower Cretaceous Cloverly Formation of Wyoming. Journal of Vertebrate Paleontology, 32(4), 883-902.

Dodson P. 1975. Taxonomic implications of relative growth in lambeosaurine hadrosaurs. Systematic Biology, 24(1), 37-54.

Erickson G.M. 2005. Assessing dinosaur growth patterns: a microscopic revolution. Trends in ecology & evolution, 20(12), 677-684.

Erickson, G.M., Rogers, K.C., Yerby, S.A. 2001. Dinosaurian growth patterns and rapid avian growth rates. Nature, 412: 429-433.

Evans D.C., Forster C.A., Reisz R.R. 2005. The type specimen of *Tetragonosaurus erectofrons* (Ornithischia: Hadrosauridae) and the identification of juvenile Lambeosaurines. In: Currie PJ, Koppelhaus EB, eds. Dinosaur Provincial Park. Bloomington: Indiana University Press. pp 349-366.

Francillon-Vieillot H., De Buffrénil V., Castanet J., Géraudie J, Meunier F.J, Sire J.Y., Zylberberg L., De Ricqlès A. 1990. Microstructure and mineralization of vertebrate skeletal tissues. Skeletal biomineralization: patterns, processes and evolutionary trends 175-234.

Gilmore C.W. 1925. A nearly complete articulated skeleton of *Camarasaurus*, a saurischian dinosaur from the Dinosaur National Monument, Utah. Carnegie Institute.

Gilmore C.W. 1936. Osteology of *Apatosaurus* with special reference to specimens in the Carnegie Museum. Memoirs of the Carnegie Museum 11: 175-300.

Grey H. 1858. Anatomy: descriptive and surgical. London: Parker & Son. pp. 983.

Griebeler E.M., Klein N., Sander P.M. 2013. Aging, Maturation and Growth of Sauropodomorph Dinosaurs as Deduced from Growth Curves Using Long Bone Histological Data: An Assessment of Methodological Constraints and Solutions. PLOS ONE, 8(6), e67012.

Harris J.D. 2006a. Cranial osteology of *Suuwassea emilieae* (Sauropoda: Diplodocoidea: Flagellicaudata) from the Upper Jurassic Morrison Formation of Montana, USA. Journal of Vertebrate Paleontology, 26: 88-102.

Harris J.D. 2006b. The significance of *Suuwassea emilieae* (Dinosauria: Sauropoda) for flagellicaudatan intrarelationships and evolution. Journal of Systematic Palaeontology, 4: 185-198.

Hatcher J.B. 1901. *Diplodocus* Marsh: its osteology, taxonomy, and probable habits, with a restoration of the skeleton. Carnegie institute.

Hatcher J.B. 1903. Osteology of *Haplocanthosaurus* with additional remarks on *Diplodocus*. Memoirs Carnegie Museum, 1: 1-75.

Hedrick B.P., Tumarkin-Deratzian A.R., Dodson P. 2012. Bone microstructure and relative age of the holotype specimen of the diplodocoid sauropod dinosaur *Suuwassea emilieae*. Acta Palaeontologica Polonica.

Holland W.J., 1924. The skull of *Diplodocus*. Memoirs of the Carnegie Museum 9: 379-403.

Hopson J.A., 1975. The evolution of cranial display structures in hadrosaurian dinosaurs. Paleobiology, 1: 21-43.

Hopson J.A. 1979. Paleoneurology; pp. 39–146 in C. Gans (ed.), Biology of the Reptilia Volume 9: Neurology A. Academic Press, London.

Horner J.R., de Ricqlès A., Padian K. 2000. Long bone histology of the hadrosaurid dinosaur *Maiasaura peeblesorum*: growth dynamics and physiology based on an ontogenetic series of skeletal elements. Journal of Vertebrate Paleontology, 20: 115-129.

Horner, J. R., de Ricqlès, A., & Padian, K. 2010. Variation in dinosaur skeletochronology indicators: implications for age assessment and physiology.

Horner J.R., Goodwin M.B. 2006. Major cranial changes during *Triceratops* ontogeny. Proceedings of the Royal Society B: Biological Sciences, 273: 2757-2761.

Horner J.R., Goodwin M.B. 2009. Extreme cranial ontogeny in the Upper Cretaceous dinosaur *Pachycephalosaurus*. PLoS One, 4: e7626.

Horner J.R., Padian K. 2004. Age and growth dynamics of *Tyrannosaurus rex*. Proceedings of the Royal Society of London. Series B: Biological Sciences, 271: 1875-1880.

Huttenlocker A.K., Woodward H.N., Hall B.K. 2013. The biology of bone. In: Bone Histology of Fossil Tetrapods: Advancing Methods, Analysis, and Interpretation, edited by K. Padian, and ET Lamm. Berkeley: University of California Press, 13-34.

Janensch W. 1935. Die Schädel der Sauropoden *Brachiosaurus, Barosaurus* und *Dicraeosaurus* aus den Tendaguruschichten Deutsch-Ostafrikas (Anfang). Palaeontographica-Supplementbände, 2: 145-248.

Janensch W. 1929. Die Wirbelsaule der Gattung *Dicraeosaurus*. Palaeontographica, Supplement 7 (I) 2:1-34.

Klein N., Sander M. 2008. Ontogenetic stages in the long bone histology of sauropod dinosaurs. Paleobiology, 34: 247-263.

Knoll F., Witmer L.M., Ortega F., Ridgely R.C., Schwarz-Wings, D. 2012. The braincase of the basal sauropod dinosaur *Spinophorosaurus* and 3D reconstructions of the cranial endocast and inner ear. PloS one, 7(1), e30060.

Lee A.H., Werning, S. 2008. Sexual maturity in growing dinosaurs does not fit reptilian growth models. Proceedings of the National Academy of Sciences, 105(2), 582-587.

Lehman T.M., Woodward H.N. 2008. Modelling growth rates for sauropod dinosaurs. Paleobiology 34: 264–281.

Lovelace D.M., Hartman S.A., Wahl W.R. 2007. Morphology of a specimen of *Supersaurus* (Dinosauria, Sauropoda) from the Morrison Formation of Wyoming, and a re-evaluation of diplodocid phylogeny. Arquivos do Museu Nacional, Rio de Janeiro, 65: 527-544.

Lull R.S. 1919. The sauropod dinosaur *Barosaurus* Marsh: redescription of the type specimens in the Peabody Museum, Yale University (Vol. 6). Connecticut Academy of Arts and Sciences.

Marpmann J.S., Carballido J.L, Sander P.M., Knötschke N. 2014. Cranial anatomy of the Late Jurassic dwarf sauropod *Europasaurus holgeri* (Dinosauria, Camarasauromorpha): ontogenetic changes and size dimorphism. Journal of Systematic Palaeontology (advance online publication) DOI:10.1080/14772019.2013.875074

Marsh O.C. 1877. Notice of new dinosaurian reptiles from the Jurassic Formation. American Journal of Science 14:514-516.

Mazzetta G.V., Christiansen P., Farina, R.A. 2004. Giants and bizarres: body size of some southern South American Cretaceous dinosaurs. Historical Biology, 16(2-4), 71-83.

McIntosh J.S. 1981. Annotated catalogue of the dinosaurs (Reptilia, Archosauria) in the collections of Carnegie Museum of Natural History.

McIntosh, J.S. 1990. Species determination in sauropod dinosaurs with tentative suggestions for their classification. Dinosaur systematics: approaches and perspectives, 53-69.

McIntosh, J.S. 2005. The genus *Barosaurus* Marsh (Sauropoda, Diplodocidae). Thunder-Lizards: The Sauropodomorph Dinosaurs: Indiana University Press, Bloomington, 38-77.

Michelis I. 2004. Taphonomie des Howe Quarry's (Morrison-Formation, Oberer Jura), Bighorn County, Wyoming, USA. Unpublished PhD thesis, Institute of Palaeontology, University of Bonn, 41 pp.

Mook, C.C. 1917. The fore and hind limbs of *Diplodocus*. Bulletin of the American Museum of Natural History 37: 815-819.

Myers T.S. 2004. Taphonomy of the Mother's Day Quarry: Implications for Gregarious Behavior in Sauropod Dinosaurs. MS thesis, University of Cincinnati, Cincinnati.

Nash J.F. 1950. Equilibrium Points in N-person Games. Proceedings of the National Academy of Sciences 36 (36): 48-9.

Osborn H.F., Mook C.C. 1921. *Camarasaurus*, *Amphicoelias*, and other sauropods of Cope. Memoirs of the American Museum of Natural History (new series) 3: 249-387.

Ostrom, J.H., McIntosh J.S. 1966. Marsh's Dinosaurs. Yale University Press, New Haven and London. 388 pages.

Padian K., de Ricqlès A.J., Horner J. R. 2001. Dinosaurian growth rates and bird origins. Nature, 412(6845), 405-408.

Padian K., Lamm, E.T. (Eds.). 2013. Bone Histology of Fossil Tetrapods: Advancing Methods, Analysis, and Interpretation. Univ of California Press.

Remes K. 2009. Taxonomy of Late Jurassic diplodocid sauropods from Tendaguru (Tanzania). Fossil Record, 12, 23–46.

Salgado L., Bonaparte J.F. 1991. Un nuevo saur´opodo Dicraeosauridae, *Amargasaurus cazaui* gen. et sp. nov., de la Formaci´on La Amarga, Neocomiano de la provincia del Neuqu´en, Argentina. Ameghiniana, 28: 333-346.

Sampson S.D., Ryan M.J., Tanke D.H. 1997. Craniofacial ontogeny in centrosaurine dinosaurs (Ornithischia: Ceratopsidae): taxonomic and behavioral implications. Zoological Journal of the Linnean Society 121: 293-337.

Sander P.M., Tuckmantel C. 2003. Bone lamina thickness, bone apposition rates, and age estimates in sauropod humeri and femora. Palaontologische Zeitschrift 77:161–172.

Sander PM, Christian A, Clauss M, Fechner R, Gee CT, Griebeler E-M, Gunga HC, Hummel J, Mallison H, Perry SF, Preuschoft H, Rauhut OWM, Remes K, Tütken T, Wings O, Witzel U. 2011. Biology of the sauropod dinosaurs: the evolution of gigantism. Biological Review 86: 117-155.

Scannella J.B., Horner J.R. 2010. Torosaurus Marsh, 1891, is Triceratops Marsh, 1889 (Ceratopsidae: Chasmosaurinae): synonymy through ontogeny. Journal of Vertebrate Paleontology, 30: 1157-1168.

Scannella J.B., Fowler D.W. 2014. A stratigraphic survey of *Triceratops* localities in the Hell Creek Formation, northeastern Montana (2006–2010). Through the End of the Cretaceous in the Type Locality of the Hell Creek Formation in Montana and Adjacent Areas: Geological Society of America Special Paper, 503.

Schwarz D., Fritsch G. 2006. Pneumatic structures in the cervical vertebrae of the Late Jurassic Tendaguru sauropods Brachiosaurus brancai and Dicraeosaurus. Eclogae Geologicae Helvetiae, 99: 65-78.

Schwarz-Wings D., Frey E. 2008. Is there an option for a pneumatic stabilization of sauropod necks?–an experimental and anatomical approach. Palaeontologia Electronica, 11: 17A.

Schwarz D., Frey E., Meyer, C.A. 2007. Pneumaticity and soft-tissue reconstructions in the neck of diplodocid and dicraeosaurid sauropods. Acta Palaeontologica Polonica, 52(1), 167.

Schwarz D., Ikejiri T., Breithaupt B.H., Sander P.M., Klein N. 2007. A nearly complete skeleton of an early juvenile diplodocid (Dinosauria: Sauropoda) from the lower Morrison formation (Late Jurassic) of North Central Wyoming and its implications for early ontogeny and pneumaticity in sauropods. Hist Biol 19:225–253.

Stein, K., M. Sander. 2009. Histological core drilling: a less destructive method for studying bone histology. In: Methods In Fossil Preparation: Proceedings of the First Annual Fossil Preparation and Collections Symposium, pp. 69-80.

Tschopp E., Mateus, O. 2012. The skull and neck of a new flagellicaudatan sauropod from the Morrison Formation and its implication for the evolution and ontogeny of diplodocid dinosaurs. Journal of Systematic Palaeontology, (ahead-of-print), 1-36.

Upchurch P., Barrett P.M. Dodson P. 2004. Sauropoda. Pp. 259–322 in D. B.Weishampel, P. Dodson & H. Osmolska (eds) The Dinosauria. Second edition. University of California Press, Berkeley.

Upchurch P., Tomida Y., Barrett P.M. 2004. A new specimen of *Apatosaurus ajax* (Sauropoda: Diplodocidae) from the Morrison Formation (Upper Jurassic) of Wyoming, USA. National Science Museum Monographs, 26: i-118.

Wedel M.J., Cifelli R.L., Sanders R.K. 2000. Osteology, paleobiology, and relationships of the sauropod dinosaur *Sauroposeidon*. Acta Palaeontologica Polonica, 45: 343-388.

Wedel M.J. 2003. The evolution of vertebral pneumaticity in sauropod dinosaurs. Journal of Vertebrate Paleontology, 23: 344-357.

Wedel M.J. 2005. Postcranial skeletal pneumaticity in sauropods and its implications for mass estimates. The sauropods: evolution and paleobiology. University of California Press, Berkeley, 201-228.

Wedel M.J. 2009. Evidence for bird-like air sacs in saurischian dinosaurs. Journal of Experimental Zoology A 311: 1-18.

Wedel M.J., Taylor M.P. 2013. Neural spine bifurcation in sauropod dinosaurs of the Morrison Formation: ontogenetic and phylogenetic implications. Palarch's Journal of Vertebrate Palaeontology 10(1): 1-34. ISSN 1567-2158.

Whitlock J.A., Harris J.D. 2010. The dentary of *Suuwassea emilieae* (Sauropoda: Diplodocoidea). Journal of Vertebrate Paleontology, 30: 1637-1641.

Whitlock J.A., Wilson J.A., Lamanna M.C. 2010. Description of a nearly complete juvenile skull of *Diplodocus* (Sauropoda: Diplodocoidea) from the Late Jurassic of North America. Journal of Vertebrate Paleontology, 30: 442-457.

Whitlock J.A. 2011. A phylogenetic analysis of Diplodocoidea (Saurischia: Sauropoda). Zoological Journal of the Linnean Society, 161: 872-915.

Wilson J.A., Smith M. 1996. New remains of *Amphicoelias* Cope (Dinosauria: Sauropoda) from the Upper Jurassic of Montana and diplodocoid phylogeny. Journal of Vertebrate Paleontology, 16(3 Suppl.): 73A.

Wilhite R. 1999. Ontogenetic variation in the appendicular skeleton of the genus *Camarasaurus*. Master's thesis. Brigham Young University, Provo, Utah.

Wilhite R. 2003. Biomechanical reconstruction of the appendicular skeleton in three North American Jurassic sauropods. Ph.D. dissertation. Louisiana State University, Baton Rouge.

Wilhite R., Curtice B. 1998. Ontogenetic variation in sauropod dinosaurs. Journal of Vertebrate Paleontology 18(Suppl. to No. 3):86A.

Woodward H.N., Lehman T.M. 2009. Bone histology and microanatomy of *Alamosaurus sanjuanensis* (Sauropoda: Titanosauria) from the maastrichtian of Big Bend National Park, Texas. Journal of Vertebrate Paleontology, 29: 807-821.

Woodruff, D.C., Fowler, D.W. 2012. Ontogenetic influence on neural spine bifurcation in Diplodocoidea (Dinosauria: Sauropoda): a critical phylogenetic character. *Journal of morphology*, *273*(7), 754-764.

Woodruff, D.C., Fowler, D.W., Horner, J.R. 2013. Changes in vertebral morphology associated with histologic data support significant change through ontogeny in diplodocid sauropods. Journal of Vertebrate Paleontology 32(5, abstracts vol): 239

Woodruff, D.C, Fowler, D.W. 2014. The Effects Of Ontogeny In Regards To Morrison Sauropod Diversity. Mid-Mesozoic: The Age Of Dinosaurs In Transition (abstract volume).

SUPPLEMENTARY INFORMATION

The material contained within this Supplemental Information serves to addresses comments, points, and questions raised by Wedel and Taylor (2013) concerning the vertebral ontogentic changes reported by Woodruff and Fowler (2012). The structural hierarchy of this Supplemental Information initiates with sauropod genera followed by particular specimens highlighting said topics.

Diplodocus

Diplodocus cervical vertebra MOR 790 8-10-96-204: Serial and ontogenetic mis-assignment?

The Mother's Day quarry is located in the upper equivalent Salt Wash Member of the Morrison Formation in south central Montana (Myers, 2004). It contains a bone bed of juvenile sauropod bones that has been excavated by the MOR and the CMC. The material collected by both institutions to date represents fifteen individuals (G. Storrs per. comm.) that are believed to belong to *Diplodocus* sp. (Myers, 2004; Myers and Storrs, 2007; Woodruff and Fowler, 2012). A general lack of articulated vertebrae primarily only allows for examination of individual elements whose precise serial position and exact ontogenetic stage are relatively circumstantial. The Mother's Day quarry contains an accumulation of an immature social group (Myers, 2004; Myers and Storrs, 2007), but the size of individuals (and possibly their level of maturity) vary slightly. The largest femur collected by the CMC is 112 cm long (CMC VP7747, upper juvenile to lower subadult [Curry, 1999; Myers, 2004]), while the smallest and largest collected by the

MOR are 102 cm (MOR 790 7-5-95-7, juvenile [Curry, 1999]) and 120 cm (MOR 790 7-23-95-122, subadult [Curry, 1999]). Because of this size distribution it is not surprising that there may also be slightly differing ontogenetic stages present which may result in the varying centrum lengths. A large portion of the cervical vertebrae examined exhibit partially closed neurocentral synostosis, while a majority of the dorsal vertebrae exhibited open synostosis. Many of the dorsal vertebrae are represented by only the neural processes. In almost all observed cervical vertebrae the neural spine rises and tapers into a smooth and rounded top. However, the largest prepared anterior cervical (MOR 790 8-21-95) bears a shallow "U"-shaped bifurcation. The neural spines are bifurcated in all examined dorsals, and in a majority the bifurcation is narrow and extends downward from the apex of the neural spine about ¼ of the neural spine length with a sharp and pronounced median tubercle. In the largest prepared anterior dorsal (MOR 790 8-21-94-238), the neural spine is greatly bifurcated with a steep "U"-shape that accounts for ~20% of the entire vertebral height.

However, despite the voluminous material of cranial and postcranial elements that support an overall immature status, there is some suggestion of adult sized *Diplodocus* specimens at the Mother's Day Quarry (Wedel and Taylor, 2013). As of this publication no skeletal material (such as a femur) collected by the CMC or the MOR indicates any animals larger than juvenile status (G. Storrs, per. comm.; Figure 1). Specifically, it has been suggested that Mother's Day Quarry cervical (MOR 790 8-10-96-204) examined in Woodruff and Fowler (2012) could be from a large and potentially fully mature animal because 1) the neural arches and cervical ribs are fused, 2) the elongation index is

indicative of an adult, and 3) the morphology is indistinguishable from that of an adult C4 or C5.

This analysis would strongly maintain that vertebral synostosis alone should not be used to infer age. Both Brochu (1996; 1999) and Ikejiri (2012) demonstrated that crocodilians can have drastically delayed or even a complete lack of vertebral synostosis within presacral vertebrae. This has been demonstrated before in dinosaurs, particularly within a remarkable sub-adult specimen of *Triceratops* (MOR 3027 [Horner and Lamm, 2011]; J. Scannella per. comm.) which is nearly devoid of any cranial and postcranial fusion.

We would suggest that fusion of the neural arch or ` should not be indicative of maturity. In the case of two *Apatosaurus* specimens, CM 3390 (*Apatosaurus* sp.) and CM 555 (*Apatosaurus excelsus*), the vertebral series of CM 3390 is significantly smaller than that of CM 555, yet the neurocentral fusion is just visible opposed to the completely unfused series of CM 555. As Brochu (1996; 1999) and Ikejiri (2012) demonstrated and inferred, neurocentral fusion in Dinosauria might be sporadic and should never be used to infer maturity (Figure 2).

Elongation Index: Does a high value indicate maturity?

A further claim used to support MOR 790 8-10-96-204 being from an adult animal is the vertebra's elongation index (Wedel and Taylor, 2013). Elongation index (EI) of a vertebra is a ratio between the length of the centrum divided by the cotyle diameter. The EI of MOR 790 8-10-96-204 is 4.24, while the EI of C4 and 5 from CM 84

are 3.57 and 3.96 respectfully. However, this analysis questions whether or not is EI is a suitable measure of ontogenetic assessment. To determine this, the EI was calculated for four *Diplodocus*, four *Apatosaurus*, and four *Barosaurus lentus* cervical series from several potential ontogenetic stages (Table 1). The results of these calculations show that (presumably) ontogenetically and individually, EI is extremely variable (Table 1). For *Diplodocus*, in the smallest form (SMA 0003), C2-4 range in the mid to low 2's; however from C5-15 the EI suddenly increases into the 6 range and even as high as 7.86 in C10. In a larger specimen (SMA 0004), the anterior most cervical remain rather low (in the 2 to high 3 range), but as before from C5-14 the EI is dramatically higher (particularly from C6-C9 where the EI remains in the low 7's). This is in marked contrast to the adult form (CM 84) in which from C2-C8 the EI slowly rises from 3.06 to 4.46, then slowly descends at C7 through C15 from 4.25 to finally 2.42. For the smallest *Apatosaurus* cervical series (CM 555) C2-4 average in the mid 2's, but suddenly increases up to 4.5 in C5, and from C8-14 gradually declines from 3.04 to 1.45. In larger forms (CM 563 and NSMT-PV 20375) C3-10 generally goes from mid 3 gradually down to the high 1's. It is interesting to note that although CM 563 is the smaller of the two, it cervical EI is generally higher than that of NSMT-PV 20375. While in the largest form (CM 3018) the EI rarely goes above 3. In the case of *Barosaurus lentus*, the EI is even more sporadic. In the two smallest forms (AMNH 7530 and AMNH 7535) the EI starts in the high 5's, and suddenly declines. In the case of AMNH 7535 the EI goes from 5.8 in C2 down to 4.45 in C4, up to 6.66 in C7 and immediately proceeded by 4.61 in C8, up to 9.36 in C13, and back down to 6.87 in C14. In a much larger specimen (AMNH 6341), the EI from C8-

C16 generally alternates from the high 4's to low 5's. While in the largest form (YPM 429) from C13-C16 the EI drops from 4.22 to 1.97.

While it is extremely difficult and not definitively or particularly accurate to assign a pattern based on four individuals, the elongation data would tentatively suggest that in the case of *Diplodocus* the entire cervical series (particularly the mid and posterior cervical) rapidly elongates in the smaller body lengths. In slighter larger body lengths the primary area of elongation is in the mid cervical vertebrae. Finally in the adult stage the degree and ratio of elongation is substantially lower. Throughout the *Apatosaurus* series it would appear that EI remains fairly constant with greater elongation in the anterior most cervicals while tapering to the posterior most. The trends of *Barosaurus lentus* are much more sporadic. In the smallest individuals (AMNH 7530 and AMNH 7535), the anterior most, mid, and posterior most cervicals of both specimens appear to experience rapid elongation; while in the largest forms (AMNH 6341 and YPM 429) the mid to posterior cervical vertebrae experience an EI ratio decrease. So if the EI trends among the three genera are indeed correct, that this indicates that higher EIs are potentially more indicative of an immature condition. These results support the findings of Woodruff and Fowler (2012) in that juvenile diplodocid vertebrae attain a certain vertebral length early in ontogeny, and after that point growth is primarily directed at width throughout the remainder of ontogeny (resulting in a high EI during early ontogeny, and a lower EI in later life).

The overall vertebral morphology of MOR 790 8-10-96-204

Figure 2 of Woodruff and Fowler (2012) illustrates the cervical morphology of *Mamenchisaurus*, MOR 790 7-23-95-122, and *Diplodocus carnegii* (CM 84) to demonstrate how juvenile morphology is more reminiscent of a basal form than to its own derived self. In the case of Figure 2, Wedel and Taylor (2013) are correct that the CM 84 cervical is C12, while the *Mamenchisaurus* cervical and MOR 790 7-23-95-122 are both more anterior. In a much more accurate depiction of this figure, Wedel and Taylor (2013) substitute the previously used CM 84 C12 for C5. Thus using this new depiction it is claimed that MOR 790 7-23-95-122 is now indistinguishable from the adult vertebral condition, and thus it is not a juvenile nor should a juvenile exhibit morphology expressed in an ancestor. While we agree with this more serially accurate depiction, we disagree that MOR 790 7-23-95-122 and C5 from CM 84 are indistinguishable from one another (Figure 3). While the centrum of MOR 790 7-23-95-122 and CM 84 both bear a large pneumatic fossa and inclined condyles and cotyles, the great curvature of the ventral portion of the centrum in MOR 790 7-23-95-122 is more like that of the *Mamenchisaurus* cervical. MOR 790 7-23-95-122 does have long, overhanging prezygapophyses like those of CM 84; however in MOR 790 7-23-95-122 the orientation of the prezygapophyses is more horizontal as in *Mamenchisaurus* than to the upturning curvature of the prezygapophyses from CM 84. Both MOR 790 7-23-95-122 and CM 84 have postzygapophyses that do not directly overhang the cotyle such as *Mamenchisaurus*. But the greater anterior curvature in the posterior portion of the neural arch in MOR 790 7-23-95-122 creates much more overhang than observed in CM 84.

Wedel and Taylor (2013) conclude that the only remaining difference between MOR 790 7-23-95-122 and CM 84 is the shape of the neural spine, and that this difference is serially variable. We on the other hand say that this feature in fact illustrates our point. If MOR 790 7-23-95-122 is indeed serially equivalent to CM 84, then their vertebral morphologies should be nearly identical. In all three vertebra the incline of the neural spine is rather steep. In the case of C5 from CM 84, after the neural spine height has been attained, the spine quickly descends into the postzygapophyses creating a very strong neural spine peak. However in MOR 790 7-23-95-122 once the neural spine height is attained, there is a small shelf, proceeded by a gentle curvature to the postzygapophyses, which is very similar to that of *Mamenchisaurus*. Immature animals expressing ancestral conditions rather than those of adults of their own species have been previously documented in several groups of dinosaurs, and should be of no surprise to be found within sauropods (Rozhdestvenksy, 1965; Fowler et al., 2011; Tsuihiji et al., 2011). In addition MOR 790 7-23-95-122 is very similar to the anterior cervical vertebrae from SMA 0003 and SMA 0004. The morphology of MOR 790 7-23-95-122 indicates that it is not indistinguishable to the adult anterior cervical vertebra condition, but the vertebral variation in MOR 790 7-23-95-122 does display interesting almost intermediate-like morphology that hints at the evolutionary history of the cervical vertebrae (Figure 3).

Diplodocus specimen MOR 592

Collected from the upper Salt Wash Member equivalent of south western Montana, MOR 592 consists of the remains of a fairly complete sub-adult diplodocid pre-sacral vertebral column. At roughly 2/3 the size of both *Apatosaurus ajax* (NSMT-PV

20375 [Upchurch et al., 2004]) and *Diplodocus carnegii* (CM 84, [Hatcher, 1901]), the intermediate morphology of this specimen previously led to some discussion that this specimen represented a new genus. In an analysis of the femur (MOR 592-35, 124.5cm long), Wilson and Smith (1996) take special note of the cylindrical and sub-circular ("stovepipe") morphology of the diaphysis and use this to identify MOR 592 as belonging to the genus *Amphicoelias*. The "stovepipe" diaphysis was once a recognized autapomorphy of *Amphicoelias* (Cope, 1878), however this diaphysis form has since been identified in several specimens of *Diplodocus* (Foster, 2007; McIntosh, 2005; R. Wilhite per. comm.), and thus is no longer a valid autapomorphy.

Wedel and Taylor (2013) claim that the morphology of the cervical and dorsal vertebrae of MOR 592 used in Woodruff and Fowler (2012) are identical to that of CM 84. While in some respects both specimens bear similar morphology, we argue that the two are not indistinguishable (Figure 4). In regards to the anterior cervical MOR 592 7-26-91-143B, the claim is made that the bifurcation of MOR 592 7-26-91-143B is an artifact of serial position rather than ontogeny (Wedel and Taylor, 2013). However MOR 592 7-26-91-143B is most likely C6, and the morphology of the neural spine is widely different from that of C6 from CM 84 (for further descriptions of the varying vertebral morphology consult Woodruff and Fowler, 2012).

In regards to the posterior cervical vertebra MOR 592 8-24-90-91, the narrow bifurcation and centrum are suggested to both represent diagenetic artifacts (Wedel and Taylor, 2013). While this specimen does indeed displays post-depositional distortion attributable to shearing, both the narrow bifurcation and centrum width are seen in other

immature diplodocids, and such we suggest they represent products of ontogeny. The wide “U”-shape bifurcation, the presence of a median tubercule, and the lateral widening of the centrum in CM 84 are all traits that have been elaborated upon through ontogeny.

In respect to the neural spine proportions of the anterior dorsal (MOR 592 8-22-90-15), the height of bifurcation is exactly 1/3 of the overall vertebral height, while in the adult form (CM 84) the bifurcation comprises over 1/3 of the vertebral height. In MOR 592 8-22-90-15, the width of the centrum is 89% the width of bifurcation. While in CM 84 the centrum is 95% of the bifurcation width. So in general proportions these two specimens are alike, but noticeable and distinguishable differences are apparent in the bifurcation morphology. The bifurcation of MOR 592 8-22-90-15 is a steep “V”-shape that terminates with a sharp and narrow bottom. In the bifurcation of CM 84, the bifurcation trough has a much wider “V”-shape. The proximal half of the neural spines have a gentle curvature, opposed to the straight sided spines of MOR 592 8-22-90-15. The greater width of the spines results in a trough termination that is curved and significantly wider. In examining the posterior dorsal vertebrae, there are again similarities, but not indistinguishable. In the posterior dorsal MOR 592 8-22-90-77, the neural spine apices are proportionally bulbous with a slight lateral incline. The bifurcation trough is a rather tall and wide “U”-shape. The total vertebral height is almost 7.5 times the height of bifurcation, and the width of the neural spines is very near to the width of the centrum, with the centrum being just slightly wider. While the morphology of the bifurcation trough of CM 84 is very similar to that of MOR 592 8-22-90-77, other proportions vary. The neural spines themselves are more gracile and taper towards the

apex and lack the lateral incline. From the neural arch the neural spine of CM 84 is much wider and increases in width proximally. In addition the total vertebral height is approximately 6.5 times the height of bifurcation. As for the centrum, it is nearly 1.5 times the width of the neural spines.

Finally in regards to the anterior caudal vertebrae, the claim is made that there is unequivocally no evidence at all of ontogenetic neural spine bifurcation (Wedel and Taylor, 2013). The "bifurcation" reported in the MOR 592 anterior caudal (un-numbered) is anteriorly/posteriorly orientated, and is expressed in other diplodocids (such as *Apatosaurus parvus*, CM 563). The neural spine anterior/posterior projections of MOR 592 (un-numbered) likely represent osteological modifications due to the attachment site of the nuchal ligament. However in anterior view, MOR 592 (un-numbered) does not have a bifurcated neural spine, while the anterior caudal of CM 84 does. Since serial position is well supported, and the evidence does sustain MOR 592 being a sub-adult *Diplodocus*, clearly even within the caudal vertebrae, neural spine bifurcation is ontogenetic (Figure 5).

So while similar, the vertebrae of MOR 592 are not indistinguishable to those of CM 84. With the information attained from MOR 592 (and other similarly 2/3 sized diplodocids), it would appear that once a diplodocid reaches roughly 2/3 its adult length that proportionally (and potentially mechanically) it is near equivalent to the adult form. The forces acting upon a 15 meter and 27 meter animal are more similar than those acting upon a 2 meter and a 15 meter animal. Once a diplodocid reaches that 2/3 sized threshold it has achieved the skeletal adaptations needed to support the large vertebral column (i.e.

bifurcation of the neural spines). From the 2/3 size through the remainder of its life, the animal then modifies the existing structure to deal with the increasing stresses enacted upon it. This explains why the spine bifurcation changes faintly and why the centrum begins to expand along with other proportional changes. At the point of dramatic weight increase, it is far easier to modify a pre-existing structure that to suddenly develop a new feature. It would appear that from a neonate, an immature diplodocid is in a dramatic race to develop the skeletal features needed to support its eventual gigantic girth.

Apatosaurus

CM 3390

The *Apatosaurus louisae* specimen CM 3390 partially consists of a segment of six articulated cervical vertebrae. While exact serial placement of these six is precisely unknown, the morphology of the largest and most posterior of the series (here referred to a “C6” only because it is the sixth cervical of the preserved series) appears to be from the posterior region of the cervical series. These six cervicals were left in the slab matrix, however the neural spines were prepared and can be viewed obliquely. In all known *Apatosaurus* adult cervical series, all mid and posterior cervical vertebrae are strongly bifurcated. However, in the case of CM 3390, the posterior cervical vertebrae neural spines all exhibit shallow spine bifurcation. We believe this to indicate ontogenetic development of neural spine bifurcation in *Apatosaurus*.

CM 555

The other *Apatosaurus* specimen used for study by Woodruff and Fowler (2012) was the *Apatosaurus excelsus* CM 555. Collected from Quarry D in the lower Brushy Basin equivalent in Albany County, Wyoming, CM 555 consists of eleven cervical and two anterior dorsal vertebrae. Roughly similar in size to the *Apatosaurus excelsus* YPM 1980, the anterior cervical vertebrae from CM 555 have a complete lack of neurocentral fusion while the posterior cervical and anterior dorsal vertebrae exhibit neurocentral synostosis (a trait seemingly shared with YPM 1980).

Through the entire vertebral series progressing from the anterior cervicals to the dorsals, bifurcation is absent then insipiently appears, then fully appears and gradually deepens posteriorly. In anterior comparison, in C8 from both CM 555 and YPM 1980, the neural spines have completely differing morphology. In CM 555 the neural spine tapers dorsally and the apex is comprised of two connecting “humps”. In the case of CM 563 the neural spines of C8 are separated, but rather narrow, and the neural spines are fully bifurcated with the bifurcation trough being a very narrow and steep “U”-shape. For YPM 1980 the neural spines are widely offset and the bifurcation trough forms a broad and deep “U”-shape. The progression in neural spine morphology serially through these three fairly complete series demonstrates the development and change of neural spine bifurcation serially and ontogenetically.

Additional Information

Anterior Cervical Bifurcation

Wedel and Taylor (2013) claim that there is no evidence of bifurcated neural spines more anteriorly than C6 in any known North American diplodocid. While it is correct that the anterior most neural spines are damaged and reconstructed from CM 84, YPM 1980, and CM 563, resulting in unknown spine morphology for these specimens, other cervical series from North American diplodocids do show anterior bifurcation. The anterior most cervical neural spines from CM 555 are damaged, yet C4 has clearly evident bifurcation. C5 has weakly expressed bifurcation; while C6 and the remaining vertebrae have fully expressed bifurcation. Within the cervical series of SMA 0003, spine bifurcation is completely absent in C2, yet apparent in C3. In the anterior most cervical vertebrae, C3-C5 are bifurcated (the neural spine of C5 is damaged, yet the bottom most portion of the bifurcation trough is visible). From C6-C7 the neural spines are un-bifurcated, yet the apexes are very broad. Neural spine bifurcation resumes in C9 and is found in the remaining vertebrae. Even within *Barosaurus lentus* we see similar anterior most bifurcation. In AMNH 7530, the neural spine of C2 is not bifurcated, yet the neural spine of C3 clearly is. After C3, the spines of C4 and C5 are broad, but not bifurcated. The remaining cervical vertebrae are on display, and removal to examine the anterior morphology could not be permitted at the time of visitation. A slightly larger specimen AMNH 7535 exhibits similar spine morphology. The neural spine of C2 is slightly damaged at the apex, but the neural spine would appear to be bifurcated (if so it would be the anterior most documentation of spine bifurcation). C3 and C5 are missing, and the

neural spine of C4 is badly damaged. The neural spine of C6 is clearly bifurcated, yet C7-C13 are un-bifurcated. The final vertebra from this specimen, C14, does have a broad neural spine with incipient or weakly expressed bifurcation.

The claim that no North American diplodocids possessed bifurcated neural spines farther than C6 is now shown to be incorrect. In consideration of the damaged neural spine in many of the historic specimens, this is an easily conceivable and believable hypothesis. However thorough examination of several complete or nearly so cervical series, we now see that in diplodocids neural spine bifurcation does generally occur between C3-C5 (Figure 6). It is interesting to see that in the anterior most cervical vertebrae that there is a small span of bifurcation pre and proceeded by a lack of bifurcation. If the hypothesis of Woodruff and Fowler (2012) is correct that bifurcation is developed in sauropods to maintain horizontal lateral mobility, the presence of select anterior most bifurcation might indicate greater cranial mobility. As rightfully demonstrated by Wedel and Taylor (2013), serial position is critical. If serial position was unknown in these specimens then there would be a valid argument to place these bifurcated anterior cervicals more posteriorly. However, as such we can now accurately say and demonstrate that North American diplodocids do indeed have neural spine bifurcation prior to C6, and we would call for the damaged historic specimens to be reconstructed with such.

Camarasaurus Spine Bifurcation

A minor point we would like to bring to light is the recognition of neural spine bifurcation within the basal macronarian *Camarasaurus*. Woodruff and Fowler (2012) note that in specimens from the Kenton Quarry, the neural spines of immature *Camarasaurus* sp. are morphologically similar to immature diplodocids in that the neural spines are short and non-bifurcated. No in depth examination on *Camarasaurus* sp. was carried out in the preliminary analysis (but is currently underway by DCW), but the possibility of *Camarasaurus* spine ontogeny was favored by Wedel and Taylor (2013). While display features can be modified throughout ontogeny (i.e. male Peacock plumage and Cassowary and Helmeted Guinea fowl casques), it would seem unusual that a biomechanical feature could be ontogenetic in one form, yet static in another. In examination of the cervical and dorsal series from the immature *Camarasaurus lentus* (CM 11338), the neural spines are bifurcated, but the depth of bifurcation is shallow and the neural spine apices are much closer together than in a fully mature animal. A slightly larger *Camarasaurus* sp. specimen (JRF 220) has cervical and dorsal neural spines that likewise exhibit shallow bifurcation and narrow neural spines. These features alone have been previously thought to be valid autapomorphies of a new genus (N. Murphy and K. Carpenter pers. comm.). However, since neural spine bifurcation in *Camarsaurus* sp. would likewise appear to be developmentally ontogenetic, we believe that JRF 220 merely represents an immature animal. As such we would strongly call for an ontogenetic analysis coupled with a morphological analysis of JRF 220 before any taxonomic or phylogenetic assumptions are made.

Haplocanthosaurus

Wedel and Taylor (2013) perform a laudable job verifying that the genus *Haplocanthosaurus* is not a juvenile *Apatosaurus* or *Diplodocus* (the specific lines of reasoning will not be addressed here but we strongly recommend referral to their text). Being one of the rarest of Morrison taxa, *Haplocanthosaurus* is known from three species: *H. delfsi*, *H. priscus*, and "*H. utterbacki*". Collected from the lower Brushy Basin, CM 572 (*H. priscus*) and CM 879 ("*H. utterbacki*") both were found meters away from each other in the Marsh-Felch Quarry 1. Based on numerous features CM 879 is assuredly an immature form (however the definitive answer via histology has not been performed as yet), possibly of *H. priscus* (the differences and validity between *H. priscus* and *H. delfsi* shall not be addressed here). This same conclusion was reached by McIntosh and Williams (1988) and Wedel and Taylor (2013). As Wedel (2009) illustrates, CM 572 exhibits widespread neurocentral synostosis, while CM 879 exhibits primarily completely unfused neural arches (similar to CM 555) (however, remember that vertebral fusion is not conclusively indicative of ontogeny within dinosaurs). Though very weakly expressed and exceedingly rare, incipient neural spine bifurcation has been observed within some specimens of *Haplocanthosaurus* (Figure 7). Neural spine bifurcation is observed in a posterior dorsal of CM 879, and within an anterior dorsal of CM 572. We are well aware of the importance of serial position and the morphological differences between such vertebrae, however due to the rarity of this feature and the relative proximity a comparison shall still be made. In a posterior cervical of CM 879, the bifurcation is formed by a connection of two closely spaced "humps" (reminiscent of

bifurcation observed in CM 555). Within an anterior dorsal of CM 572 these "humps" are spaced and the bifurcation trough is a shallow "V"-shape. It would appear that biomechanically *Haplocanthosaurus* did not require neural spine bifurcation as did members of Diplodocidae. In fully conjunction with McIntosh and Williams (1988) and Wedel and Taylor (2013), we would consider "*H. utterbacki*" as a *nomen dubia*, and instead propose for the time being that it represents an immature form of *H. priscus*. In addition to this, the variation between the two specimens would suggest that while incipient, the neural spine bifurcation observed in *Haplocanthosaurus* may also be ontogenetic.

In regards to the phylogenetic assignment of *Haplocanthosaurus*, we would again stress for the care and recognition of ontogenetic stages. In his 2010 analysis of Diplodocoidea, J. Whitlock shows that the character matrix for *Haplocanthosaurus* is a combination of several specimens including CM 879 ("*H. utterbacki*"), CM 572 (*H. priscus*), and CMNH 10380 (*H. delfsi*). While these individuals were included to complete otherwise missing characters from other incomplete specimens, could the taxonomic uncertainty of *Haplocanthosaurus* be due to the fact that the characters states representing it are from a combination of varying ontogenetic stages and potentially separate species?

Questionable Small Statured Diplodocid Taxa

Previous studies on diplodocid ontogeny have questioned and debated the validity of small statured taxa (Woodruff and Fowler, 2012; Hedrick et al., 2012; Wedel and

Taylor, 2013). Previously these forms have been described as possessing unique combinations of basal and derived traits, with such trait combinations being explained as environmental adaptations (Harris, 2006b). In regards to *Suuwassea emilieae* (ANS 21122), some works claim that it is a valid genus, while opposing that it is in fact also not a juvenile animal (Hedrick et al., 2012; Wedel and Taylor, 2013). At times *Suuwassea* ranges from a basal apatosaurinae (Harris and Dodson, 2004), a Laurasian dicraeosaurid (Whitlock and Harris, 2010), to an immature diplodocid (Woodruff and Fowler, 2012).

Some of the debated morphologies of *Suuwassea* include: narrow spine bifurcation, anterior prominence at the dentary symphysis (a ‘‘chin’’), curvature of the tooth row, decreased vertebral pneumaticity, postparietal “foramen”, unfused scapula-coracoid, and elongate pedal phalanges (see Woodruff and Fowler [2012] for the initial ontogenetic suggestion). In regards to *Suuwassea’s* status, Woodruff and Fowler (2012) state that until a histologic analysis, no statements and inferences can be definitive. Hedrick et al. (2012) laudably did just that, and from analysis of the holotype tibia, they conclude that *Suuwassea* is HOS 8-9 out of 13. However from this HOS, Hedrick et al. (2012) concluded that the holotype of *Suuwassea* (ANS 21122) was nearly full grown, had reached sexual maturity, was a valid genus, and that the plesiomorphic characters were not related to immaturity. We remain cautious to these interpretations, and still strongly suggest comparison to the SOS Stage 3 *Diplodocus* MOR 592 for taxonomic clarity Figure 8).

The *Diplodocus* MOR 592 displays the same plesiomorphic characters observed in *Suuwassea*. Originally referred to as *Amphicoelias* on the basis of possessing a

"stovepipe" femur (Wilson and Smith, 1996), and some subsequent discussion on the possibility of being a new genus, this specimen has since been largely recognized and accepted as an immature *Diplodocus* (Woodruff and Fowler, 2012). Aside from the plesiomorphic characters, MOR 592 also has a similar femur length (124.5 cm versus the calculated 135 cm of *Suuwassea* [Hedrick et al., 2012]). Likewise thin sectioning of the MOR 592 femur indicates that it is HOS 9 out of 13. Further, thin sectioning of a thoracic rib of MOR 592 and ANS 21122 records a minimum of eight preserved LAGs in both specimens (Figure 8). Both specimens exhibit similar morphology, both exhibit similar histology, and yet two different interpreted ontogenetic outcomes.

Opposed to the suggestion that MOR 592 should be recognized as a basal diplodocid or a second Laurasian dicraeosaurid (Whitlock and Harris, 2010), the parsimonious explanation is that it is an immature *Diplodocus* (*sensu* Woodruff and Fowler, 2012). Likewise the abundance of commonalities between MOR 592 and ANS 21122 should parsimoniously be indicative of ontogeny (Figure 8), and that both specimens be classified as SOS Stage 3. While the characters between MOR 592 and ANS 21122 arguably denote ontogeny, the specific vertebral morphologies of *Suuwassea* bear more resemblance and commonality to other immature *Apatosaurus* individuals (such as CM 555, YPM 1980, and CM 563). In consideration of the fact that now both morphological and histologic analyses by separate investigating parties (Hedrick et al., 2012; Woodruff and Fowler, 2012; this analysis) have reached comparable results, we formally consider *Suuwassea emilieae* (ANS 21122) as a *nomen dubium*, and synonymize it into the genus *Apatosaurus*.

Implications Regarding Sauropod Growth Rates

The preserved LAG records in the sampled thoracic ribs are testaments to the rapid growth of these dinosaurian individuals. A juvenile diplodocid that is seven meters long is a minimum of six years old, while a twenty-seven meter adult is at least twenty-four years old. These growth rates are not nearly as accelerated as those recorded in other dinosaurs - such as a three meter body length within the first year in *Maiasaura* (Woodward et al., in review) – but they still testify to rapid growth rates. In terms of longevity, sauropods have run the estimation gambit – attaining maximum body size within a decade (Curry, 1999) up to several centuries (and finally sexually mature at seventy-two years of age!; Case, 1978). This titanic variability in longevity estimates has allowed for practically every possible life history strategy, and sadly little consensus. In lieu of complete life histories or growth series, studies that incorporate more individual life history data are largely being recognized as the more accurate methodology. For instance in *Apatosaurus*, by estimating limb length and body mass for each LAG interval and applying this data into the von Bertalanffy growth equation, the life history of the individual animal could be extrapolated (Woodward and Lehman, 2009). In re-analyzing the *Apatosaurus* specimens of Curry (1999), Woodward and Lehman (2009) calculated that *Apatosaurus* adult mass was attained by seventy years (and an even shorter interval within Titanosauria). While the now extensive (and growing) work on dinosaur life histories can safely dismiss the previous centennial age estimations, these newer works present a slight crux: apparently more realistic values (Curry, 1999; Erickson et al., 2001) versus more grounded methodology (Woodward and Lehman, 2009).

Woodward and Lehman (2009) demonstrated that the histological interpretations of Curry (1999) could have been affected from the types of elements examined (scapulae, radii, and ulnae), and Myhrvold (2013) sufficiently and in extreme depth demonstrated that the Developmental Mass Extrapolation method of Erickson and Tumanova (2000) is highly suspect. The methods of more inclusive life history data, (such as Sander and Tuckmantel, 2003; Woodward and Lehman, 2009; Campione and Evans, 2012; Griebeler et al., 2013) theoretically should be more accurate representations because at the level of the individual these methodologies account for more individual variation and importantly the actual life history of each animal.

Although this analysis as yet could not ascertain exact diplodocid growth rates, thoracic rib and femoral data does allow for mass estimations and mass based ontogentic trends to be theorized. The femoral data applied to the Mazzetta et al. (2004) limb bone allometry based formula can calculate projected body masses. Numerous other variables can also be considered and compared, but one highly important comparison is that between body mass and the number of LAGs present. From this comparison morphologic features could be applied to the graph to determine the mass and aged based timing of ontogenetic events (Figure 9). All juvenile *Diplodocus* examined thus far have fairly short and rounded cervical neural spine apices. If the age determinate histology from the Mother's Day Quarry specimens is correct, then theses young animals are collectively under approximately 2,400 kg and six years of age. The sub-adult size range approximately represents the change to a taller and initial bifurcating spine apex, and this would seem to correlate with animals equal to or greater than 3,500 kg and a minimum of

eight years of age. Finally the adult stage signifies animals with fully bifurcated cervical spine apices and correlates to animals approximately 7,000 kg and at least twenty years of age. If these categorizations are indeed correct, it would appear that the biomechanics of the vertebral column dictate that at least within *Diplodocus*, the neural spine morphology and degree of spine bifurcation are directly correlated with mass.

It is interesting to note the calculated body masses compared to femora circumferences between *Apatosaurus* and *Diplodocus*. The data of this analysis would suggest that *Apatosaurus* potentially achieved a significantly greater body mass throughout ontogeny compared to *Diplodocus* (Figure 9). As yet an age determinate examination of *Apatosaurus* has yet to be conducted, but one could hypothesize that perhaps *Apatosaurus* had a faster growth rate than *Diplodocus*, and if spine morphology is correlated to body mass, perhaps an immature *Apatosaurus* possessed greater spine bifurcation earlier in ontogeny than a similarly aged *Diplodocus*.

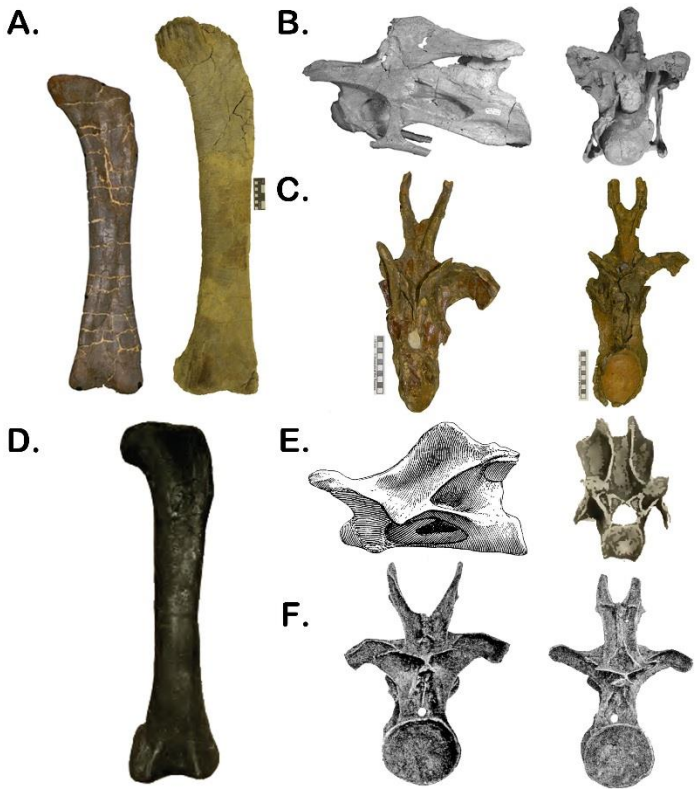

Figure 1: The SOS Stage 2 *Diplodocus* specimens of the Mother's Day Quarry (here represented by MOR 790) compared to the SOS Stage 4 *Diplodocus carnegii* CM 84 (from Hatcher, 1901). A. MOR 790 7-5-95-7 and MOR 790 7-23-95-122. B. Cervical vertebra MOR 790 8-10-96-204 in anterior and left lateral view. C. Anterior dorsal MOR 790 8-21-95-238 and posterior dorsal MOR 790 7-8-95-17 in anterior view. D. *Diplodocus* CM 84 femur. E. Anterior cervical in anterior and left lateral view. F. Anterior and posterior dorsal vertebrae in anterior view. D-F from Hatcher (1901). Not to scale.

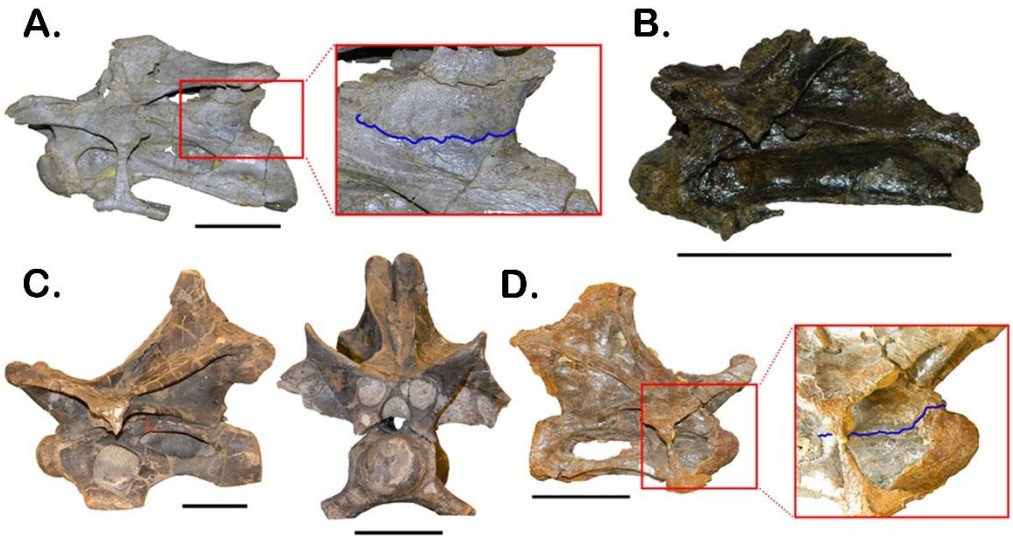

Figure 2: The degrees and variation of neurocentral fusion in diplodocid cervical vertebrae indicate that fusion is not indicative of maturity. A. The posteriorly unfused MOR 790 8-10-96-204, B. The completely fused MOR 714 7-22-3-53, C. The completely unfused CM 555, D. The anteriorly unfused MOR 592. Red inset boxes highlight the visible sutures (in blue). Not to scale. Scale bar = 10 cm.

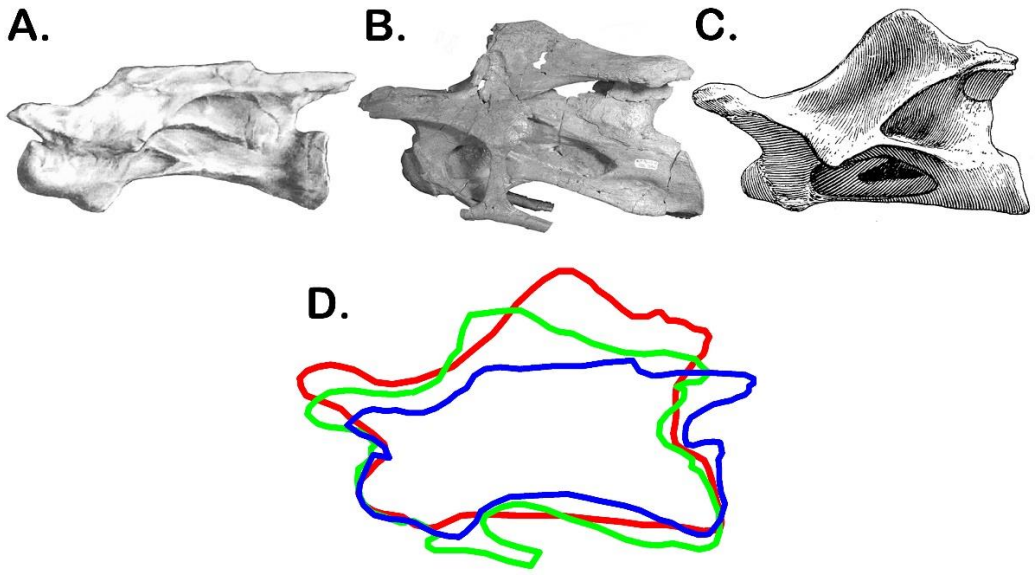

Figure 3: Anterior cervical vertebrae of *Mamenchisaurus youngi* (A.; C7 from Ouyang and Ye, 2002), *Diplodocus* (B.; MOR 790 8-10-96-204), and *Diplodocus carnegii* (C.; C5 from Hatcher, 1901). D. Outlines of *Mamenchisaurus* (blue), MOR 790 8-10-96-204 (green), and *Diplodocus carnegii* (red) to illustrate the varying vertebral morphologies and commonalities. Not to scale.

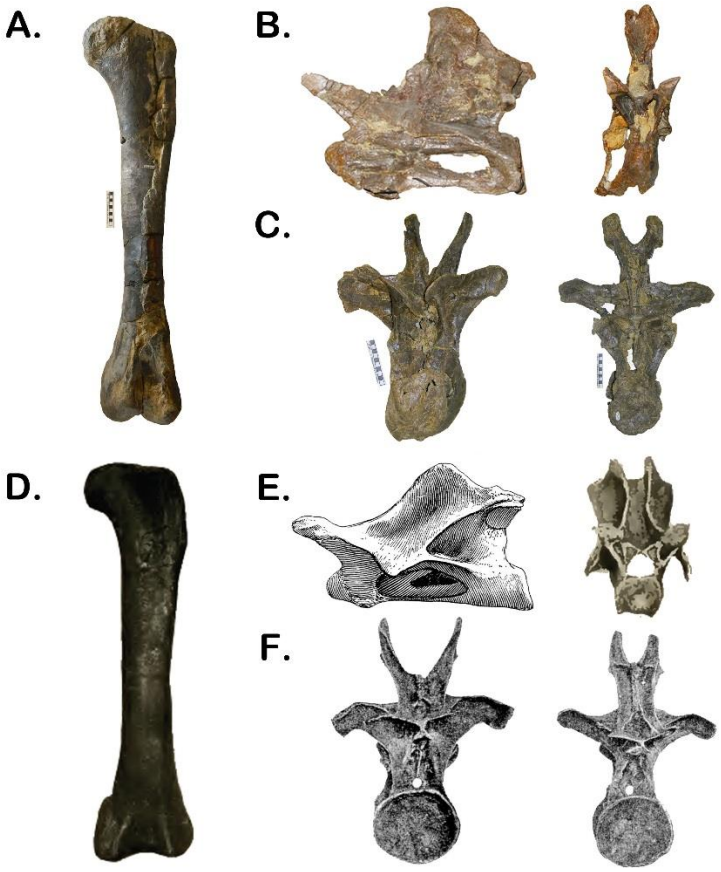

Figure 4: The SOS Stage 3 *Diplodocus* specimen MOR 592 compared to the SOS Stage 4 *Diplodocus carnegii* CM 84. A. MOR 592-35. B. Cervical vertebrae MOR 592 7-26-91-143B in anterior and lateral view. C. Anterior dorsal MOR 592 8-22-90-15 and posterior dorsal MOR 592 8-22-90-77 in anterior view. D. *Diplodocus* CM 84 femur. E. Anterior cervical in anterior and left lateral view. F. Anterior and posterior dorsal vertebrae in anterior view. D-F from Hatcher (1901). Not to scale.

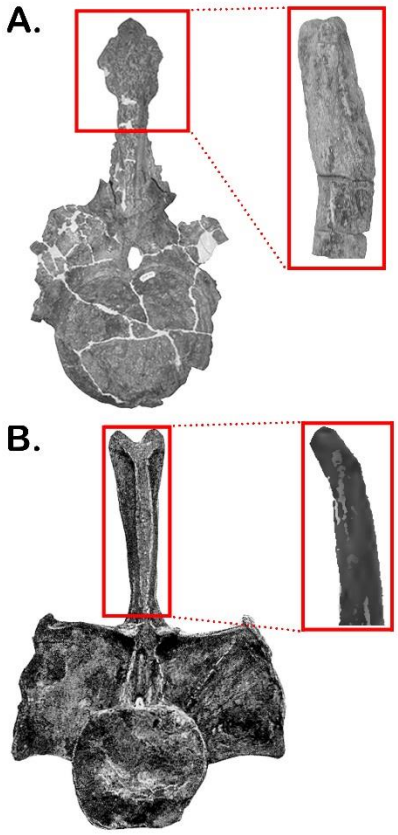

Figure 5: Neural spine morphology in the caudal vertebrae of SOS Stage 3 *Diplodocus* MOR 592 (A.) and SOS Stage 4 *Diplodocus* CM 84 (B.; from Hatcher, 1901) indicates ontogenetic spine bifurcation. A. and B. in anterior view. Red inset boxes showing the neural spines in lateral view. Note the unbifurcated spine apex of MOR 592 opposed to that of CM 84. Not to scale.

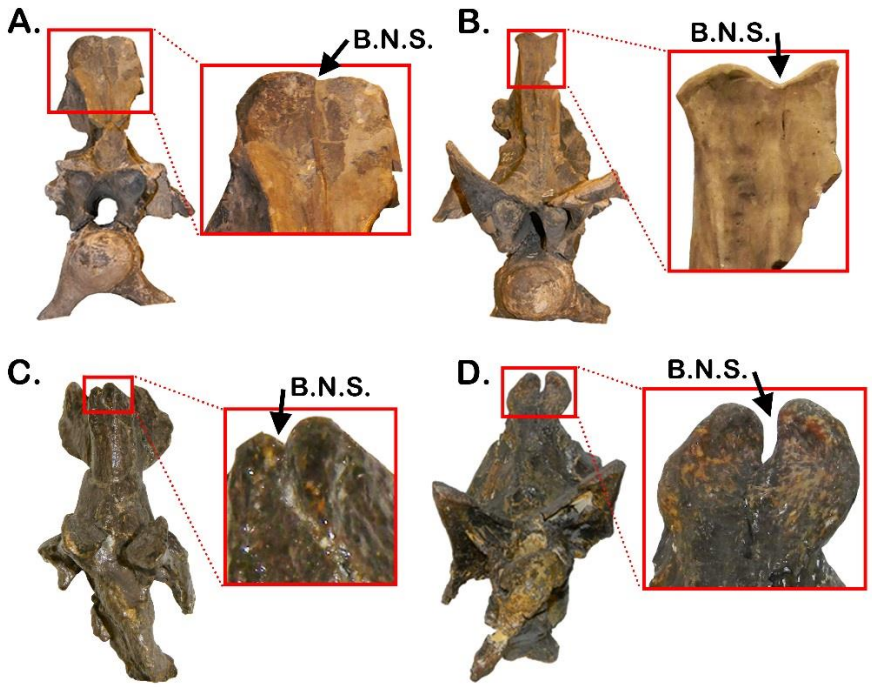

Figure 6: Neural spine bifurcation in diplodocid anterior most cervical vertebrae. A. and B. *Apatosaurus* CM 555; C. *Barosaurus* AMNH 7530; D. *Diplodocus* MOR 592. B.N.S = Bifurcated Neural Spine. All cervical vertebrae in anterior view. Not to scale.

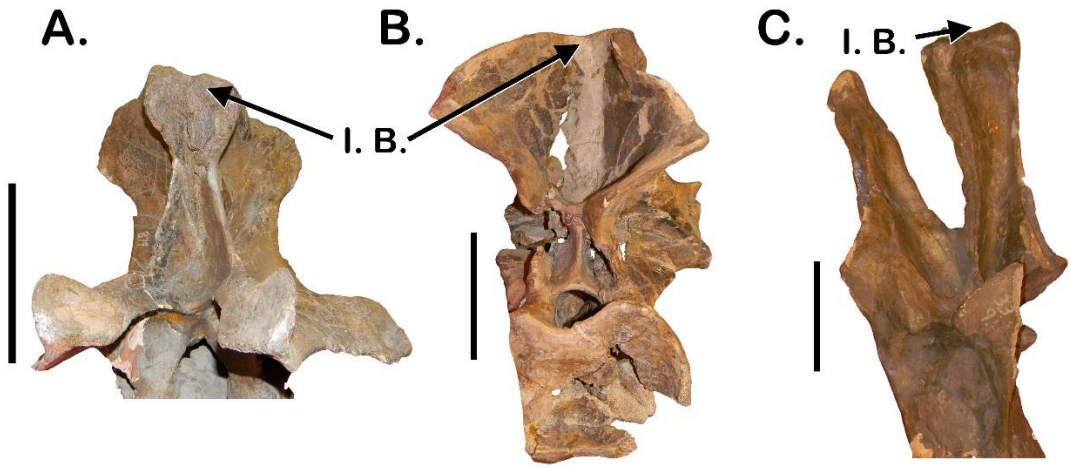

Figure 7: *Haplocanthosaurus* incipient neural spine bifurcation. A. *H.* "*utterbacki*" (CM 879) anterior dorsal in anterior view; B. *H. priscus* (CM 529) anterior dorsal in posterior view; C. *H.* "*utterbacki*" (CM 879) posterior dorsal in anterior view. I.B. = Incipient Bifurcation. Not to scale. Scale bar = 10 cm.

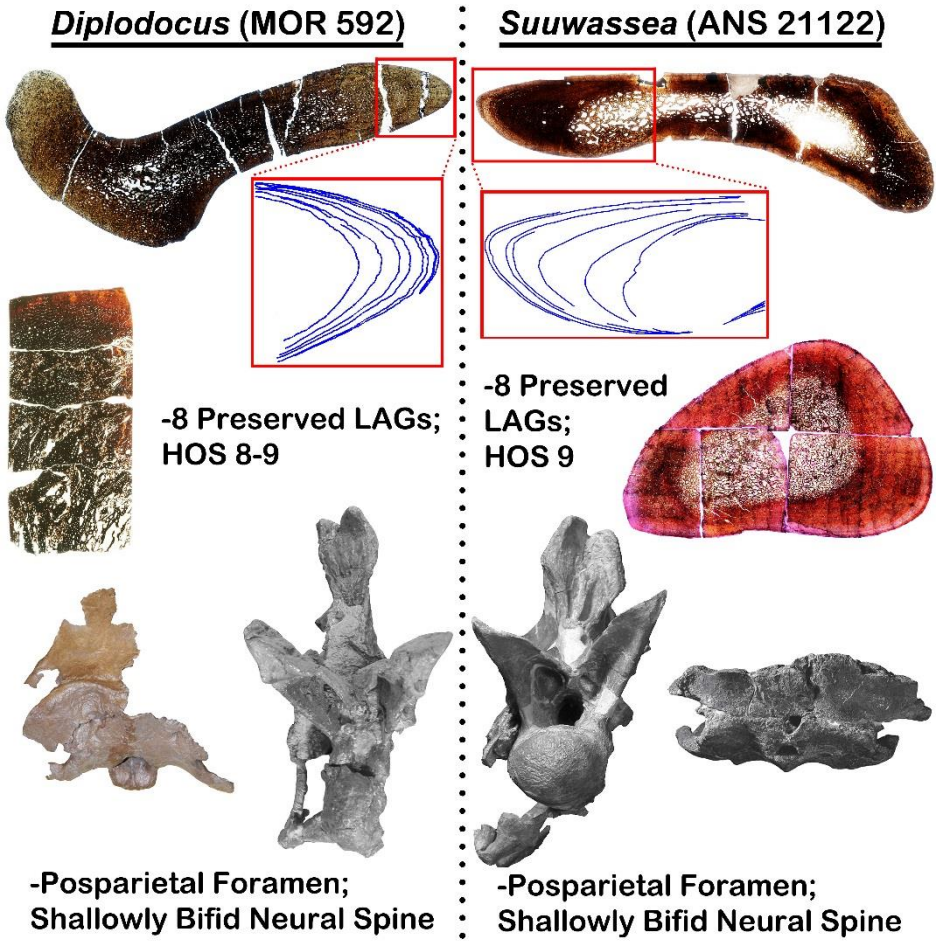

Figure 8: Histologic and morphologic commonalities of *Diplodocus* (MOR 592) and *Suuwassea emilieae* (ANS 21122) which demonstrate immature maturational states for both animals (SOS Stage 3).

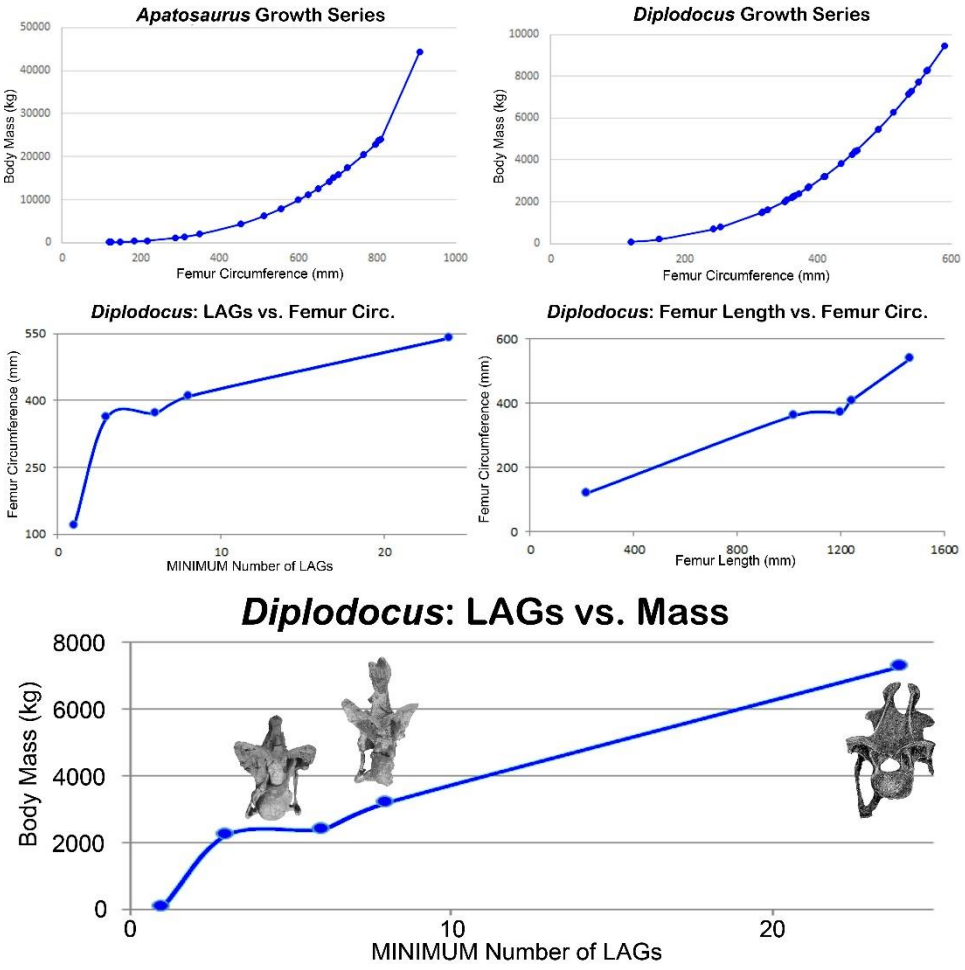

Figure 9: Calculated body masses for the Morrison diplodocids *Apatosaurus* (A) and *Diplodocus* (B) using the formula of Mazzetta et al. (2004) (log Body Mass = 2.955 • log Femur Circumference − 4.166); C. LAG count vs. femur circumference for *Diplodocus*; D. Femur length vs. femur circumference for *Diplodocus*; E. LAG count vs. body mass for *Diplodocus* with cervical vertebrae marking each size range to illustrate the correlation between mass and spine morphology. Data for all diplodocid specimens can be found in MS Table 3.

Table 1: Elongation Index (E.I. = centrum length divided by cotyle diameter).

Diplodocus

HQ 1 SMA 0003

	Centrum Length (mm)	Cotyle Diameter (mm)	EI
C2	84	37	2.27027
C3	105.5	31	3.40323
C4	131	46.5	2.8172
C5	184	30.5	6.03279
C6	228	46	4.95652
C7	280	44	6.36364
C8	376	55.5	6.77477
C9	375	71	5.28169
C10	385	49	7.85714
C11	431	75	5.74667
C12	458	74	6.18919
C13	454	58.5	7.76068
C14	463	77	6.01299
C15	474	77	6.15584

HQ 2 SMA 0004

	Centrum Length (mm)	Cotyle Diameter (mm)	EI
C2	83.5	35	2.38571
C3	107	27	3.96296
C4	132	-	-
C5	158	28	5.64286
C6	192	26.5	7.24528
C7	218	37	5.89189
C8	247	34.5	7.15942
C9	264	38	6.94737
C10	296	53	5.58491
C11	295	51	5.78431
C12	316	56	5.64286
C13	326	66	4.93939
C14	314	61	5.14754

MOR 592

	Centrum Length (mm)	Cotyle Diameter (mm)	EI
C2	114.4	41.2	2.7767
C3	128.3	41.9	3.06205
C4	-	-	-
C5	163.6	49	3.33878
C6	-	-	-
C7	247	37.5	6.58667
C8	256.5	47.4	5.41139
C9	271.6	67.8	4.0059
C10	291	62.4	4.66346
C11	279.4	103.5	2.69952
C12	266.7	112.5	2.37067
C13	239.2	180.8	1.32301
C14	349.3	73.2	4.77186
C15	304.8	96.2	3.1684

CM 84

	Centrum Length (mm)	Cotyle Diameter (mm)	EI
C2	165	54	3.05556
C3	243	69	3.52174
C4	289	81	3.5679
C5	372	94	3.95745
C6	442	99	4.46465
C7	485	114	4.25439
C8	512	120	4.26667
C9	525	159	3.30189
C10	595	175	3.4
C11	605	210	2.88095
C12	627	225	2.78667
C13	638	231	2.7619
C14	642	295	2.17627
C15	595	245	2.42857

MOR 790 8-10-96-204

Centrum Length (mm)	Cotyle Diameter (mm)	EI
304.8	71.86	4.24158

Apatosaurus

CM 555

	Centrum Length (mm)	Cotyle Diameter (mm)	EI
C2	140	63	2.22222
C3	221	84	2.63095
C4	274	96	2.85417
C5	270	60	4.5
C6	295	114	2.58772
C7	316	-	-
C8	344	113	3.04425
C9	380	-	-
C10	-	-	-
C11	480	193	2.48705
C12	460	245	1.87755
C13	-	-	-
C14	378	260	1.45385
C15	-	-	-

CM 563

	Centrum Length (mm)	Cotyle Diameter (mm)	EI
C3	250	80	3.125
C4	300	125	2.4
C5	342	134	2.55224
C6	-	-	-
C7	415	170	2.44118
C8	415	205	2.02439
C9	445	215	2.06977
C10	475	250	1.9

NSMT-PV 20375

	Centrum Length (mm)	Cotyle Diameter (mm)	EI
C3	352	97	3.62887
C4	-	-	-
C5	375	155	2.41935
C6	395	195	2.02564
C7	420	220	1.90909
C8	395	195	2.02564
C9	380	235	1.61702
C10	390	-	-
C11	-	-	-

C12	475	240	1.97917
C13	-	-	-
C14	450	305	1.47541

CM 3018

	Centrum Length (mm)	Cotyle Diameter (mm)	EI
C2	190	85	2.23529
C3	280	100	2.8
C4	370	100	3.7
C5	-	-	-
C6	440	150	2.93333
C7	450	190	2.36842
C8	485	225	2.15556
C9	510	230	2.21739
C10	530	250	2.12
C11	550	240	2.29167
C12	490	265	1.84906
C13	480	-	-

Barosaurus

AMNH 7530

	Centrum Length (mm)	Cotyle Diameter (mm)	EI
C2	80	14	5.71429
C3	75	26	2.88462
C4	97	37	2.62162
C5	123	62	1.98387

C6-C12 are on display and could not be measured first hand

AMNH 7535

	Centrum Length (mm)	Cotyle Diameter (mm)	EI
C2	87	15	5.8
C3	-	-	-
C4	102.5	23	4.45652
C5	-	-	-
C6	135	25	5.4
C7	140	21	6.66667

C8	166	36	4.61111
C9	-	-	-
C10	-	-	-
C11	234	32	7.3125
C12	-	-	-
C13	281	30	9.36667
C14	323	47	6.87234

AMNH 6341 (*from McIntosh, 2005*)

	Centrum Length (mm)	Cotyle Diameter (mm)	EI
C8	618	130	4.75385
C9	685	123	5.56911
C10	737	168	4.3869
C11	775	145	5.34483
C12	813	155	5.24516
C13	850	180	4.72222
C14	865	155	5.58065
C15	840	160	5.25
C16	750	250	3

YPM 429 (*from McIntosh, 2005*)

	Centrum Length (mm)	Cotyle Diameter (mm)	EI
C13	930	220	4.22727
C14	890	345	2.57971
C15	-	300	-
C16	720	365	1.9726

REFERENCES CITED

Brochu C.A. 1996. Closure of neurocentral sutures during crocodilian ontogeny: implications for maturity assessment in fossil archosaurs. Journal of Vertebrate Paleontology, 16: 49-62.

Brochu C.A., 1999. Phylogeny, systematics, and historical biogeography of Alligatoroidea. Society of Vertebrate Paleontology Memoir 6:9-100.

Campione N.E., Evans D.C. 2011. Cranial growth and variation in edmontosaurs (Dinosauria: Hadrosauridae): implications for latest Cretaceous megaherbivore diversity in North America. PLoS One, 6(9), e25186.

Case T.J. 1978. Speculations on the growth rate and reproduction of some dinosaurs. Paleobiology, 320-328.

Cope E.D. 1878. On the Vertebrata of the Dakota Epoch of Colorado: Proceedings of the American Philosophical Society, v. 17, p.233-247.

Curry K.A. 1999. Ontogenetic histology of *Apatosaurus* (Dinosauria: Sauropoda): new insights on growth rates and longevity. Journal of Vertebrate Paleontology, 19: 654-665.

Erickson G.M. Tumanova T.A. 2000. Growth curve of *Psittacosaurus mongoliensis* Osborn (Ceratopsia: Psittacosauridae) inferred from long bone histology. Zool. J. Linn. Soc. 130, 551±566.

Erickson, G.M., Rogers, K.C., Yerby, S.A. 2001. Dinosaurian growth patterns and rapid avian growth rates. Nature, 412: 429-433.

Foster J. 2007. Jurassic West: the dinosaurs of the Morrison Formation and their world. Indiana University Press.

Fowler D.W., Woodward H.N., Freedman E.A., Larson P.L., Horner J.R. 2011. Reanalysis of ‘‘*Raptorex kriegsteini*’’: A Juvenile Tyrannosaurid Dinosaur from Mongolia. PLoS ONE 6(6): e21376. doi:101371/journalpone.0021376.

Griebeler E.M., Klein N., Sander P.M. 2013. Aging, Maturation and Growth of Sauropodomorph Dinosaurs as Deduced from Growth Curves Using Long Bone Histological Data: An Assessment of Methodological Constraints and Solutions. PLOS ONE, 8(6), e67012.

Harris J.D., Dodson P. 2004. A new diplodocoid sauropod dinosaur from the Upper Jurassic Morrison Formation of Montana, USA. Acta Palaeontologica Polonica, 49: 197-210.

Hatcher J.B. 1901. *Diplodocus* (Marsh): Its osteology,taxonomy, and probable habits, with a restoration of the skeleton. Memoirs of the Carnegie Museum 1: 1-63.

Hedrick B.P., Tumarkin-Deratzian A.R., Dodson P. 2012. Bone microstructure and relative age of the holotype specimen of the diplodocoid sauropod dinosaur *Suuwassea emilieae*. Acta Palaeontologica Polonica.

Horner J.R., Lamm E.T. 2011. Ontogeny of the parietal frill of *Triceratops*: a preliminary histological analysis. C. R. Pelevol 10: 439-452.

Ikejiri T. (2012). Histology-Based Morphology of the Neurocentral Synchondrosis in *Alligator mississippiensis* (Archosauria, Crocodylia). The Anatomical Record, 295(1), 18-31.

Mazzetta G.V., Christiansen P., Farina, R.A. 2004. Giants and bizarres: body size of some southern South American Cretaceous dinosaurs. Historical Biology, 16(2-4), 71-83.

McIntosh J.S. 2005. The genus *Barosaurus* Marsh (Sauropoda, Diplodocidae). Thunder-Lizards: The Sauropodomorph Dinosaurs: Indiana University Press, Bloomington, 38-77.

McIntosh J.S, Williams, ME. 1988. A new species of sauropod dinosaur, *Haplocanthosaurus delfsi* sp. nov., from the Upper Jurassic Morrison Fm. of Colorado. Kirtlandia, 43, 3-26.

Myers T.S. 2004. Taphonomy of the Mother's Day Quarry: Implications for Gregarious Behavior in Sauropod Dinosaurs Unpublished M.S. thesis. University of Cincinnati.

Myers T.S, Storrs GW. 2007. Taphonomy of the Mother's Day Quarry, Upper Jurassic Morrison Formation, south−central Montana, USA. Palaios 22: 651–666.

Myhrvold N.P. 2013. Revisiting the Estimation of Dinosaur Growth Rates. PloS one, 8(12), e81917.

Ouyang H., Ye Y. 2002. The first mamenchisaurian skeleton with complete skull (*Mamenchisaurus youngi*). pp. 111.

Rozhdestvensky A.K. 1965. Growth Changes in Asian Dinosaurs and Some Problems of Their Taxonomy, Paleontological Journal 3:95-109 [in Russian].

Sander P.M., Tuckmantel C. 2003. Bone lamina thickness, bone apposition rates, and age estimates in sauropod humeri and femora. Palaontologische Zeitschrift 77:161–172.

Tsuihiji T, Watabe M, Tsogtbaatar K, Tsubamoto T, Barsbold R, Suzuki S, Lee AH, Ridgely RC, Kawahara Y, Witmer LM. 2011. Cranial Osteology of a Juvenile Specimen of *Tarbosaurus bataar* (Theropoda, Tyrannosauridae) from the Nemegt Formation (Upper Cretaceous) of Bugin Tsav, Mongolia. Journal of Vertebrate Paleontology 31: 497-517.

Upchurch P, Tomida Y, and Barrett PM. 2004. A new specimen of *Apatosaurus ajax* (Sauropoda: Diplodocidae) from the Morrison Formation (Upper Jurassic) of Wyoming, USA. National Science Museum Monographs 26:1–107.

Wedel M.J. 2009. Evidence for bird-like air sacs in saurischian dinosaurs. Journal of Experimental Zoology A 311: 1-18.

Wedel M.J., Taylor M.P. 2013. Neural spine bifurcation in sauropod dinosaurs of the Morrison Formation: ontogenetic and phylogenetic implications. Palarch's Journal of Vertebrate Palaeontology 10(1): 1-34. ISSN 1567-2158.

Whitlock J.A., Harris J.D. 2010. The dentary of *Suuwassea emilieae* (Sauropoda: Diplodocoidea). Journal of Vertebrate Paleontology, 30: 1637-1641.

Whitlock J.A., Wilson J.A., Lamanna M.C. 2010. Description of a nearly complete juvenile skull of *Diplodocus* (Sauropoda: Diplodocoidea) from the Late Jurassic of North America. Journal of Vertebrate Paleontology, 30: 442-457.

Whitlock J.A. 2011. A phylogenetic analysis of Diplodocoidea (Saurischia: Sauropoda). Zoological Journal of the Linnean Society, 161: 872-915.

Wilson J.A., Smith M. 1996. New remains of *Amphicoelias* Cope (Dinosauria: Sauropoda) from the Upper Jurassic of Montana and diplodocoid phylogeny. Journal of Vertebrate Paleontology, 16(3 Suppl.): 73A.

Woodruff D.C., Fowler D.W. 2012. Ontogenetic influence on neural spine bifurcation in Diplodocoidea (Dinosauria: Sauropoda): a critical phylogenetic character. Journal of morphology, 273(7), 754-764.

Woodward H.N., Lehman T.M. 2009. Bone histology and microanatomy of *Alamosaurus sanjuanensis* (Sauropoda: Titanosauria) from the maastrichtian of Big Bend National Park, Texas. Journal of Vertebrate Paleontology, 29: 807-821.

CUMULATIVE REFERENCES CITED

Abramoff MD., Magalhaes P.J., Ram S.J. 2004. Image Processing with ImageJ. Biophotonics International, volume 11, issue 7, pp. 36-42.

Ashdown RR, Done SH, Barnett SW. 2010. Color Atlas of Veterinary Anatomy, Vol. 1, Amsterdam: The Ruminants (Mosby). pp 272.

Balanoff AM., Bever GS., Ikejiri T. 2010. The braincase of *Apatosaurus* (Dinosauria: Sauropoda) based on computed tomography of a new specimen with comments on variation and evolution in sauropod neuroanatomy. American Museum Novitates, 1-32.

Beadnell HJL. 1902. A Preliminary Note on *Arsinoitherium zitteli*, Beadn., from the Upper Eocene Strata of Egypt. National Printing Department.

Benjamin M, Kumai T, Milz S, Boszczyk BM, Boszczyk AA, Ralphs JR. 2002. The skeletal attachment of tendons—Tendon 'entheses.' Comp Biochem Physiol A Mol Integr Physiol 133: 931-945.

Berman DS., McIntosh JS. 1978. Skull and relationships of the Upper Jurassic sauropod *Apatosaurus* (Reptilia, Saurischia).

Bonaparte JF. 1985. A horned Cretaceous carnosaur from Patagonia. Natl Geogr Res 1: 149-151.

Bonnan MF. 2004. Morphometric analysis of humerus and femur shape in Morrison sauropods: implications for functional morphology and paleobiology. Paleobiology, 30: 444-470.

Brochu CA. 1996. Closure of neurocentral sutures during crocodilian ontogeny: implications for maturity assessment in fossil archosaurs. Journal of Vertebrate Paleontology, 16: 49-62.

Brochu CA., 1999. Phylogeny, systematics, and historical biogeography of Alligatoroidea. Society of Vertebrate Paleontology Memoir 6:9-100.

Budras K-D, Habel RE. 2003. Bovine Anatomy: An Illustrated Text. Hanover, Germany: Schlütersche. pp 138.

Campione NE., Evans DC. 2011. Cranial growth and variation in edmontosaurs (Dinosauria: Hadrosauridae): implications for latest Cretaceous megaherbivore diversity in North America. PLoS One, 6(9), e25186.

Carballido JL., Marpmann JS., Schwarz-Wings D., Pabst B. 2012. New information on a juvenile sauropod specimen from the Morrison Formation and the reassessment of its systematic position. Palaeontology, 55: 567-582.

Case TJ. 1978. Speculations on the growth rate and reproduction of some dinosaurs. Paleobiology, 320-328.

Castanet J., Francillon-Vieillot H., Meunier FJ., De Ricqles A. 1992. Bone and lndividual Aging. Bone: A Treatise Volume 7: 245.

Coombs WPJ. 1975. Sauropod habits and habitats. Palaeogeogr Palaeoclimatol Palaeoecol 17:1-33.

Cope ED. 1877. On a gigantic saurian from the Dakota Epoch of Colorado. Palaeontological Bulletin 25:5-10.

Cope ED. 1890. The cetacea. Am Nat 24: 599-616.

Cormick W. 2010. Enthesopathy—a personal perspective on its manifestations, implications and treatment. Aust J Ultrasound Med 13: 19–23.

Currey JD. 1984. The Mechanical Adaptations of Bones. Princeton University Press. Princeton: New Jersey. pp 294.

Curry KA. 1999. Ontogenetic histology of *Apatosaurus* (Dinosauria: Sauropoda): new insights on growth rates and longevity. Journal of Vertebrate Paleontology, 19: 654-665.

Desilva U, Fitch J. 1995. Ankole-Watusi. From Breeds of Livestock Project, Oklahoma State University Department of Animals Sciences. Available at: http://www.ansi.okstate.edu/breeds/cattle/. Last accessed on 2013.

Dimery NJ, Alexander RM, Deyst KA. 1985. Mechanics of the ligamentum nuchae of some artiodactyls. J Zool 206: 341-351.

De Ricqlès A., Meunier FJ., Castanet J., Francillon-Vieillot H. 1991. Comparative microstructure of bone. Bone, 3: 1-78.

D'Emic MD., Foreman BZ. 2012. The beginning of the sauropod dinosaur hiatus in North America: insights from the Lower Cretaceous Cloverly Formation of Wyoming. Journal of Vertebrate Paleontology, 32(4), 883-902.

Dodson P. 1975. Taxonomic implications of relative growth in lambeosaurine hadrosaurs. Systematic Biology, 24(1), 37-54.

Dürst JU. 1899. Die Rinder Von Babylonien, Assyrien Undü Agypten Und Ihr Zusammanhang Mit Den Rindern Der Alten Welt; Georg Reimer: Berlin, Germany.

Dzemski G, Christian A. 2007. Flexibility along the neck of the ostrich (Struthio camelus) and consequences for the reconstruction of dinosaurs with extreme neck length. J Morphol 268:701-714.

Erickson GM. 2005. Assessing dinosaur growth patterns: a microscopic revolution. Trends in ecology & evolution, 20(12), 677-684.

Erickson GM. Tumanova T.A. 2000. Growth curve of *Psittacosaurus mongoliensis* Osborn (Ceratopsia: Psittacosauridae) inferred from long bone histology. Zool. J. Linn. Soc. 130, 551±566.

Erickson, GM., Rogers, K.C., Yerby, S.A. 2001. Dinosaurian growth patterns and rapid avian growth rates. Nature, 412: 429-433.

Evans DC., Forster CA., Reisz RR. 2005. The type specimen of *Tetragonosaurus erectofrons* (Ornithischia: Hadrosauridae) and the identification of juvenile Lambeosaurines. In: Currie PJ, Koppelhaus EB, eds. Dinosaur Provincial Park. Bloomington: Indiana University Press. pp 349-366.

Folkard C. 2003. Guinness Book of World Records. New York: Guinness World Records Ltd. pp 288.

Foster J. 2007. Jurassic West: the dinosaurs of the Morrison Formation and their world. Indiana University Press.

Fowler DW., Woodward HN., Freedman EA., Larson PL., Horner JR. 2011. Reanalysis of ‘‘*Raptorex kriegsteini*’’: A Juvenile Tyrannosaurid Dinosaur from Mongolia. PLoS ONE 6(6): e21376. doi:101371/journalpone.0021376.

Francillon-Vieillot H., De Buffrénil V., Castanet J., Géraudie J., Meunier FJ., Sire JY., Zylberberg L., De Ricqlès A. 1990. Microstructure and mineralization of vertebrate skeletal tissues. Skeletal biomineralization: patterns, processes and evolutionary trends 175-234.

Frey E. 1988. Anatomie des Küorperstammes von *Alligator mississippiensis* Daudin. Stuttgarter Beitrüage zur Naturkunde 24: 1-106.

Gilmore CW. 1925. A nearly complete articulated skeleton of *Camarasaurus*, a saurischian dinosaur from the Dinosaur National Monument, Utah. Carnegie Institute.

Gilmore CW. 1936. Osteology of *Apatosaurus* with special reference to specimens

in the Carnegie Museum. Memoirs of the Carnegie Museum 11: 175-300.

Goldfinger E. 1981. Animal Anatomy for Artists. Oxford University Press, Oxford: United Kingdom. pp 256.

Grey H. 1858. Anatomy: Descriptive and Surgical. London: Parker & Son. pp 983.

Griebeler EM., Klein N., Sander PM. 2013. Aging, Maturation and Growth of Sauropodomorph Dinosaurs as Deduced from Growth Curves Using Long Bone Histological Data: An Assessment of Methodological Constraints and Solutions. PLOS ONE, 8(6), e67012.

Grigson C. 2000. *Bos africanus* (Brehm)? Notes on the archaeozoology of the native cattle of Africa. In: Blench RM, MacDonald KC, editors. The origins and development of African livestock. pp 38-60.

Grubb P. 2005. "*Bos taurus primigenius*". In: Wilson DE, Reeder DM, editors. Mammal Species of the World, 3rd ed. Johns Hopkins University Press. Baltimore: Maryland. pp 637-722.

Hall BK. 2005. Bones and Cartilage: Developmental and Evolutionary Skeletal Biology. Academic Press. San Diego: California. pp 792.

Harris JD. 2006a. Cranial osteology of *Suuwassea emilieae* (Sauropoda: Diplodocoidea: Flagellicaudata) from the Upper Jurassic Morrison Formation of Montana, USA. Journal of Vertebrate Paleontology, 26: 88-102.

Harris JD. 2006b. The significance of *Suuwassea emilieae* (Dinosauria: Sauropoda) for flagellicaudatan intrarelationships and evolution. Journal of Systematic Palaeontology, 4: 185-198.

Hatcher JB. 1901. *Diplodocus* (Marsh): Its osteology,taxonomy, and probable habits, with a restoration of the skeleton. Mem Carnegie Mus 1: 1-63.

Hatcher JB. 1903. Osteology of *Haplocanthosaurus* with additional remarks on *Diplodocus*. Memoirs Carnegie Museum, 1: 1-75.

Hedrick BP., Tumarkin-Deratzian AR., Dodson P. 2012. Bone microstructure and relative age of the holotype specimen of the diplodocoid sauropod dinosaur *Suuwassea emilieae*. Acta Palaeontologica Polonica.

Holland WJ., 1924. The skull of *Diplodocus*. Memoirs of the Carnegie Museum 9: 379-403.

Hopson JA., 1975. The evolution of cranial display structures in hadrosaurian dinosaurs. Paleobiology, 1: 21-43.

Hopson JA. 1979. Paleoneurology; pp. 39–146 in C. Gans (ed.), Biology of the Reptilia Volume 9: Neurology A. Academic Press, London.

Horner JR., Goodwin MB. 2006. Major cranial changes during *Triceratops* ontogeny. Proceedings of the Royal Society B: Biological Sciences, 273: 2757-2761.

Horner JR., Goodwin MB. 2009. Extreme cranial ontogeny in the Upper Cretaceous dinosaur *Pachycephalosaurus*. PLoS One, 4: e7626.

Horner JR., Lamm ET. 2011. Ontogeny of the parietal frill of *Triceratops*: a preliminary histological analysis. C. R. Pelevol 10: 439-452.

Horner JR., Padian K. 2004. Age and growth dynamics of *Tyrannosaurus rex*. Proceedings of the Royal Society of London. Series B: Biological Sciences, 271: 1875-1880.

Horner JR., de Ricqlès A., Padian K. 2000. Long bone histology of the hadrosaurid dinosaur *Maiasaura peeblesorum*: growth dynamics and physiology based on an ontogenetic series of skeletal elements. Journal of Vertebrate Paleontology, 20: 115-129.

Horner, JR., de Ricqlès, A., Padian, K. 2010. Variation in dinosaur skeletochronology indicators: implications for age assessment and physiology.

Huttenlocker AK., Woodward HN., Hall BK. 2013. The biology of bone. In: Bone Histology of Fossil Tetrapods: Advancing Methods, Analysis, and Interpretation, edited by K. Padian, and ET Lamm. Berkeley: University of California Press, 13-34.

Ikejiri T. 2012. Histology-Based Morphology of the Neurocentral Synchondrosis in *Alligator mississippiensis* (Archosauria, Crocodylia). The Anatomical Record, 295(1), 18-31.

Ikejiri T, Tidwell V, Trexler DL. 2005. New adult specimens of *Camarasaurus lentus* highlight ontogenetic variation within the species. Thunder-Lizards: The Sauropodomorph Dinosaurs. In: Tidwell V, Carpenter K, editors. Bloomington, IN: Indiana University Press. Pp. 154-179.

Janensch W. 1935. Die Schädel der Sauropoden *Brachiosaurus*, *Barosaurus* und *Dicraeosaurus* aus den Tendaguruschichten Deutsch-Ostafrikas (Anfang). Palaeontographica-Supplementbände, 2: 145-248.

Janensch W. 1929. Die Wirbelsaule der gattung *Dicraeosaurus* Palaeontographica (Supplement 7) 3: 39-133.

Keller C. 1905. Naturgeschichte Der Haustiere. Berlin, Germany: Paul Parey.

Klein N., Sander M. 2008. Ontogenetic stages in the long bone histology of sauropod dinosaurs. Paleobiology, 34: 247-263.

Knoll F., Witmer LM., Ortega F., Ridgely RC., Schwarz-Wings, D. 2012. The braincase of the basal sauropod dinosaur *Spinophorosaurus* and 3D reconstructions of the cranial endocast and inner ear. PloS one, 7(1), e30060.

Lee AH., Werning, S. 2008. Sexual maturity in growing dinosaurs does not fit reptilian growth models. Proceedings of the National Academy of Sciences, 105(2), 582-587.

Lehman TM., Woodward HN. 2008. Modelling growth rates for sauropod dinosaurs. Paleobiology 34: 264–281.

Linder JF, Longhurst P, Johnson NW. 1981. A paraffin-celloidin embedding method for studying soft-hard tissue interfaces. Arch Oral Biol 26: 753-755.

Lull RS. 1919. The sauropod dinosaur *Barosaurus* Marsh: redescription of the type specimens in the Peabody Museum, Yale University (Vol. 6). Connecticut Academy of Arts and Sciences.

Lovelace DM., Hartman SA., Wahl WR. 2007. Morphology of a specimen of *Supersaurus* (Dinosauria, Sauropoda) from the Morrison Formation of Wyoming, and a re-evaluation of diplodocid phylogeny. Arquivos do Museu Nacional, Rio de Janeiro, 65: 527-544.

Marpmann JS., Carballido JL, Sander PM., Knötschke N. 2014. Cranial anatomy of the Late Jurassic dwarf sauropod *Europasaurus holgeri* (Dinosauria, Camarasauromorpha): ontogenetic changes and size dimorphism. Journal of Systematic Palaeontology (advance online publication) DOI:10.1080/14772019.2013.875074

Marsh OC. 1877. Notice of new dinosaurian reptiles from the Jurassic Formation. American Journal of Science 14:514-516.

Mateus O, Maidment SC, Christiansen NA. 2009. A new longnecked 'sauropod-mimic' stegosaur and the evolution of the plated dinosaurs. Proc Royal Soc B Biol Sci 276: 1815-1821.

Mazzetta GV., Christiansen P., Farina, RA. 2004. Giants and bizarres: body size of some southern South American Cretaceous dinosaurs. Historical Biology, 16(2-4), 71-83.

McIntosh JS. 1981. Annotated catalogue of the dinosaurs (Reptilia, Archosauria) in the collections of Carnegie Museum of Natural History.

McIntosh, JS. 1990. Species determination in sauropod dinosaurs with tentative suggestions for their classification. Dinosaur systematics: approaches and perspectives, 53-69.

McIntosh, JS. 2005. The genus *Barosaurus* Marsh (Sauropoda, Diplodocidae). Thunder-Lizards: The Sauropodomorph Dinosaurs: Indiana University Press, Bloomington, 38-77.

McIntosh JS, Williams, ME. 1988. A new species of sauropod dinosaur, *Haplocanthosaurus delfsi* sp. nov., from the Upper Jurassic Morrison Fm. of Colorado. Kirtlandia, 43, 3-26.

Mescher AL. 2010. Junqueira's Basic Histology: Text & Atlas. Mcgraw-hill medical, New York: New York. pp. 480.

Michelis I. 2004. Taphonomie des Howe Quarry's (Morrison-Formation, Oberer Jura), Bighorn County, Wyoming, USA. Unpublished PhD thesis, Institute of Palaeontology, University of Bonn, 41 pp.

Mook, CC. 1917. The fore and hind limbs of *Diplodocus*. Bulletin of the American Museum of Natural History 37: 815-819.

Myers TS. 2004. Taphonomy of the Mother's Day Quarry: Implications for Gregarious Behavior in Sauropod Dinosaurs. MS thesis, University of Cincinnati, Cincinnati.

Myers TS, Storrs GW. 2007. Taphonomy of the Mother's Day Quarry, Upper Jurassic Morrison Formation, south−central Montana, USA. Palaios 22: 651–666.

Myhrvold NP. 2013. Revisiting the Estimation of Dinosaur Growth Rates. PloS one, 8(12), e81917.

Nash JF. 1950. Equilibrium Points in N-person Games. Proceedings of the National Academy of Sciences 36 (36): 48-9.

Novas FE, Pol D, Canale JI, Porfiri JD, Calvo JO. 2009. A bizarre Cretaceous theropod dinosaur from Patagonia and the evolution of Gondwanan dromaeosaurids. Proc Royal Soc London B Biol Sci 276: 1101-1007.

Organ CL, Adams J. 2005. The histology of ossified tendon in dinosaurs. J Vertebrate Paleontol 25: 602-613.

Osborn HF. 1898. Additional characters of the great herbivorous dinosaur *Camarasaurus*. Bull Am Mus Nat Hist 10: 219-233.

Osborn HF., Mook CC. 1921. *Camarasaurus*, *Amphicoelias*, and other sauropods of Cope. Memoirs of the American Museum of Natural History (new series) 3: 249-387.

Ostrom, JH., McIntosh JS. 1966. Marsh's Dinosaurs. Yale University Press, New Haven and London. 388 pages.

Ouyang H., Ye Y. 2002. The first mamenchisaurian skeleton with complete skull (*Mamenchisaurus youngi*). pp. 111.

Padian K., de Ricqlès AJ., Horner JR. 2001. Dinosaurian growth rates and bird origins. Nature, 412(6845), 405-408.

Padian K, Lamm ET. 2013. Bone Histology of Fossil Tetrapods: Advancing Methods, Analysis, and Interpretation. University of California Press, Oakland: California.

Post L. 2012. The Whale Building Book: A Step-By-Step Guide To Preparing And Assembling Medium Sized Whale Skeletons. print on demand. pp. 1-69.

Rauhut O. 2005. Osteology and relationships of a new theropod dinosaur from the Middle Jurassic of Patagonia. Paleontology 48: 87-110.

Remes K. 2009. Taxonomy of Late Jurassic diplodocid sauropods from Tendaguru (Tanzania). Fossil Record, 12, 23–46.

Romer AS. 1956. Osteology of the Reptiles. University of Chicago Press, Chicago: Illinois. pp. 1-772.

Rozhdestvensky AK. 1965. Growth Changes in Asian Dinosaurs and Some Problems of Their Taxonomy, Paleontological Journal 3:95-109 [in Russian].

Ruffer MA. 1921. Studies in the Palaeopathology of Egypt. Chicago, IL: University of Illinois Press. Pp. 1-372.

Salgado L., Bonaparte JF. 1991. Un nuevo saur´opodo Dicraeosauridae, *Amargasaurus cazaui* gen. et sp. nov., de la Formaci´on La Amarga, Neocomiano de la provincia del Neuqu´en, Argentina. Ameghiniana, 28: 333-346.

Sampson SD., Ryan MJ., Tanke DH. 1997. Craniofacial ontogeny in centrosaurine dinosaurs (Ornithischia: Ceratopsidae): taxonomic and behavioral implications. Zoological Journal of the Linnean Society 121: 293-337.

Sander PM., Tuckmantel C. 2003. Bone lamina thickness, bone apposition rates, and age estimates in sauropod humeri and femora. Palaontologische Zeitschrift 77:161–172.

Sander PM, Christian A, Clauss M, Fechner R, Gee CT, Griebeler E-M, Gunga HC, Hummel J, Mallison H, Perry SF, Preuschoft H, Rauhut OWM, Remes K, Tütken T, Wings O, Witzel U. 2011. Biology of the sauropod dinosaurs: the evolution of gigantism. Biological Review 86: 117-155.

Scannella JB., Horner JR. 2010. Torosaurus Marsh, 1891, is Triceratops Marsh, 1889 (Ceratopsidae: Chasmosaurinae): synonymy through ontogeny. Journal of Vertebrate Paleontology, 30: 1157-1168.

Scannella JB., Fowler DW. 2014. A stratigraphic survey of *Triceratops* localities in the Hell Creek Formation, northeastern Montana (2006–2010). Through the End of the Cretaceous in the Type Locality of the Hell Creek Formation in Montana and Adjacent Areas: Geological Society of America Special Paper, 503.

Schwarz D., Fritsch G. 2006. Pneumatic structures in the cervical vertebrae of the Late Jurassic Tendaguru sauropods Brachiosaurus brancai and Dicraeosaurus. Eclogae Geologicae Helvetiae, 99: 65-78.

Schwarz-Wings D., Frey E. 2008. Is there an option for a pneumatic stabilization of sauropod necks?–an experimental and anatomical approach. Palaeontologia Electronica, 11: 17A.

Schwarz D., Frey E., Meyer, CA. 2007. Pneumaticity and soft-tissue reconstructions in the neck of diplodocid and dicraeosaurid sauropods. Acta Palaeontologica Polonica, 52(1), 167.

Schwarz D., Ikejiri T., Breithaupt BH., Sander PM., Klein N. 2007. A nearly complete skeleton of an early juvenile diplodocid (Dinosauria: Sauropoda) from the lower Morrison formation (Late Jurassic) of North Central Wyoming and its implications for early ontogeny and pneumaticity in sauropods. Hist Biol 19:225–253.

Stein, K., Sander M. 2009. Histological core drilling: a less destructive method for studying bone histology. In: Methods In Fossil Preparation: Proceedings of the First Annual Fossil Preparation and Collections Symposium, pp. 69-80.

Stock C. 1930. Quarternary antelope remains from a second cave deposit in the Organ Mountains, New Mexico. Los Angel Mus Sci Ser Paleontol 2: 1-18.

Sumida SS. 1990. Vertebral morphology, alternation of neural spine height, and structure in Permo-Carboniferous tetrapods, and a reappraisal of primitive modes of terrestrial locomotion. University of California Press, Oakland: California.

Tambussi CP, de Mendoza R, Degrange FJ, Picasso MB. 2012. Flexibility along the neck of the Neogene terror bird *Andalgalornis steulleti* (Aves Phorusrhacidae). PLoS One 7(5): e37701.

Tschopp E., Mateus, O. 2012. The skull and neck of a new flagellicaudatan sauropod from the Morrison Formation and its implication for the evolution and ontogeny of diplodocid dinosaurs. Journal of Systematic Palaeontology, (ahead-of-print), 1-36.

Tsuihiji T. 2004. The ligament system in the neck of *Rhea americana* and its implication for the bifurcated neural spines of sauropod dinosaurs. J Vertebrate Paleontol 24: 165-172.

Tsuihiji T, Watabe M, Tsogtbaatar K, Tsubamoto T, Barsbold R, Suzuki S, Lee AH, Ridgely RC, Kawahara Y, Witmer LM. 2011. Cranial Osteology of a Juvenile Specimen of *Tarbosaurus bataar* (Theropoda, Tyrannosauridae) from the Nemegt Formation (Upper Cretaceous) of Bugin Tsav, Mongolia. Journal of Vertebrate Paleontology 31: 497-517.

Upchurch P., Barrett P.M. Dodson P. 2004. Sauropoda. Pp. 259–322 in D. B.Weishampel, P. Dodson & H. Osmolska (eds) The Dinosauria. Second edition. University of California Press, Berkeley.

Upchurch P., Tomida Y., Barrett P.M. 2004. A new specimen of *Apatosaurus ajax* (Sauropoda: Diplodocidae) from the Morrison Formation (Upper Jurassic) of Wyoming, USA. National Science Museum Monographs, 26: i-118.

Vaughn PP. 1964. Vertebrates from the Organ Rock shale of the Cutler Group, Permian of Monument Valley and vicinity, Utah and Arizona. J. Paleont 38: 567-583.

Vickaryous MK, Olson WM. 2007. Sesamoids and ossicles in the appendicular skeleton. Fins and Limbs: Evolution, Development and Transformation. In: Hall BK, editor. Chicago, IL: University of Chicago Press. pp 323-341.

von Eggeling H. 1922. Die Gabelung der Halswirbeldornen undihre Ursache. Anat Anz 55: 33-94.

Wedel MJ., Cifelli RL., Sanders R.K. 2000. Osteology, paleobiology, and relationships of the sauropod dinosaur *Sauroposeidon*. Acta Palaeontologica Polonica, 45: 343-388.

Wedel MJ. 2003. The evolution of vertebral pneumaticity in sauropod dinosaurs. Journal of Vertebrate Paleontology, 23: 344-357.

Wedel MJ. 2005. Postcranial skeletal pneumaticity in sauropods and its implications for mass estimates. The sauropods: evolution and paleobiology. University of California Press, Berkeley, 201-228.

Wedel MJ. 2009. Evidence for bird-like air sacs in saurischian dinosaurs. Journal of Experimental Zoology A 311: 1-18.

Wedel MJ, Taylor MP. 2013. Neural spine bifurcation in sauropod dinosaurs of the Morrison Formation: Ontogenetic and phylogenetic implications. Palarch's J Vertebrate Palaeontol 10: 1-34.

Wedel MJ, Cifelli RL, Sanders RK. 2000. Osteology, paleobiology, and relationships of the sauropod dinosaur *Sauroposeidon*. Acta Palaeontol Pol 45: 343-388.

Whitlock JA., Harris JD. 2010. The dentary of *Suuwassea emilieae* (Sauropoda: Diplodocoidea). Journal of Vertebrate Paleontology, 30: 1637-1641.

Whitlock JA. 2011. A phylogenetic analysis of Diplodocoidea (Saurischia: Sauropoda). Zoological Journal of the Linnean Society, 161: 872-915.

Whitlock JA., Harris JD. 2010. The dentary of *Suuwassea emilieae* (Sauropoda: Diplodocoidea). Journal of Vertebrate Paleontology, 30: 1637-1641.

Whitlock JA., Wilson JA., Lamanna MC. 2010. Description of a nearly complete juvenile skull of *Diplodocus* (Sauropoda: Diplodocoidea) from the Late Jurassic of North America. Journal of Vertebrate Paleontology, 30: 442-457.

Wilson JA., Smith M. 1996. New remains of *Amphicoelias* Cope (Dinosauria: Sauropoda) from the Upper Jurassic of Montana and diplodocoid phylogeny. Journal of Vertebrate Paleontology, 16(3 Suppl.): 73A.

Wilhite R. 1999. Ontogenetic variation in the appendicular skeleton of the genus *Camarasaurus*. Master's thesis. Brigham Young University, Provo, Utah.

Wilhite R. 2003. Biomechanical reconstruction of the appendicular skeleton in three North American Jurassic sauropods. Ph.D. dissertation. Louisiana State University, Baton Rouge.

Wilhite R., Curtice B. 1998. Ontogenetic variation in sauropod dinosaurs. Journal of Vertebrate Paleontology 18(Suppl. to No. 3):86A.

Woodward HN., Lehman TM. 2009. Bone histology and microanatomy of *Alamosaurus sanjuanensis* (Sauropoda: Titanosauria) from the maastrichtian of Big Bend National Park, Texas. Journal of Vertebrate Paleontology, 29: 807-821.

Woodruff DC, Fowler DW. 2012. Ontogenetic influence on neural spine bifurcation in Diplodocoidea (Dinosauria: Sauropoda): A critical phylogenetic character. J Morphol 273: 754-764.

Woodruff, DC, Fowler, DW. 2014. The Effects Of Ontogeny In Regards To Morrison Sauropod Diversity. Mid-Mesozoic: The Age Of Dinosaurs In Transition (abstract volume).

Woodruff, DC., Fowler, DW., Horner, JR. 2013. Changes in vertebral morphology associated with histologic data support significant change through ontogeny in diplodocid sauropods. Journal of Vertebrate Paleontology 32(5, abstracts vol): 239.

Zazula GD, MacKay G, Andrews TD, Shapiro B, Letts B, Brock F. 2009. A late Pleistocene steppe bison (*Bison priscus*) partial carcass from Tsiigehtchic, Northwest Territories, Canada. Quat Sci Rev 28: 2734-2742.